A Comparative Study of Ryanodine Receptors (RyRs) Gene Expression Levels in the Basal Ray-Finned Fish, Bichir (*Polypterus ornatipinnis*) and the Derived Euteleost Zebrafish (*Danio rerio*)

Siavash Fazel Darbandi

Supervisor: Dr. Jens Franck

A Thesis Submitted to the Faculty of Graduate Studies in Partial Fulfilment of the Requirements for the Masters of Science Degree.

Department of Biology
Masters of Science in BioScience, Technology and Public Policy Program
The University of Winnipeg
Winnipeg, Manitoba, Canada
July 2010

ABSTRACT

Ryanodine receptors (RyR) mediate the controlled release of intracellular stores of calcium from the sarcoplasmic reticulum. This release of calcium, triggered by membrane-depolarization, is responsible for initiating muscle contraction. Three RyR genes have been identified in mammals, two of which are expressed in specific tissues; RyR1 (skeletal muscle), RyR2 (cardiac muscle), and, RyR3, that is ubiquitously distributed. The RyR1 and RyR3 isoforms are co-expressed at equal levels in teleost fish skeletal muscle. Additionally, fish express fiber type-specific RyR1 paralogous genes in fast-twitch and slow-twitch muscles, termed RyR1-fast (RyR1b) and RyR1-slow (RyR1a) respectively. Bichir, (*Polypterus ornatipinnis*), a ray-finned fish, is considered to be one of the most basal extant species of this lineage. Utilizing a genomic survey of the genome of bichir for the presence of candidate RyR genes, 134 genomic clones were obtained. These cloned sequences were grouped into four cognate groups representing four RyR genes called RyR1a, RyR1b, RyR2, and RyR3 that phylogenetically cluster with their vertebrate orthologs. Quantitative real-time PCR and *in situ* hybridization show fibre type-specific expression of the RyR1a and RyR1b genes. However, the RyR3 gene is down regulated in bichir in contrast to derived teleosts including zebrafish (*Danio rerio*) in which the RyR1 and RyR3 genes are co-expressed at equivalent levels. Succinate dehydrogenase staining revealed that bichir and zebrafish possess similar red muscle fiber arrangements in their skeletal muscle; however, zebrafish possess a higher concentration of red muscle fibers, which could have contributed to the further diversification of the teleost lineage.

ACKNOWLEDGEMENTS

The task of completing a Biology Masters thesis project is one that could not have been accomplished without the help of many spectacular people along the way. First I would like to acknowledge the help and guidance of my supervisor Dr. Jens Franck. His unbelievable patience and kindness were invaluable throughout the year and truly made the project a great success. Also, thanks to my committee members Dr. Alberto Civetta and Dr. Sara Good-Avila who served as voices of reason and inspiration throughout my research journey. I am very thankful to have had committee members and a supervisor that were always willing to take the time to answer any questions I had. In addition, I would like to acknowledge the efforts of Saro Bascaramurty (NRC-CNRC) for her tremendous help and support with cryosectioning portion of my thesis project. My sincere appreciations to Dr. Eileen Denovan-Wright for her tremendous help with the *in situ* hybridization portion of the thesis. Lastly, a big high five to the RyR crew, including Ian Kasloff, Rebecca Vanderhooft and Rolland Gillies who's tormenting made this research journey very interesting.

Of course, no one could survive University life without the support of friends and family. Thanks to friends and family, especially my girlfriend Jill, for putting up with my constant rambling about fish, ryanodine receptors, and spending long hours in the lab even on holidays! The support of my whole family has made my life easier and I am certain that they are proud of my accomplishments. I am very fortunate to be surrounded by wonderful people both in and out of school.

TABLE OF CONTENT

LIST OF TABLES

LIST OF FIGURES

LIST OF APPENDICES

ABBREVIATIONS AND NOMENCLATURE

cDNA: Complementary DNA (reverse transcribed from RNA)

PCR: Polymerase chain reaction

RyR: Ryanodine receptors

DHPR: Dihydropyridine receptor

Ca^{2+}: Calcium cation

Mg^{2+}: Magnesium cation

TE: Tris Ethylenediaminetetraacetic acid (Tris EDTA)

dNTP: Deoxyribonucleotide triphosphate

RNasin: Ribonuclease inhibitor

ddH_2O: Doubled-distilled water (RNase-free water)

SDH: Succinate dehydrogenase

qRT-PCR: quantitative Real Time PCR

1 Kbp: 1 Kilobase pairs

bp: base pair

HEPES: 4-(2-hydroxyethyl)-1-piperazineethanesulfonic acid

Bi: Bichir

ZF: Zebrafish

CICR: Calcium-induced calcium release

DICR: Depolarization-induced calcium release

qRT-PCR: quantitative Real-Time PCR

$MgCl_2$: Magnesium chloride

MS222: Tricaine methane sulphonate

ABBREVIATIONS AND NOMENCLATURE (CONT'D)

CODEHOP: Consensus-Degenerate Hybrid Oligonucleotide Primers

DGF5: Degenerate Forward primer 5

DFR4: Degenerate Reverse primer 4

S.N.A.P.: Simple Nucleic Acid Purification

IPTG: Isopropyl β-D-1-thiogalactopyranoside

PHYLIP: Phylogeny Inference Package

NADH: Nicotinamide Adenine Dinucleotide

PBS: Phosphate Buffer Saline

SSC: Saline Sodium Citrate buffer

EDTA: Ethylenediaminetetraacetic acid

DEPC: Diethylpyrocarbonate

BLAST: Basic Local Alignment Search Tool

Ef1α: Eukaryotic Elongation factor 1 alpha

X-Gal: 5-bromo-4-chloro-3-indolyl- beta-D-galactopyranoside

NZCYM: NaCl, Zinc, Casamino acid, Yeast extract and Magnesium chloride (powder broth)

PUBLICATION:

Much of the research discussed in this thesis is available in the following publication:

Darbandi, S. and J. P. C. Franck. 2009. A comparative study of Ryanodine Receptors (RyRs) gene expression levels in basal ray-finned fishes, Bichir (*Polypterus ornatipinnis*) and the derived euteleosts Zebrafish (*Danio rerio*). *Comparative Biochemistry and Physiology Part B* **154:** 443 – 448.

CHAPTER 1: LITERATURE REVIEW

1.1 RYANODINE RECEPTORS (RYRS) STRUCTURE

Ryanodine receptors (RyRs) are intracellular calcium release channels that are widely expressed, but are particularly prevalent in skeletal muscles (Williams *et al*., 2001). In muscle cells, neuron-induced depolarization of transverse-tubules (t-tubules) is translated into a signal for calcium release from the sarcoplasmic reticulum (SR) at structures known as triad junctions, where RyRs respond to the signal (Fill and Copello, 2002). RyRs are large homotetrameric proteins with a total molecular mass of approximately 2.2 – 2.3 million Daltons (Figure 1a; Sharma and Wagenknecht, 2004). RyRs contain at least two distinct functional domains, which are referred to as the cytoplasmic assembly (CA) and the transmembrane assembly (TA; Figure 1b; Frank, 1996). The cytoplasmic assembly was first recognized as a foot structure in electron micrographs of sectioned muscle (Franzini-Armstrong and Jorgensen, 1994). Radermacher and colleagues suggested that about half of the volume of the CA is occupied by solvent and its characteristic square form is made up of reproducible, interconnected globular proteins or domains (Radermacher *et al*., 1994). These domains were allocated numerical designations 1 – 10 (Figure 1a and 1b; Radermacher *et al*., 1994). The topology of the TA of RyRs has not been fully described. There is a consensus agreement that most of the transmembrane helices occur in the amino terminal region of the RyR subunits' sequence. However, the number and locations of the helical segments within the sequence are still debated (Zhao *et al*., 1999).

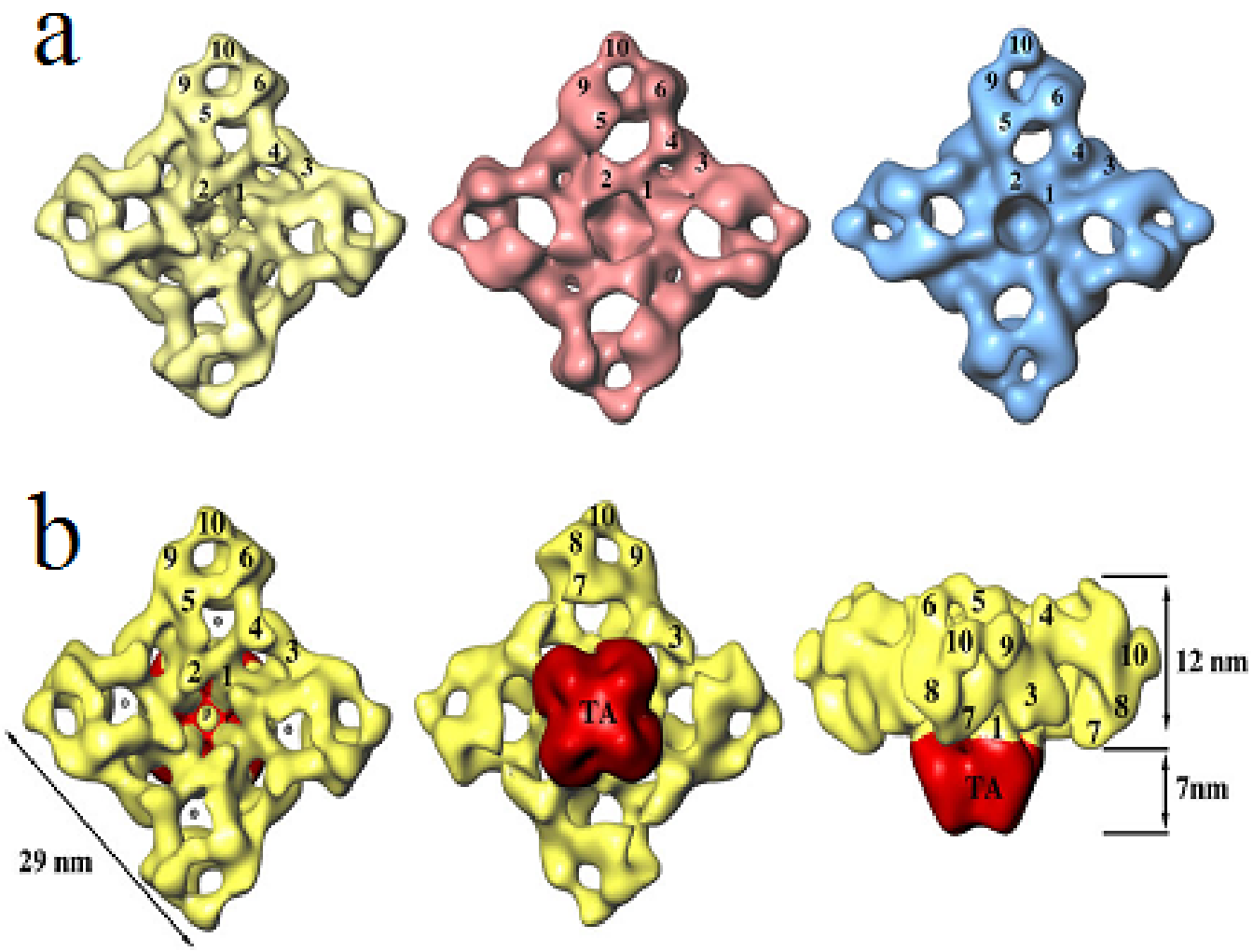

Figure 1: (a) Cryo-electron microscopy and 3D reconstruction of three RyR genes are shown as viewed from the cytoplasmic face. RyR1 (yellow), RyR2 (red) and RyR3 (blue). Functional domains are numbered 1-10 in one subunit of the tetrameric molecule. Structural differences among the isoforms could be due to functional differences in the mechanism of E-C coupling (Sharma and Wagenknecht, 2004). (b) Surface representation of RyR1 in three different orientations. Cytoplasmic assembly (CA) is presented in yellow and transmembrane assembly (TA) is in red (Radermacher *et al*., 1994; Sharma and Wagenkencht, 2004).

1.2 RYANODINE RECEPTORS GENES

The three RyR genes that have been identified in mammals have an overall amino acid identity of 66-70% (Rossi and Sorrentino, 2002). The RyR gene that is expressed primarily in skeletal muscle is referred to as RyR1, while RyR2 is predominantly expressed in cardiac muscle. The RyR3 gene is widely expressed and has been found in the diaphragm, skeletal muscle, and in non-contractile tissue such as brain, and is known to play a role in developmental processes (Inoue *et al*., 2004). In mammals, the three copies of RyRs are products of three different genes (Fill and Copello, 2002). The RyR genes first identified in non-mammals (for instance, amphibians such as frog) were originally designated as α-RyR and β-RyR, because the orthology of these genes to mammals was uncertain (O'Brien *et al*., 1995). In a study conducted by O'Brien and colleagues (1993) RyR expression was investigated by immunoblotting of RyR antibodies to protein extracted from toad fish swimming muscles. This investigation described the equal co-expression of RyR1 and RyR3 proteins in the skeletal muscles of teleost fish. Further investigation by O'Brien and colleagues (1995) was performed utilizing [^{3}H]ryanodine binding properties of the two distinct non-mammalian RyR channels, which was complemented with binding studies on single-channel conductance of the two different channels in fish swimming muscle (O'Brien *et al*., 1995). The presence of two RyR genes (RyR1 and RyR3) with different properties in most non-mammalian vertebrate skeletal muscles has important implications for the mechanism of Ca^{2+} release (O'Brien *et al*., 1995) and evolution of E-C coupling. It has been determined that these genes are homologous to RyR1 and RyR3 respectively (O'Brien *et al.,* 1995). Moreover, two distinct RyR1 genes have been shown to be discretely expressed in slow

and fast twitch muscle in fish. These have been designated as RyR1-slow (RyR1a) and RyR1-fast (RyR1b), respectively (Franck *et al.*, 1998; Hirata *et al.*, 2007). Slow and fast twitch muscles in fish are discretely compartmentalized which makes them a good model organism to study expression of these genes.

1.3 GENOME DUPLICATION EVENTS

There is evidence that at least two rounds of whole-genome duplication took place during vertebrate evolution. Supporting evidence comes from studies of the *Hox* gene family (Amores *et al.*, 2004; Blomme *et al.*, 2006). *Hox* genes have a dynamic evolutionary history hallmarked by tandem and whole-cluster duplications (Holland and Garcia-Fernandez, 1996). These gene clusters possess the phenomenon of co-linearity, in which the position of the gene and its spatiotemporal expression pattern in embryonic development are related (Chiu *et al*., 2004). In a study directed by Chiu and colleagues, it was suggested that bichir (*Polypterus senegalus*) contains one *Hox*A cluster that is mosaic in its pattern of non-coding sequence conservation and gene retention relative to the single *Hox*A cluster of human, and duplicated *Hox*Aα and *Hox*Aβ clusters in zebrafish and pufferfish (Chiu *et al*., 2004). Chiu and colleagues concluded that the genome duplication leading to two copies of the *Hox*A cluster occurred after the divergence of bichir (Polypteridae lineage) from the rest of the ray-finned fishes. Another study conducted by Ledje and colleagues (2002) suggested that bichir (*Polypterus palmas*) possesses five groups of nine *Hox* genes, indicating there are four *Hox* clusters in the genome of bichir (Ledje *et al.*, 2002), whereas teleosts including zebrafish and medaka possess seven *Hox* clusters (Ledje *et al.*, 2002). All *Hox* gene-mapping studies of teleosts have revealed proof of at least one extra *Hox* gene duplication event in the teleost

lineage (Prohaska and Stadler, 2004). Loss of *Hox* genes is not a rare event (Stellwag, 1999). It is possible that the number of *Hox* clusters in zebrafish and medaka, seven rather than eight, is due to secondary loss of a whole cluster. Mapping experiments have identified the predicted adjacent chromosome fragments of an extra *Hox*D cluster in zebrafish (Amores *et al.*, 1998), which could confirm the hypothesis that one copy of *Hox* cluster genes has been lost in the teleost lineage.

The first whole-genome duplication probably predates the Cambrian explosion (530 MYA), and occurred during early chordate evolution coincident with the divergence of cephalochordates (Meyer and Van de Peer, 2005; Xian-guang *et al.,* 2002). This original duplication gave rise to RyR2-like and RyR3-like genes from the invertebrate ancestral RyR gene (Figure 2). Supporting evidence comes from previous work done by a former honours student (Reimer, 2007) who surveyed the hagfish genome (representative of Agnatha lineage) for the number of RyR paralogs. Utilizing a PCR-based approach, he provided sufficient evidence that hagfish only possesses orthologs for RyR2 and RyR3 (Reimer, 2007). The second duplication is estimated to have occurred during the early Devonian (359 MYA) prior to the divergence of teleosts and tetrapods (Figure 2). It is believed that during the second whole-genome duplication followed by a gene loss, RyR3 diverged into RyR1-like and RyR3-like genes, early in the evolution of vertebrates (Franck *et al.*, in preparation). This hypothesis is supported by genomic survey of horn shark (*Heterodontus francisci*; representative of the Chondrichthiomorphi lineage), done by a previous honours student (Nguyen, 2009). Utilizing a PCR-based approach she provided sufficient evidence that horn shark only possesses orthologs for RyR1, RyR2 and RyR3 in its genome. Additionally, strong evidence also exists for a third round of

whole-genome duplication (also referred to as the Fish-Specific Genome-Duplication; FSGD) that occurred during the early divergence of teleost fish from sarcopterygians (Figure 2; Finn and Kristoffersen, 2007; Meyer and Van de Peer, 2005). Comparative synteny mapping by Franck *et al*. (in preparation) suggests that the RyR1a and RyR1b paralogs are the result of a local gene duplication event followed by transposition (Figure 2).

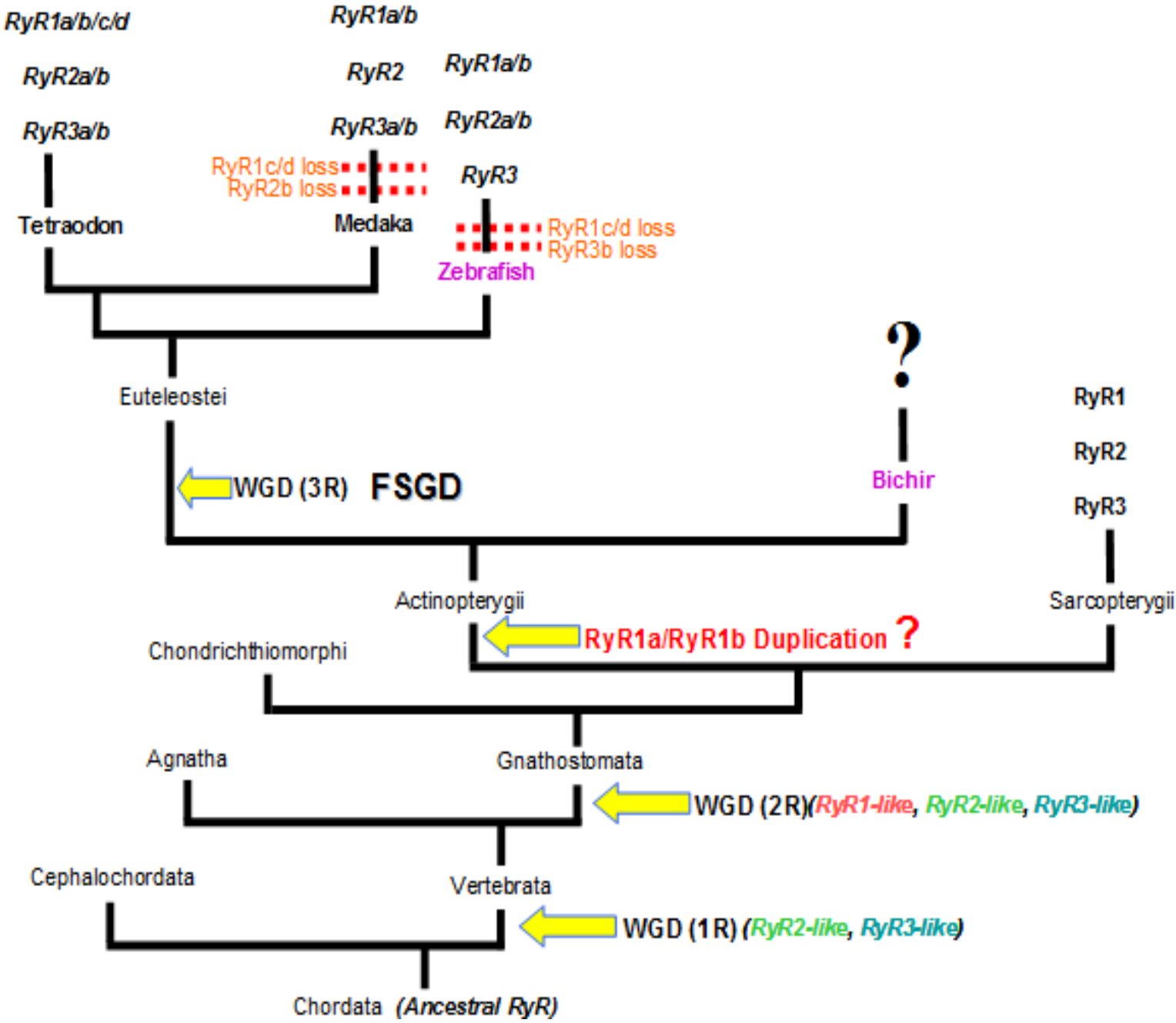

Figure 2: Proposed History of RyR Gene Duplication. The proposed molecular evolution of the RyR gene family is shown within a conventional vertebrate species tree. The evolution of the fiber type-specific RyR1 genes is believed to be the result of a Fish-Specific Genome-Duplication (FSGD); however, the timing of this event is debated. Also since no work has been done on the genome of bichir, investigating the number of paralogs copies of RyRs present in its genome would provide further evidence as for the timing of duplication event that gave rise to multiple RyR copies within fish lineage. WGD = Whole-Genome Duplication, 1R = first round of whole-genome duplication, 2R = second round of whole-genome duplication, and 3R = third round of whole-genome duplication.

Gene duplication, whether due to a whole-genome or a local duplication event leads to one of several potential outcomes. Duplicated genes may be subsequently lost due to redundancy through selection, or may be retained as a backup with no change in function (Force *et al*., 1999). Duplicate genes could also lose their function and become non-functionalized resulting in the formation of a pseudogene (Lynch and Force, 2000). The duplicated genes may also diversify to take on completely new roles; an outcome known as neofunctionalization (Lynch and Force, 2000). Duplicated genes may also undergo subfunctionalization, in which case duplicated copies partition the original functions of the ancestral gene. The subfunctionalized genes are sometimes expressed at different times (temporal separation) or in different tissues (spatial separation) (Figure 3; Force *et al.*, 1999; Lynch and Force, 2000). Subfunctionalization best describes the divergence of the RyR1a and RyR1b paralogs in red and white skeletal muscle fibers respectively.

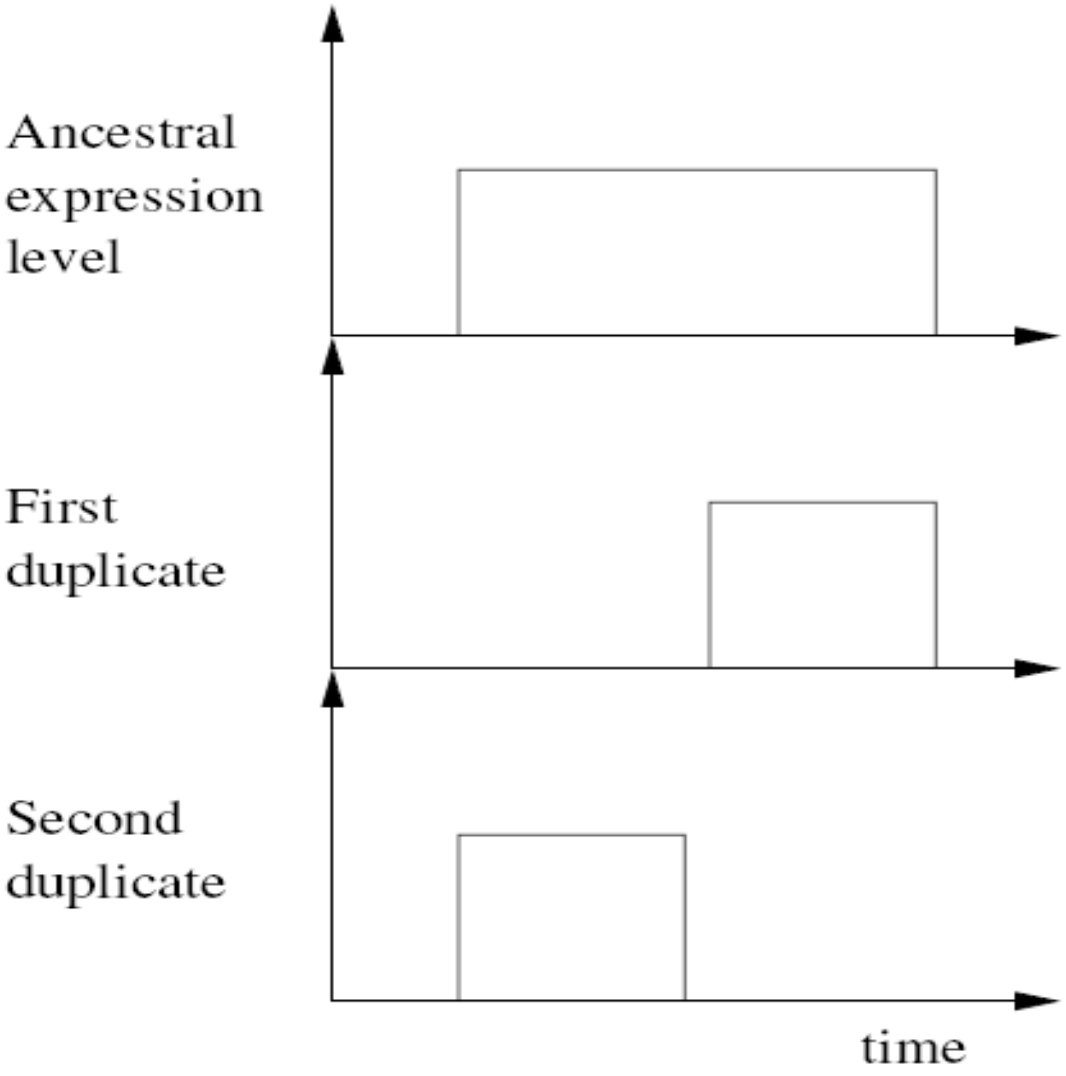

Figure 3: Spatial subfunctionalization, illustrated here by the spatial expression patterns of a hypothetical ancestor and two evolved duplicates. The expression level of the duplicates has evolved such that the ancestral expression pattern is maintained in complementary temporal domains via the combined expression of the two duplicates (Figure adapted from MacCarthy and Bergman, 2007). RyR1a and RyR1b are classic examples of spatial subfunctionalization in the fish lineage, since they share an ancestral function, yet expressed differentially in red and white muscle fibers respectively.

1.4 ROLE OF RYANODINE RECEPTORS

Ryanodine receptors serve as an important channel responsible for the regulated release of intracellular stores of calcium (Ca^{2+}) from the sarcoplasmic reticulum of muscle cells. This release of Ca^{2+}, triggered by membrane depolarization, is responsible for initiation of the muscle contraction process. Excitation–contraction (E-C) coupling describes the tight relationship between an excitatory nerve impulse and the resulting muscular contraction (Sherwood *et. al.*, 2005). The cytoplasmic concentration of calcium in resting cells is much lower relative to extracellular and sarcoplasmic reticulum calcium concentrations. In skeletal muscle the transverse tubules (t-tubules) of muscle cells allow RyRs to directly contact with the dihydropyridine receptors (DHPRs) on the cell membrane (Sherwood *et al.*, 2005). Once a nerve impulse reaches the DHPR, it induces a conformational change, leading to the mechanical opening of the RyR, a process referred to as depolarization–induced calcium release (DICR). In cardiac muscle, calcium enters via the voltage-gated calcium channels for extracellular stores and acts as a ligand to open RyR channels. This is referred to as calcium–induced calcium release (CICR; Sherwood *et al.*, 2005).

1.5 EVOLUTION OF EXCITATION-CONTRACTION COUPLING

Genome duplications during the evolution of vertebrates were major steps that allowed for the differentiation of muscle specific myosin II into separate cardiac and skeletal genes and thus the appearance of a separate cardiac system (McGuigan *et al.*, 2004). The molecular evolution of the RyR gene family has been implicated as a critical contributor to the divergence of the vertebrate lineage, particularly with respect to the evolution of muscle activation (Di Biase and Franzini-Armstrong, 2005; Franzini-

Armstrong and Kish, 1995). The divergence of vertebrates from ancestral invertebrates included physiological changes in the E-C coupling mechanism in skeletal muscle tissues (Inoue *et al.*, 2002). The DHPR-RyR interaction is indirect in more ancestral organisms such as invertebrates, and probably involves calcium as a short-range transmitter, which is imported from extracellular fluids into the cell. Contraction, then, takes place via the CICR mechanism (Sorrentino *et al.*, 2000; Nabauer *et al*., 1989; Gyorke and Palade, 1993; Franzini-Armstrong and Protasi, 1997). Conversely, the RyRs in vertebrate skeletal muscle (RyR1) are mechanically gated by the voltage sensitive DHPRs and do not require extracellular calcium as a ligand; thus, the E-C coupling occurs via a depolarization-induced calcium release (DICR; Sorrentino *et al.*, 2000). Skeletal and cardiac muscles of higher vertebrates differ in both the mechanism of muscle activation (E-C coupling), and in the proteins involved. The evolution from a single mechanism of E-C coupling for all muscle fibers to one that differentiates between cardiac and skeletal muscles seems to have occurred at the transition between chordates and vertebrates in parallel to the myosin II dichotomy (Inoue *et al.,* 1994; Franzini-Armstrong *et al.*, 1999). This transition involved the appearance of separate calcium release channels for the two types of striated muscles (Chugun *et al*., 2003), as well as the acquisition by skeletal muscle of a novel mechanism for controlling the initiation of contraction.

The two main components essential to E-C coupling are DHPRs and RyRs. DHPRs are L-type channels that sense membrane voltage and are located in junctional domains of the plasmalemma and its invaginations (t-tubules). RyRs are calcium release channels of the endoplasmic reticulum or sarcoplasmic reticulum (SR) in muscle cells. Di Biase and Franzini-Armstrong (2005) suggested that in muscle cells, both RyRs and

DHPRs are strategically located within calcium release units (CRUs), so that RyRs can receive a signal from the DHPRs; however, this is achieved by different mechanisms in skeletal and cardiac muscle. In skeletal muscle direct RyR-DHPR interaction is mediated by a specific link between the two molecules; whereas, in cardiac muscle, RyRs and DHPRs interact indirectly and are only loosely associated (Di Biase and Franzini-Armstrong, 2005). The structural arrangement of the specific RyR-DHPR association is revealed by the presence of DHPR in tetrads, dictated by their link with the tetrameric RyR structures, in which four DHPRs associate with the corners of the four equal subunits of the RyR (Figure 4; Di Biase and Franzini-Armstrong, 2005; Franzini-Armstrong *et al.*, 1999; Protasi *et al.*, 1997). Although DHPRs are distributed equally in the CRUs of smooth muscle and cardiac muscle, DHPRs are not arranged in tetrad structures, and there is no evidence for direct association between DHPRs and RyRs in smooth and cardiac muscle fibers (Takekura and Franzini-Armstrong, 2002). Structural and functional differences between skeletal and cardiac muscles are uniquely dependent on the composition of CRUs (ratio of DHPRs:RyRs). The presence of tetrads gives an explicit structural support for concerted expression of skeletal muscle-specific isoforms of both DHPRs and RyRs (Di Biase and Franzini-Armstrong, 2005).

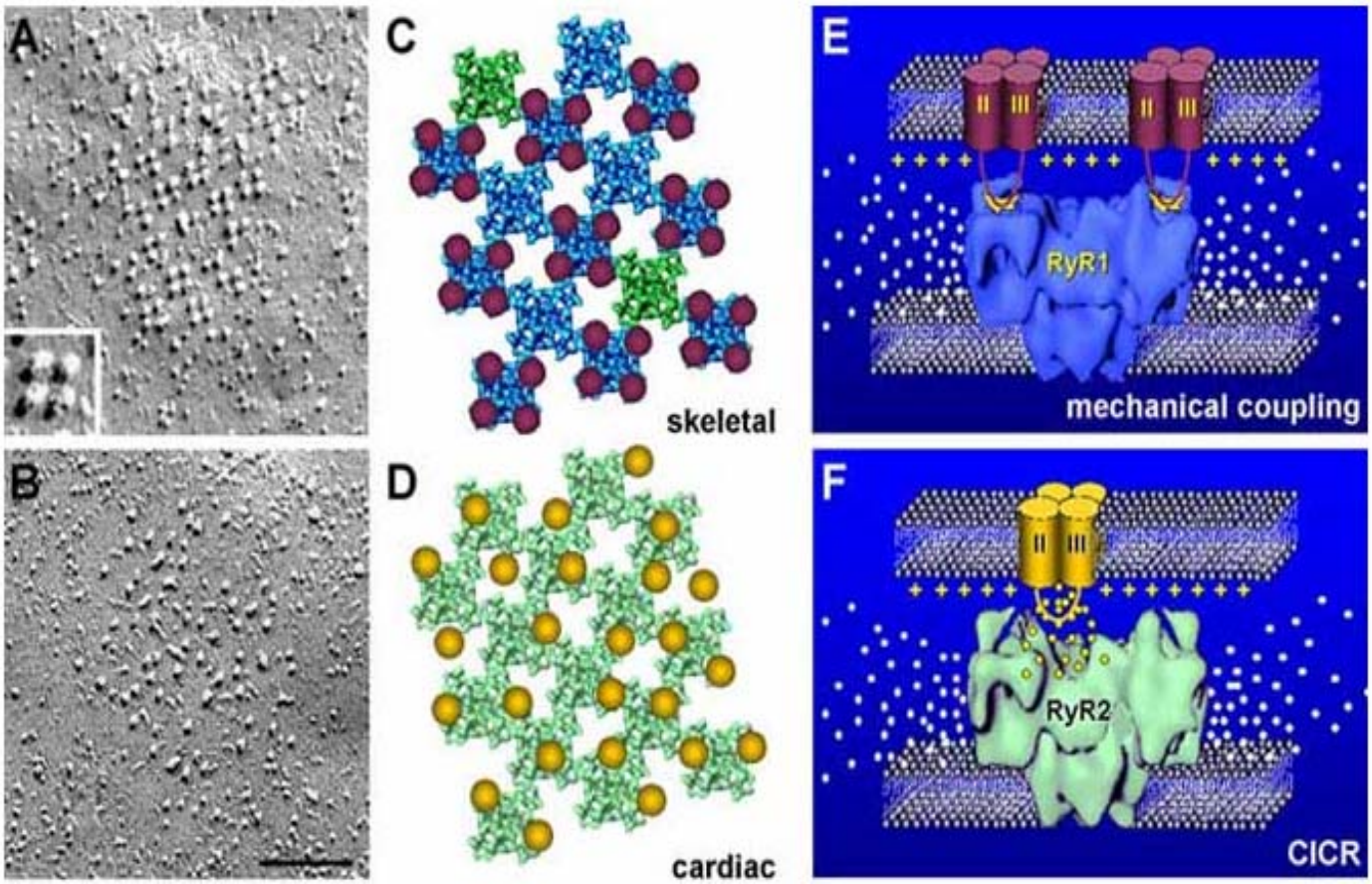

Figure 4: Structure/function correlation: lack of tetrads in cardiac cells explains the need of Ca^{2+} in DHPR/RyR communication. A and B) DHPRs clustered respectively in peripheral coupling of BC3H1 cells (A) and in chicken ventricle (B). DHPRs form tetrads in the first, while in the second are randomly disposed in the junctional domain. C and D) both RyR1 (blue, C) and RyR2 (pale green, D) form ordered arrays. However, the specific link that allows associations of tetrads to alternate RyR1s in skeletal muscle cells is missing in the heart. The role and intracellular localization of RyR3 in skeletal muscle fibers is still not completely clear: RyR3 (green, C) may occupy some of the uncoupled positions of the RyR arrays. E and F) Cartoons illustrating the two different mechanisms that allow DHPRs and RyRs to communicate in E-C coupling: mechanical coupling in skeletal fibers and CICR in cardiac myocytes. Need of external Ca^{2+} in heart (F) is the result of lack of a direct link between the two molecules; this link probably involves the II-III loop of the DHPR in skeletal fibers (E) (Figure used with permission from Sharma and Wagenknecht, 2004).

1.6 MODEL ORGANISMS

Bichir (*Polypterus ornatipinnis*), and zebrafish (*Danio rerio*) have been utilized as vertebrate model organisms throughout this research. These organisms are valuable for the study of the evolution of physiological and developmental processes. Bichir is a representative of the most basal extant species of ray-finned (Actinopterygii) fish lineage possessing ancestral morphological features (Chiu *et al.*, 2004). Bichir is also an interesting model organism for studying the timing of the third round of whole-genome duplication (FSGD), which is hypothesized to have given rise to multiple RyR paralogs in the fish lineage, since the number of paralogous copies of RyRs have not been investigated in the genome of this organism.

Zebrafish (*Danio rerio*) represents a model species from the derived euteleost lineage. Since the genome of zebrafish is sequenced and is available through various databases, it provides additional insights on the evolution of the RyR multigene family. It provides an opportunity to compare and contrast the molecular evolutionary and gene expression data obtained from bichir (basal ray-finned fish) and to create a clearer image of patterns of evolution in the RyR multigene family.

1.7 OBJECTIVES:

The first objective of this study was to survey the genome of bichir (*P. ornatipinnis*) for the presence and number of RyR genes. This was of particular interest, since it allowed me to further investigate the timing of the Fish-Specific Genome Duplication, which was hypothesized to give rise to multiple copies of RyRs. The genes were annotated by similarity searches against the GenBank database and analyzed using

phylogenetic methodologies. Subsequent to this investigation, I was interested to compare the expression levels of RyRs discovered from the genomic survey of bichir with expression levels of RyRs in zebrafish in different tissue sources such as skeletal muscle, cardiac muscle, and brain. This involved the use of quantitative Real Time PCR (qRT-PCR) to determine the relative expression levels of the RyR orthologs in comparison to actin and eukaryotic elongation factor 1 alpha (ef1α) housekeeping genes (HKG). The results obtained from qRT-PCR will shed more light on the patterns of evolution of E-C coupling throughout fish lineages. The third objective of this thesis was to examine the spatial arrangement of red and white muscle fibers in the bichir and the zebrafish transverse sections as revealed by succinate dehydrogenase (SDH) staining of the thin cut transverse sections. Furthermore, spatial expression of RyR1 paralogs and RyR3 were examined in different tissues of bichir and zebrafish, such as skeletal muscle and brain by utilizing *in situ* hybridization of ^{33}P labelled oliognucleotide probes to thin cut sections. Spatial expression of RyR1 and RyR3 were examined due to their significant contribution to the evolution of E-C coupling. The results of this portion of the research was also used to provide supporting evidence for the results obtained from previous sections of this thesis, namely, qRT-PCR as well as muscle fiber arrangement observed in histological staining methods .

CHAPTER 2: MATERIALS AND METHODS

2.0 GENOMIC DNA EXTRACTION FROM FRESH SAMPLES:

Overall, 9 bichir fish were obtained from a local tropical fish store (Fish Gallery, Winnipeg) and sacrificed following a protocol approved by the Senate Animal Care Committee issued to Dr. Franck. The organisms were euthanized immediately after being received in the lab by immersion in 0.6 mg/ml MS222 (Tricaine Sulfate; 300 mg MS222 dissolved in 500 mL of ddH_2O; pH adjusted to 7.0 by adding 1 M NaOH) followed by pithing. Tissues were dissected from the specimens using a dissecting microscope. Skeletal muscle, cardiac muscle, and brain were carefully dissected and instantly frozen in liquid nitrogen. 50 mg of tissue was cut into small pieces and incubated in 1 mL of DNAzol reagent supplemented with 100 μg/mL of proteinase K (Invitrogen Life Technologies). The mixture was incubated overnight at room temperature. Subsequently, the mixture was centrifuged for 10 min at 10 000 ×g at room temperature. DNA was precipitated by adding 0.5 mL of 95% ethanol per 1mL of DNAzol. After precipitation, DNA was pelleted via centrifugation at 5 000 ×g and washed with 0.8 – 1.0 mL of 75% ethanol and centrifuged at 7 500 ×g. Lastly DNA was dissolved in 0.2 – 0.3 mL of 8 mM sodium hydroxide (8 mM NaOH) and neutralized utilizing 101 μL of 0.1 M HEPES to pH 8.0.

2.1 RNA EXTRACTION FORM FRESH SAMPLES:

100 mg of tissue was homogenized in 1 mL of TRIzol reagent (Invitrogen Life Technologies). The tissues were homogenized with a motorized Teflon pestle and glass mortar. TRIzol reagent uses phenol chloroform to separate RNA from other cellular

components (primarily protein; Chomczynski and Sacchi, 1987). Total RNA was precipitated with 95% ethanol, pelleted by centrifugation at maximum speed (14 000 ×g) and dried by speed-vacuum evaporation. The dried RNA was resuspended in 50 μL RNase free water, and quantified using a nanophotometer (UV_{260} was measured; Birds, 2005).

2.2 cDNA Synthesis from Extracted RNA:

10 – 20 μg of total RNA was used as template to synthesize first strand cDNA. A 20 μL solution of the total RNA and 0.05 μg/μL of Oligo dT_{15} primer was heated to 95°C for five minutes and immediately chilled on ice. Once the solution was chilled, 12 μL of 5X Oligo dT_{15} buffer, 2 μL of 10 mM dNTPs, 24 μL double distilled H_2O (ddH_2O), 1 μL RNAsin and 1 μL of reverse transcriptase (SS II RT) were added and mixed. The solution was incubated at room temperature for 15 minutes, followed by 30 minutes incubation at 37°C. The reaction was stopped by adding 40 μL of 10X TE buffer at room temperature (pH 8.0). The first strand cDNA was precipitated by adding 10 μL of 3M sodium acetate and 250 μL of 95% ethanol. The cDNA was precipitated at -20°C for several hours in this solution and pelleted by centrifugation at 14 000 ×g for 15 minutes, washed with 95% ethanol and centrifuged again at 3 000 – 4 000 ×g for 5 minutes. The pellet was dissolved in 100 μL of distilled, RNase and DNase free water (Invitrogen Life Technologies).

2.3 Polymerase Chain Reaction (DNA Amplification):

Partial RyR sequences were amplified from both genomic DNA and cDNA using degenerate primer pairs. The CODEHOP program (Rose *et al*., 1998) was used to design

degenerate primers for highly conserved blocks of RyR sequence **(**Figure 5**)**. The conserved sequence blocks were identified from a multiple amino acid sequence alignment of published RyR sequences using the Blocks Multiple Alignment Processor (http://blocks.fhcrc.org/blocks/process_blocks.html). The forward (DGF5; 5′-GTGAACGGAACGATCGGAMRNCARATGGT-3′) and reverse primer (DGR4; 5′-TCTTGGCGGCTCCCADDATYTCDAT-3′) pair amplified a partial RyR sequence corresponding to amino acid position 4414 – 4555 in human RyR1. In the primer sequence, R donates G or A, Y donates C or T, M donates A or C, and N donates A, C, G or T. The calculated melting points under standard conditions for DGF5 and DGR4 were between 58°C and 61°C. Theoretically, the pool of degenerate PCR products represents a survey of all RyR genes in the bichir genome; thus, these primers were then used to amplify RyR messages from the genomic DNA. 22.5 μL of master mix and 2.5 μL of template (equivalent of approximately 3 ng of DNA template) were used for each PCR reaction. The master mix contained 2.5μL of 10X PCR buffer (Invitrogen Life Technologies), 0.75 μL of 50 mM $MgCl_2$, 0.5 μL of 10 mM dNTPs, 0.5 μM of each primers, 0.2 μL recombinant Taq DNA Polymerase (0.5 U) and 18.05 μL of ddH2O (RNase free water). The initial denaturation step was 95°C for 9 minutes. The subsequent denaturation step was 95°C for 1 minute, followed by an annealing step at 57°C for 1 minute and 30 seconds and an extension step at 72°C for 1 minute. These 3 steps were cycled 35 times and a final extension step at 72°C for 7 minutes completed the reaction. PCR reaction products were fractionated on a 1% low melting point agarose gel containing 0.5 μg/μL ethidium bromide and viewed on a Bio-Rad UV transilluminator (Universal Hood II), and purified by either gel purification (Wizard® PCR Preps DNA

Purification System, Promega) or with S.N.A.P. Gel Purification Kit (Invitrogen Life Technologies) following the manufacturer's protocol.

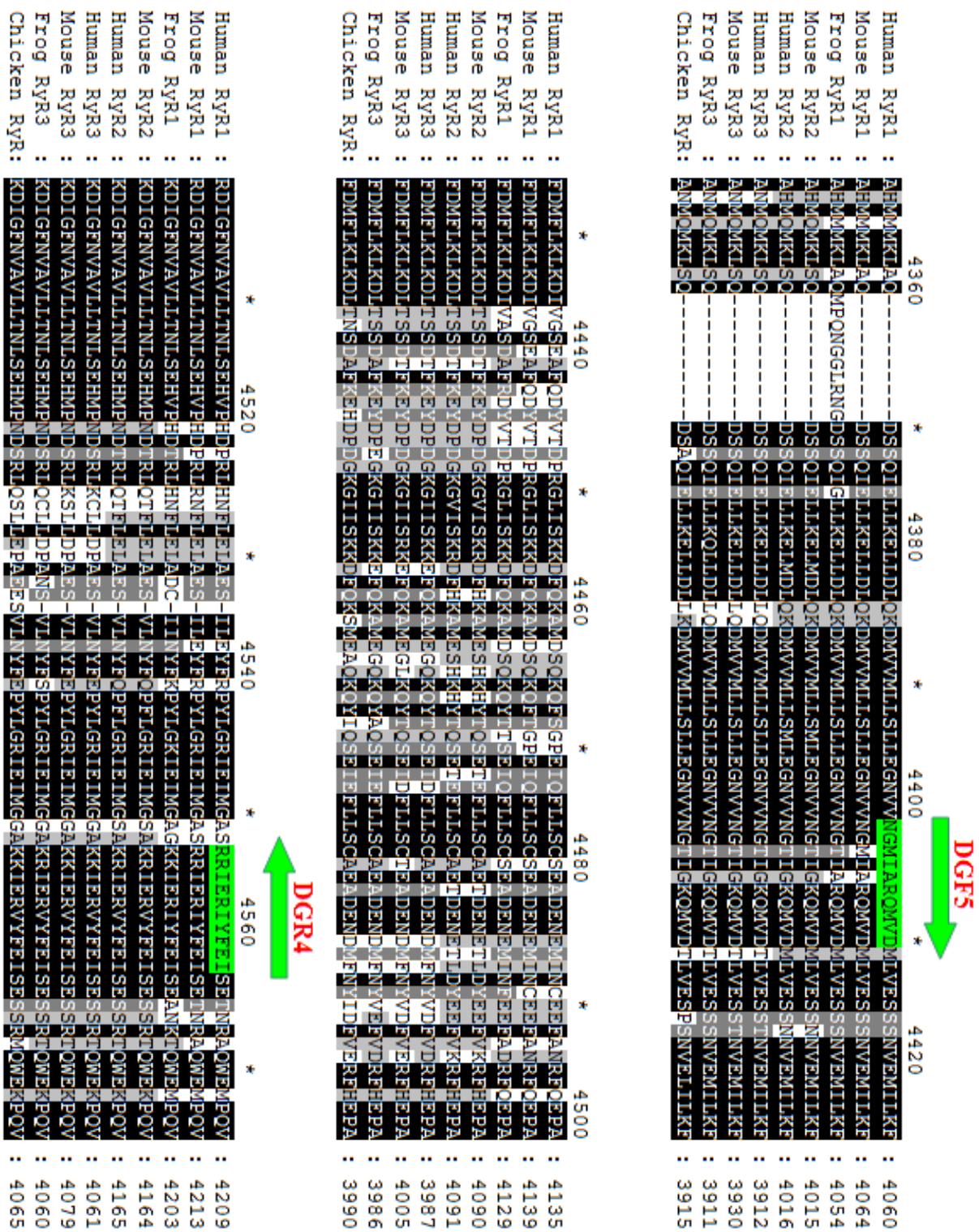

Figure 5: Amino acid alignment of published RyR sequences used to design degenerate primer pairs. Highly conserved blocks of published RyR sequences (shown in green) were used as target region for primer design.

2.4 CLONING OF PCR PRODUCTS:

Cloning was performed to separate the pool of PCR products amplified by the degenerate primers; this step was essential since each PCR reaction tube would presumably contain a mixture of partial RyR gene sequences present in the genome of the organism. The purified PCR products were ligated with pGEM® – T Easy vectors (Promega Biotech, Appendix 1). The ligated products were transformed into *Escherichia coli* JM109 strain (*E. coli* JM109; Promega Biotech) competent cells. The cells were then plated on NZCYM growth media supplemented with 50 μg/mL ampicillin, 40 μg/mL X-gal and 0.1 mM IPTG. IPTG acted as an inducer of the *lac* operon in *E. coli* while X-gal was a visual indicator of β-galactosidase activity. The activity of IPTG in combination with X-gal allowed for screening of colonies. Plates were incubated at 37°C overnight. Colonies with a functional *lac* operon appeared blue; however, recombinant colonies appeared white due to disruption of the β-galactosidase gene. Since pGEM® – T Easy vectors contain an antibiotic resistance gene, the media was supplemented with ampicillin (50 μg/ml) to prevent the growth of non-transformed bacteria.

2.5 PCR DETECTION OF RECOMBINANTS AND PLASMID PURIFICATION:

Bacterial colonies were randomly selected for screening from each plate. Each colony was touched with a sterile pipette tip and was allowed to incubate in a PCR tube containing 15 μL of PCR master mix containing 1.5 μL 10X PCR buffer, 0.9 μL 50 mM $MgCl_2$, 0.075 μL of 100 μM M13 forward primer, 0.075 μL of 100 μM M13 reverse primer, 11.925 μL ddH_2O, and 1.5 μL Taq DNA Polymerase, for approximately one minute at room temperature. PCR was performed using M13 forward (5′-GTTTTCCCAGTCACGAC-3′) and M13 reverse (5′-CAGGAAACAGCTATGAC-3′)

primer pairs to amplify the cloned insert. The PCR program consisted of an initial denaturation step at 95°C for five minutes. The second step was 95°C for one minute, followed by an annealing step at 55°C for thirty seconds and an extension step at 72°C for one minute. The second, third and fourth steps were cycled 35 times. The reaction products were fractionated on a 1% agarose gel containing 0.5 μg/μL ethidium bromide and viewed on a Bio-Rad UV transilluminator (Universal Hood II). Bacterial cultures corresponding to PCR products of expected size were grown overnight in NZCYM broth containing 50 μg/mL ampicillin. Plasmids were purified from bacterial cultures using the S.N.A.P. PureLink™ Quick Plasmid Miniprep Kit following manufacturer's protocol (Invitrogen Life Technology).

2.6 SEQUENCING AND PHYLOGENETIC ANALYSIS:

Plasmids were sequenced on both strands with M13 forward and reverse primers by The Centre for Applied Genomics (The Hospital for Sick Children, University of Toronto). The cloned bichir PCR products were aligned using the CLUSTALX program (Thompson *et al.*, 1997) and grouped into four cognate classes based on sequence identity. The consensus sequence from each cognate class was searched against the GenBank database using the BLASTx program (Altschul *et al.*, 1990) to determine putative orthology to the published RyR sequences. Phylogenetic analysis of the bichir RyR sequences was performed using programs from the PHYLIP package (Felsenstein, 1993). A multiple sequence alignment of the deduced amino acid sequences from the four bichir consensus sequences with selected published RyR sequences was generated using the program CLUSTALX (Thompson *et al.*, 1997). In addition to the RyR consensus sequences from bichir, the alignment included human, (*Homo sapiens*) RyR1 (Hsa RyR1,

GenBank accession number NM_001042723), bullfrog (*Rana catesbeina*) RyR1 (Rca RyR1, D21070), mouse (*Mus musculus*) RyR1 (Mmu RyR1, NM_009109), zebrafish (*Danio rerio*) RyR1a (Dre RyR1a, XM_001923259), zebrafish RyR1b (Dre RyR1b, NM_001102571), human RyR2 (Hsa RyR2, NP_001026), mouse RyR2 (Mmu RyR2, NM_023868), zebrafish RyR2a (Dre RyR2a, XM_001922082), zebrafish RyR2b (Dre, XM_001921102), human RyR3 (Hsa RyR3, NM_001036), mouse RyR3 (Mmu RyR3, NM_177652), frog RyR3 (Rca RyR3, D21071), zebrafish RyR3 (Dre RyR3, XM_001922078), and the nematode *Caenorhabditis elegans* (Cel RyR, BAA08309). The aligned RyR sequences were used as input for the Boot program of PHYLIP to generate 100 pseudo-replicate alignments. The Protdist program was then used to generate 100 distance matrices using the Dayhoff PAM distance matrix (Dayhoff *et al.*, 1972). The Neighbor program of PHYLIP generated 100 neighbour-joining trees and a majority rule consensus tree was generated using the Consense program. The consensus tree was viewed using the Treeview program (Page, 1996).

2.7 QUANTITATIVE REAL-TIME PCR (qRT-PCR):

Quantitative real time PCR was performed with a MiniOpticon real time cycler (Bio-Rad Technologies). The actin and ef1α sequences were amplified using degenerate primers designed using CODEHOP program (Table 1). PCR products were cloned and sequenced, which yielded one cognate class for each gene. Gene-specific primers for the four bichir RyR sequences and the actin and ef1α housekeeping gene sequences were designed using the Primer 3 program (Table 2; Rozen and Skaletsky, 2000). Specificity of the primers was confirmed by performing reverse transcriptase PCR and direct sequencing of the PCR products (appendix 2 and 3). The expression level of the bichir

and zebrafish RyR genes were measured relative to the expression of actin and ef1α housekeeping genes (Appendix 4 and 5).

Table 1: Degenerate primer pair sequence used to amplify actin and ef1α HKG from genomic DNA of bichir and zebrafish.

Gene	Forward Primer	Reverse Primer
Actin	5′-TGATGGTGGGCATGGGNCARAA-3′	5′-CGTAGCCCTCGTAGATGGGNACRTTRTG-3′
ef1α	5′-CACCGGCCACCTGATCTAYAARTGYGG-3′	5′-GATGCCGCCGATCTTGTANACRTCYTG-3′

Table 2: Gene-specific primers used for quantitative real-time PCR (qRT-PCR) analyses.

P. ornatipinnis	Forward Primer	Reverse Primer
Actin	5′-AGC TCA GAG CAA GAG GGG TA-3′	5′-ACC GGT TGT ACG ACC AGA AG-3′
ef1a	5′-AAT GGT GGT GAC CTT TGC TC-3′	5′-GCT GAT CTG TCC AGG ATG GT-3′
RyR1a	5′-CGG ACG ACA GAT GGT TGA TA-3′	5′-TGG CTT TCC ATA GCT TTC TGA-3′
RyR1b	5′-TCC TGC TCA GAA GCA GAT GA-3′	5′-ATC TGC CTG CTC CAA AAA GTT-3′
RyR2	5′-TTC GAT ACG ACC CAG GAA AG-3′	5′-CCA TGA ACC TGC AAA AGA CA-3′
RyR3	5′-GCT ATG GAA AGC CAA AAG CA-3′	5′-GGC CTA GGT AGG GCT CAA AG-3′

D. rerio	Forward Primer	Reverse Primer
Actin	5′-ACT GGG ACG ACA TGG AGA AG-3′	5′-ACA TAG CGG GGA CAT TGA AG-3′
ef1a	5′-GAT GCA CCA CGA GTC TCT GA-3′	5′-TGA TGA CCT GAG CGT TGA AG-3′
RyR1a	5′-ATC CAT GGA CAG CCA GAA AC-3′	5′-CAT GTT CGG AGA GGT TGG TT-3′
RyR1b	5′-CTT TCA AGA GCC TGC CAA AG-3′	5′-AGC ACC CAT GAT CTC GAT TC-3′
RyR2a	5′-GGC ACT ATT GGC AAG CAG AT-3′	5′-ATT GCC TTG TGG AAA TCT CG-3′
RyR2b	5′-GTT TTC ACG AAC CGG CTA AA-3′	5′-TCC TTC CAA GAT GAG GAT GG-3′
RyR3	5′-AAG GAC AGT GGG ATC GTT TG-3′	5′-AAA GTC CAG CGC ACT CTT GT-3′

A 15 μL total reaction volume was used for each qRT-PCR reaction, consisting of 7.5 μL SYBR Green master mix, 1.5 μL each of forward and reverse primers at 10 μM concentration, 1 μL cDNA template and 3.5 μL ddH_2O. The initial denaturation step was 95°C for 9 min, followed by a subsequent denaturation step of 95°C for 1 min, an annealing step at 60°C for 60s and a 90s extension step at 72°C. The reaction was cycled 35 times. The PCR plate was read after each cycle to measure the signal intensity emitted from the reaction. After the final cycle, a melting curve was monitored by gradually heating the plate from 55°C to 95°C and measuring expression at 0.5°C intervals. A

single peak was determinant of a single PCR product in the test tube. In case of DNA contamination in the PCR tube, the peak corresponding to the contaminant would appear upstream in the melting curve analysis. The results of the qRT-PCR analysis were collected and analyzed using the Opticon Monitor 2.1 software (Bio-Rad). For all replicates, the threshold value was manually set at 0.010. In order to determine the relative expression of each RyR gene, the efficiency of designed primers in binding and amplifying the target gene was determined by generating a standard curve from undiluted and 10^{-1}, 10^{-2}, 10^{-3} and 10^{-4} dilutions of cDNA template. Trials were run in triplicates and the average concentration threshold (Ct) value was plotted against the log(dilution). The slope of the best-fit line was used as a parameter to determine the efficiency (E) value ($E = 10^{\frac{-1}{slope}}$; thus a lower slope, implies greater primer efficiency in binding to and amplifying the target). The actual E value for each primer pair did not vary significantly and was very close to 2. The RyR mean normalized expression (MNE) levels in different tissues of bichir and zebrafish were also calculated in triplicate runs (3 biological and 3 experimental sets) since it is statistically more robust than normalized expression; MNE = $\frac{(E_{\mathrm{Re}\,f})^{\overline{Ct_{ref}}}}{(E_{T\,\mathrm{arg}\,et})^{\overline{Ct_{t\,\mathrm{arg}\,et}}}}$. Subsequently the standard error of MNE (SEMNE) was calculated as an estimate of standard deviation, computed from the data sample being analyzed.

$$\text{SEMNE} = \left(\frac{(E_{\mathrm{Re}\,f})^{\overline{Ct_{ref}}}}{(E_{T\,\mathrm{arg}\,et})^{\overline{Ct_{t\,\mathrm{arg}\,et}}}}\right)\times\left(\sqrt{\left((\ln(E_{ref})\times(SE\overline{Ct_{ref}})^2+(\ln(E_{t\,\mathrm{arg}\,et})\times(SE\overline{Ct_{t\,\mathrm{arg}\,et}})^2\right)}\right),$$

where $SE = \sqrt{\left(\frac{\sum_{i=1}^{n}(x_i-x)^2}{n\times(n-1)}\right)}$. The tissue with the lowest expression level (i.e. highest Ct value) was chosen as the control or calibrator tissue.

2.8 EMBEDDING AND CRYOSECTIONING OF FRESH TISSUE SAMPLES

One bichir and one zebrafish were immediately euthanized by immersion into an overdose concentration of MS222 (0.6 mg/ml MS222, pH = 7.0), followed by pithing prior to the embedding procedure. Specimens were dissected carefully to remove internal organs and then cut into 5 mm thick cross-sections. Fresh sections were embedded using cryomatrix embedding medium (Thermo Shandon; Fisher Scientific). A thin layer of cryomatrix was applied to the embedding mold and placed on a cold glass petri dish, which was chilled in liquid nitrogen. Tissue was positioned onto the mold and pressed lightly in order to eliminate entrapped air. Additional cryomatrix was added to provide a supporting coat for the tissue section. Lastly, the mold and the chilled glass petri dish were floated back on liquid nitrogen and the matrix was allowed to harden. Molds were stored at -80°C until ready for sectioning. 10 μm sections were obtained from the embedded specimen, utilizing a LEICA CM3050S cryostat-microtome. The chamber temperature was set at -21°C and the blade temperature was adjusted to -18°C in order to optimize the quality of sections.

2.9 SUCCINATE DEHYDROGENASE STAINING:

Sections of bichir and zebrafish were collected immediately after being produced; using superfrost®/plus microscope slides (Fisher Brand). Once sections were successfully obtained from the embedded specimen, slides were incubated at room temperature for 30 minutes in a cocktail of 10 mg NADH, 4 mL ddH_2O, 2 mL of 0.145 M saline solution, 10 mL of 2 mg/mL Nitro Blue Tetrazolium (NBT), and 2 mL phosphate buffer (for detailed composition of solutions refer to Appendix 6). Following incubation, slides were rinsed

with ddH_2O and mounted using Immu-mounting media. Stains were visualized using a Nikon Stereoscopic Zoom Microscope (SMZ1500).

2.10 *IN SITU* HYBRIDIZATION:

Tissue sections were obtained as per section 2.8 in triplicates for each gene (RyR1a, RyR1b and RyR3) and organism (bichir and zebrafish) respectively. 50 bp gene-specific oligonucleotide probes were designed based on RyR gene sequences amplified from bichir and zebrafish. Slides were stored in an RNase-free slide box and were shipped on dry ice along with the designed oligonucleotide probes. *In situ* hybridization was performed by Dr. Eileen Denovan-Wright, Department of Pharmacology at Dalhousie University.

2.10.1 PROBE PREPARATION:

Lyophilized oligonucleotide probes (Table 3) were reconstituted in sterile, RNase-free TE buffer (10 mM Tris pH=8.0, 1 mM EDTA pH=8.0) to a final concentration of 100 μM. Working solutions of probes were obtained from a 10-fold dilution of the 100 μM stock solution using RNase-free distilled water (10 μM final concentration). Both stock and the working solution of probes were stored at -20°C until use. Probes were radioactively labelled in a 25 μL reaction, consisting of 12.5 μL ddH_2O, 5 μL of 5X TdT buffer, 1.0 μL of 10 μM oligonucleotide probes, 1.5 μL TdT enzyme, and 5.0 μL ^{33}P-dATP. Reactions were incubated at 37°C for 90 minutes. Subsequent to incubation, 5 μL 0.5 M EDTA and 20 μL of ddH_2O were added to each reaction. Mixture was loaded onto a G25 spin column and centrifuged for 2 minutes at 2 800 rpm and stored at -20°C until use. In order to ensure the quality of probes, 1 μL of the labelled probes were added to the scintillation fluid. Utilizing a liquid scintillation counter, counts (cpm) were measured

(2×10^6 counts per slide or per 200 µL of hybridization buffer is indicative of a successful labelling reaction).

Table 3: Gene-specific oligonucleotide probes used for *in situ* hybridization of RyR genes in bichir (Bi) and zebrafish (ZF).

Label	Probe sequence
Bi-RyR1a	5'-ATTGATGCTGTCCATGCTGGAGGGCAACGTTGTGAATGGTACCATTGCTCGA-3'
Bi-RyR1b	5'-GAAGGTGCCTCTGGTCATCTTTAAGCGAGAGAAGGAACTGGCTCGTAAACTTGA-3'
Bi-RyR3	5'-TCCCAGGATCTCGATGCGGCCTAGGTAGGGCTCAAAGTAACTGAGGACACTTTC-3'
ZF-RyR1a	5'-CAAGCTGAAGGACATTGTTGCGTCTGACGCGTTTCGTGACTACGTGACCGACCC-3'
ZF-RyR1b	5'-GGATGGTGCGCAGGGTTTTGACACCCATGGCAATGTCCAGCAGGTGACAGGCGA-3'
ZF-RyR3	5'-GACATCAAAGGACAGTGGGATCGTTTGGTCATTGCAACTCCGTCCTTCCC-3'

2.10.2 SLIDE PREPARATION:

Once slides were thawed, tissue sections were fixed by incubating the slides in 4% paraformaldehyde for 5 minutes. Subsequent to fixation, slides were washed twice in 1X PBS for 5 minutes, and once in 2X SSC for 20 minutes. Slides were air dried for 30 minutes and rinsed with MilliQ water.

2.10.3 HYBRIDIZATION:

For each slide, hybridization buffer consisting of 50% formamide, 5X SSC, 1X Denhardt's solution, 0.02 M sodium phosphate (pH=6.8), 0.2% SDS, 5 mM EDTA, 10 µg/mL Poly(A)n and 10% (w/v) Dextran sulphate was mixed thoroughly and denatured for 10 minutes in boiling water. Subsequent to denaturation, the solution was chilled on ice for at least 10 minutes. Appropriate amount of probe (2×10^6 cpm/ 200 µL reaction) was added to the hybridization buffer solution for each reaction. 200 µL of hybridization buffer was carefully added to the slide to avoid introducing air bubbles to the buffer. Once the hybridization buffer was added to the slide, the slide was covered with a piece of parafilm and placed in a frigoseal box with the filter paper containing formamide.

Frigoseal boxes were incubated at 42°C overnight. Following incubation overnight, slides were placed into the 1X SSC in order to remove the parafilm cover from the slides and then were transferred to a 55°C hot waterbath for subsequent washes. Slides were washed four times in 1X SSC for 30 minutes at 55°C followed by four washes in 0.5X SSC for 30 minutes at 55°C. Subsequently, slides were washed twice in 0.25X SSC for 30 minutes at room temperature. Lastly, slides were placed in RNase and DNase-free water to remove residual salt from the slides and were air dried overnight at room temperature. Once air dried, slides were aligned and placed in the cassette. Slides were exposed for 2-4 weeks before images were developed.

2.11 CRESYL VIOLET STAINING:

Slides were stained following the *in situ* hybridization experiment with cresyl violet. Frozen slides were let to thaw and were hydrated by incubating the slides in 95% ethanol for 15 min, followed by 70% ethanol for 1 min, 50% ethanol for 1 min. Subsequent to the rehydration steps in ethanol, slides were incubated in distilled water for 2 min followed by an extra 1 min incubation in distilled water. After the hydration step was completed, slides were incubated in cresyl violet solution (2.0 g cresyl violet, 300 mL ddH_2O, 30 mL 1M sodium acetate, and 170 mL 1M acetic acid, pH = 3.7 – 3.9) for 5 min, and then rinsed with distilled water for 1 min. After the staining procedure was done, slides were dehydrated by a series of ethanol washes consisting of incubating slides in 50% ethanol for 1 min, 70% ethanol for 2 min, 95% ethanol for 2 min, followed by final incubation in 100% ethanol for 1 min. Following the dehydration step, slides were mounted using Immu-mounting media and visualized using a Nikon Stereoscopic Zoom Microscope (SMZ1500).

CHAPTER 3: RESULTS

3.1 PCR AMPLIFICATION AND GEL PURIFICATION:

PCR products from genomic and first-strand cDNA were amplified using RyR degenerate primer pair DGF5 and DGR4. All lanes showed amplified bands of the expected size and the negative controls were clean, which implies absence of any contaminating template (Figure 6).

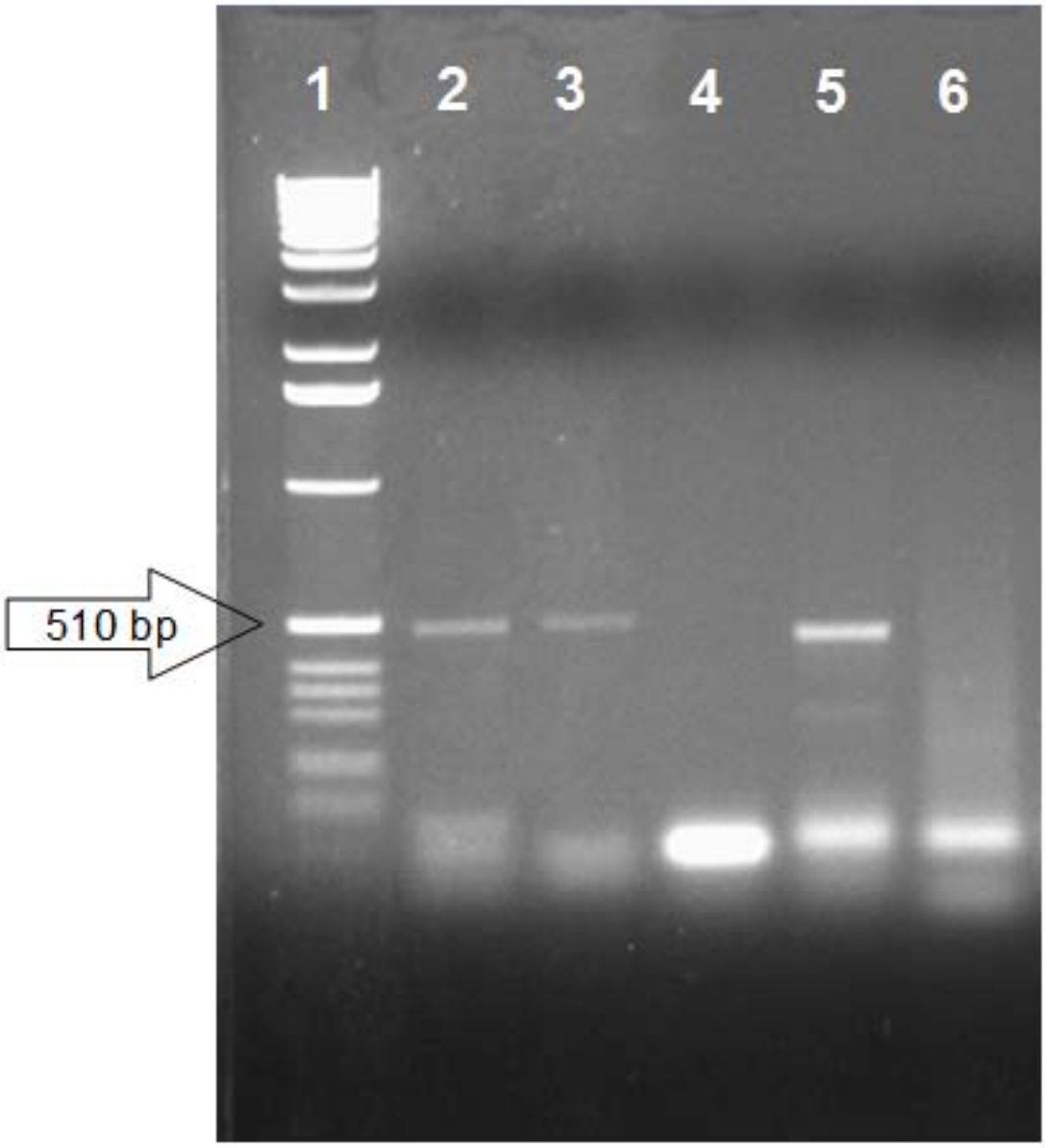

Figure 6: PCR products amplified using DGF5 and DGR4 primers on bichir genomic DNA (lane 2), bichir cDNA (lane 3), zebrafish cDNA (lane 5), and zebrafish genomic DNA (lane 6). Lane 4 is the negative control for bichir and zebrafish PCR reactions. Since negative lane for the above primer pair shows no contamination or presence of any PCR products, amplicons were identified. 1 Kbp DNA ladder is loaded on the left-hand side of the gel (lane 1; unit = bp).

3.2 DETECTION OF RECOMBINANTS

The PCR amplicons were purified from low melting-point agarose gel and cloned into pGEM®-T Easy vector. Recombinants were detected by amplifying plasmid inserts utilizing M13 forward and M13 reverse primer and using transformed colonies as template. Figure 7 shows the result of gel electrophoresis, with PCR amplicons in the expected size range present in lanes 1-8 and 10. The white color of colonies, which were used for single-colony PCR in lanes 1-8 and 10, also confirmed the presence of an insert in the vector, which indicates a successful recombination and subsequent transformation.

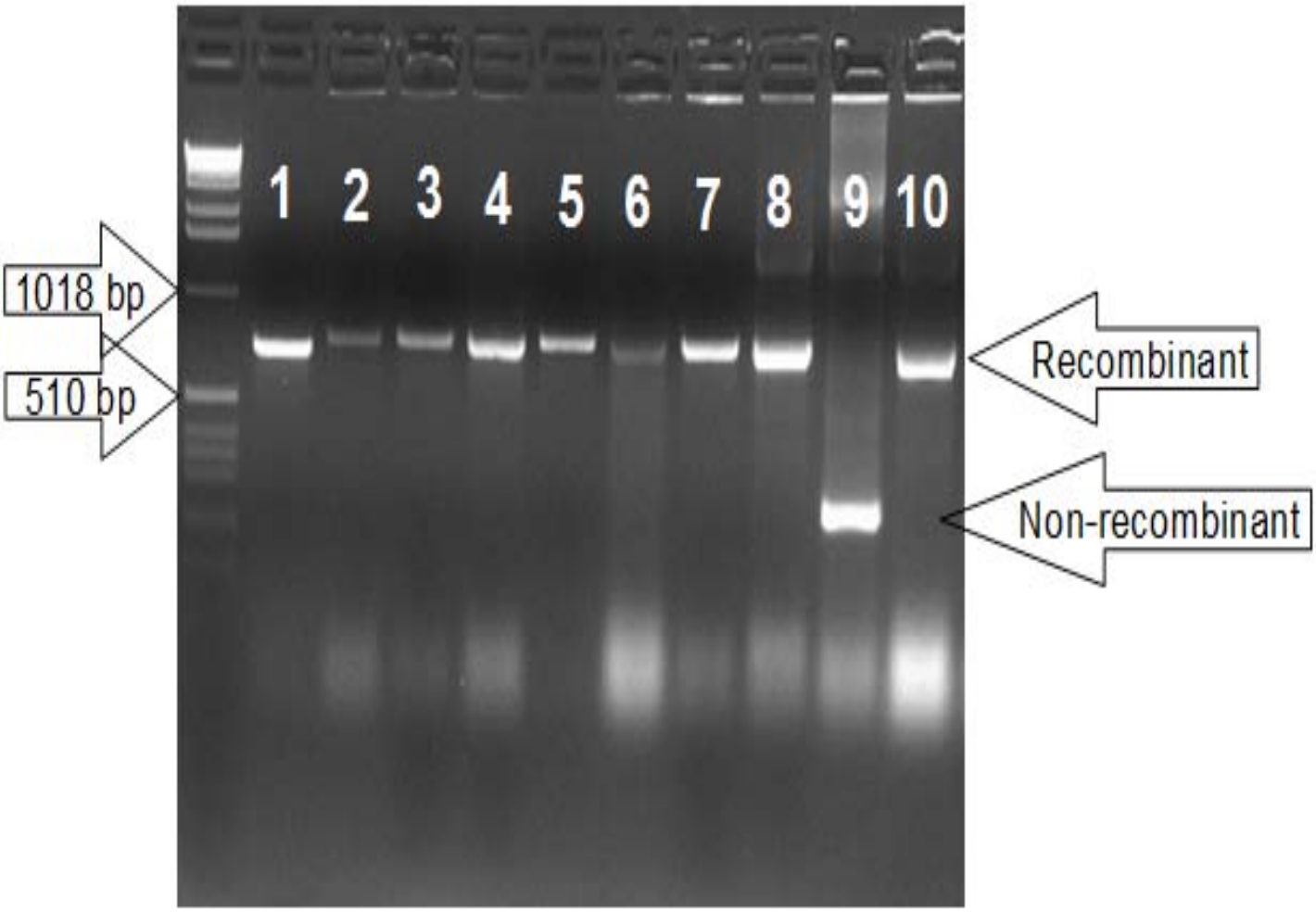

Figure 7: Gel electrophoresis showing the PCR detection of recombinants from *E. coli* JM109 colonies utilizing M13 forward and M13 reverse primers. Lanes 1-8 and 10 show the expected size of the insert of amplified RyR gene sequence. 1 Kbp ladder is located on the left hand-side of the image (unit = bp).

3.3 SEQUENCING AND PHYLOGENETIC ANALYSIS

The degenerate primer pair, DGF5 and DGR4, designed to anneal to conserved sequence blocks in all RyR gene sequences, was used to survey the genomic DNA of the primitive ray-finned fish, bichir (*P. ornatipinnis)*. 134 genomic cloned sequences were obtained from this region (using the same primer pair). All 134 cloned sequences shared sequence identity with published RyR sequences based on BLASTx analysis. BLASTx searches of GenBank databases tentatively identified the sequences as orthologs of the RyR1a, RyR1b, RyR2 and RyR3 genes (Figure 8). A multiple sequence alignment of the bichir consensus sequences and orthologous RyR sequences from selected vertebrate species (human, mouse, frog, zebrafish) was generated (Figure 9) and used to construct a neighbour-joining phylogenetic tree (Figure 10).

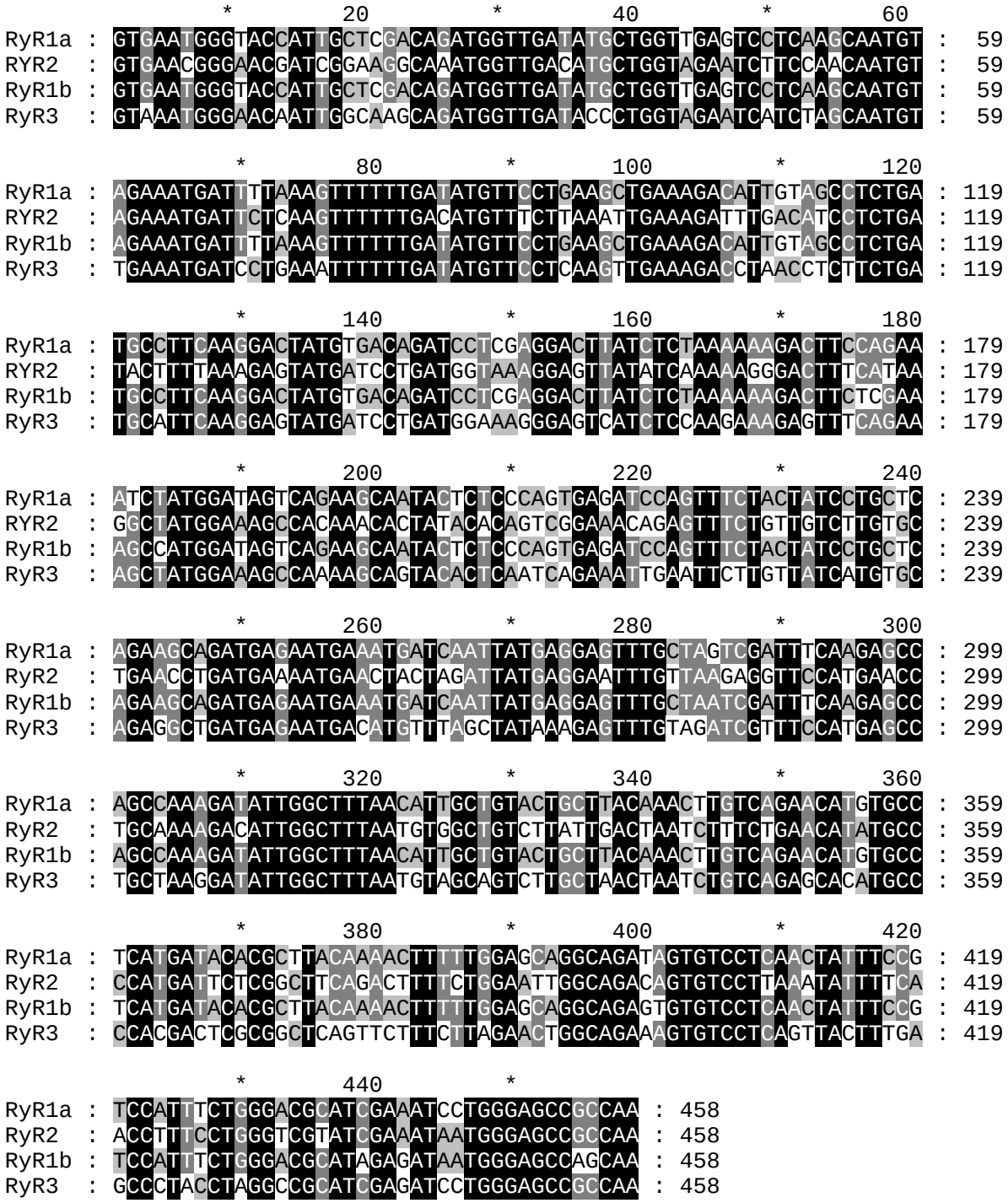

Figure 8: Alignment of bichir consensus nucleotide sequences based on genomic survey using degenerate PCR. Identical nucleotides are presented in black and less conserved nucleotides are in shades of grey.

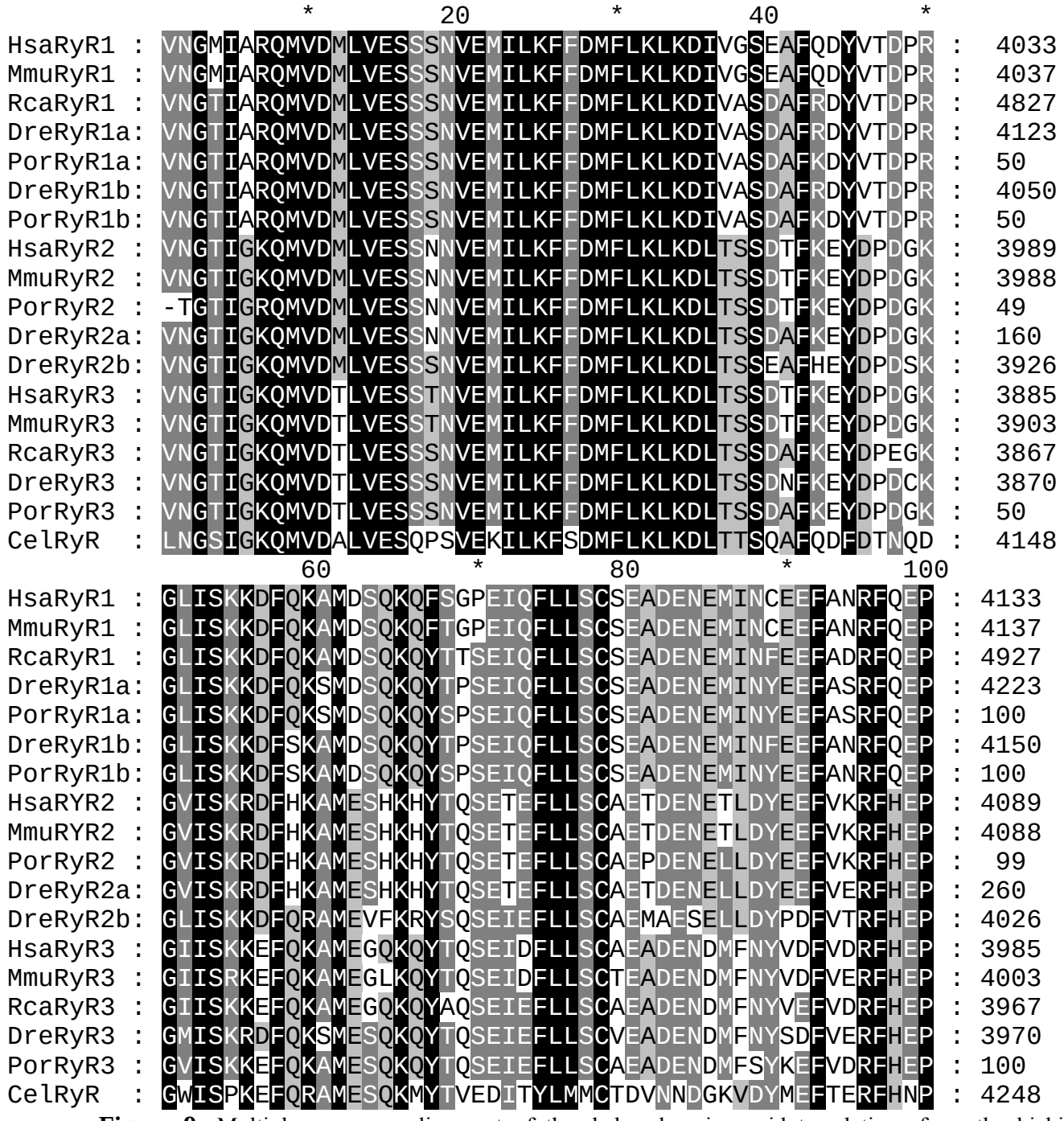

Figure 9: Multiple sequence alignment of the deduced amino acid translations from the bichir consensus partial RyR sequences with GenBank accession number presented in braket (PorRyR1a (FJ976726), PorRyR1b (FJ976727), PorRyR2 (FJ976728), and PorRyR3 (FJ976725)) are aligned with the orthologous RyR sequences of human (HsaRyR1 (NM_001042723), HsaRyR2 (NP_001026), HsaRyR3 (NM_001306)), mouse (MmuRyR1 (NM_009109), MmuRyR2 (NM_023868), MmuRyR3 (NM_177652)), bullfrog (RcaRyR1 (D21070), RcaRyR3 (D21071)), zebrafish (DreRyR1a (XM_001923259), DreRyR1b (NM_001102571), DreRyR2a (XM_001922082), DreRyR2b (XM_001921102), DreRyR3 (XM_001922078)), and the nematode *C. elegans* (CelRyR (BAA08309)). The alignment is shaded to highlight conserved amino acids. Positions of amino acid sequences are given at the right-hand-side of the figure.

```
                    *       120         *       140         *
HsaRyR1 : ARDIGFNVAVLLTNLSEHVPHDPRLHNFLELAESILEYFRPYLGRIEIMG : 4183
MmuRyR1 : ARDIGFNVAVLLTNLSEHVPHDPRLRNFLELAESILEYFRPYLGRIEIMG : 4187
RcaRyR1 : AKDIGFNVAVLLTNLSEHVPHDTRLHNFLELADCIINYFKPYLGKIEIMG : 4977
DreRyR1a: AKDIGFNIAVLLTNLSEHVPHDTRLQNFLEQAESVLNYFRPFLGRIEIMG : 4273
PorRyR1a: AKDIGFNIAVLLTNLSEHVPHDTRLQNFLEQADSVLNYFRPFLGRIEILG : 150
DreRyR1b: AKDIGFNIAVLLTNLSEHVPHDTRLQNFLEQAESVLNYFRPFLGRIEIMG : 4200
PorRyR1b: AKDIGFNIAVLLTNLSEHVPHDTRLQNFLEQAECVLNYFRPFLGRIEIMG : 150
HsaRyR2 : AKDIGFNVAVLLTNLSEHMPNDTRLQTFLELAESVLNYFQPFLGRIEIMG : 4139
MmuRyR2 : AKDIGFNVAVLLTNLSEHMPNDTRLQTFLELAESVLNYFQPFLGRIEIMG : 4138
PorRyR2 : AKDIGFNVAVLLTNLSEHMPHDSRLQTFLELADSVLKYFQPFLGRIEIMG : 149
DreRyR2a: AKDIGFNVAVLLTNLSEHMPHDSRLQTFLELAESVLNYFQPYLGRIEIMG : 310
DreRyR2b: AKEIGFNMAVLLTNLSEHMPNDARLQNFLELADSVLKYFHPHLGRIEILG : 4076
HsaRyR3 : AKDIGFNVAVLLTNLSEHMPNDSRLKCLLDPAESVLNYFEPYLGRIEIMG : 4035
MmuRyR3 : AKDIGFNVAVLLTNLSEHMPNDSRLKSLLDPAESVLNYFEPYLGRIEIMG : 4053
RcaRyR3 : AKDIGFNVAVLLTNLSEHMPNDSRLQCLLDPANSVLNYFSPYLGRIEIMG : 4017
DreRyR3 : AKDIGFNVAVLLTNLSEHMPHDSRLSTFLDLAESVLSYFEPYLGRIEIMG : 4020
PorRyR3 : AKDIGFNVAVLLTNLSEHMPHDSRLSSFLELAESVLSYFEPYLGRIEILG : 150
CelRyR  : ARDIGFNLAVLLVNLKEHITNDPRLEKIIEKAQTLLEYFDPFLGRIEIMG : 4298

HsaRyR1 : ASR : 4186
MmuRyR1 : ASR : 4190
RcaRyR1 : AGK : 4980
DreRyR1a: ASR : 4276
PorRyR1a: AA- : 152
DreRyR1b: ASK : 4203
PorRyR1b: ASK : 153
HsaRYR2 : SAK : 4142
MmuRYR2 : SAK : 4141
PorRyR2 : AAK : 152
DreRyR2a: SAK : 313
DreRyR2b: SGK : 4079
HsaRYR3 : GAK : 4038
MmuRYR3 : GAK : 4056
RcaRYR3 : GAK : 4020
DreRyR3 : GAK : 4023
PorRyR3 : AAK : 153
CelRyR  : SSK : 4301
```

Figure 9: Continued.

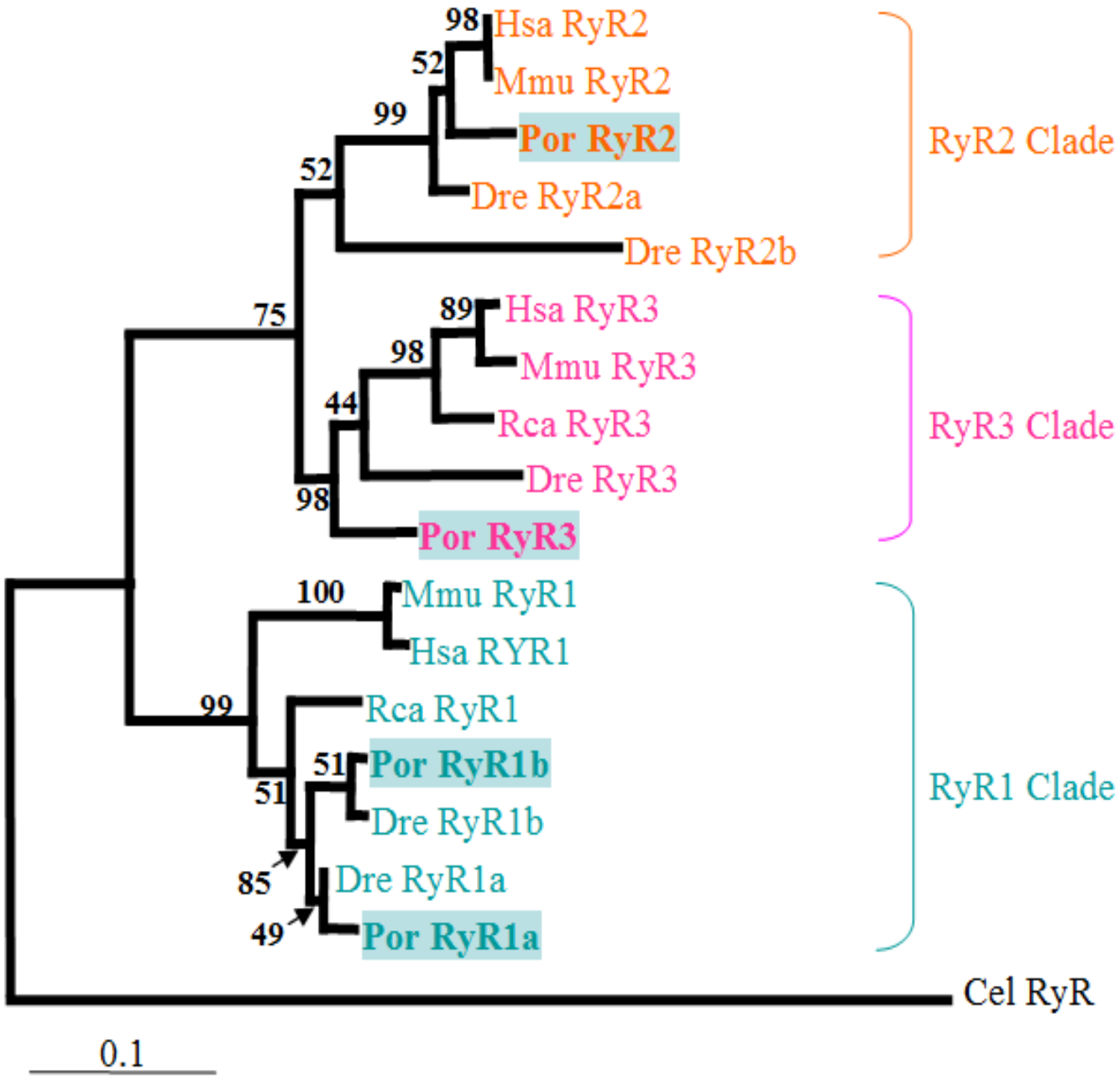

Figure 10: Bootstrapped neighbor-joining tree based on Dayhoff PAM distance matrix (Dayhoff *et al*., 1972). The multiple sequence alignment in Figure 9 was used to generate the phylogenetic tree. The consensus tree is based on the output of 100 bootstrap pseudoreplicates from the Neighbor program of PHYLIP (Felsenstein, 1993). The *C. elegans* RyR sequence was used as a designated outgroup and bootstrap values are given on the major nodes of the tree.

3.4 Expression Levels of RyR Genes in Bichir and Zebrafish

The relative expression levels for the four bichir and five zebrafish RyR genes were determined by qRT-PCR in four tissue sources: slow twitch skeletal muscle, fast twitch skeletal muscle, cardiac and brain tissues. In all tissues the expression levels were assayed relative to the expression of two housekeeping genes, actin (Appendix 4) and elongation factor 1α (ef1α [Appendix 5]; Figure 11). In zebrafish, the expression ratio measured relative to the actin housekeeping gene of RyR3 to RyR1a and RyR1b was 0.77 for both slow twitch (red) and fast twitch (white) muscle respectively (Table 4) while the RyR3 to RyR1a and RyR1b expression ratio for bichir slow twitch and fast twitch muscle was 0.16 and 0.18 respectively. These values are consistent with the ratios calculated relative to the ef1α housekeeping gene with a ratio of RyR3 to RyR1a and RyR1b expression of 0.75 and 0.64 in zebrafish slow twitch and fast twitch muscle respectively and 0.27 and 0.18 for the same comparison in bichir. A two-tailed t-test indicated that the RyR3 to RyR1 expression ratios are significantly different between bichir and zebrafish (Table 5).

Table 4: Relative expression levels[a] ± SE of RyR multigene family in selected tissues of bichir (*P. ornatipinnis*) and zebrafish (*D. rerio*).

		Relative to actin expression (±SE)		Relative to ef1α expression (±SE)	
		P. ornatipinnis	*D. rerio*	*P. ornatipinnis*	*D. rerio*
Red Skeletal Muscle	RyR1a	1.106 ± 0.3756	1.444 ± 0.0641	1.231 ± 0.2432	1.181 ± 0.0183
	RyR1b	0.171± 0.0576	0.553 ± 0.0234	0.322 ± 0.0503	0.323 ± 0.0071
	RyR2a	0.034 ± 0.0140	0.230 ± 0.0102	0.023 ± 0.0045	0.312 ± 0.0048
	RyR2b	N/A[b]	0.276 ± 0.0107	N/A[b]	0.425 ± 0.0107
	RyR3	0.176 ± 0.0752	1.106 ± 0.0428	0.331 ± 0.1013	0.886 ± 0.0223
White Skeletal Muscle	RyR1a	0.085 ± 0.0138	0.702 ± 0.943	0.085 ± 0.0205	0.644 ± 0.0290
	RyR1b	1.699 ± 0.1605	2.378 ± 0.1075	1.699 ± 0.0719	1.510 ± 0.0112
	RyR2a	0.052 ± 0.0252	0.597 ± 0.0281	0.052 ± 0.0182	0.293 ± 0.0081
	RyR2b	N/A[b]	0.603 ± 0.0238	N/A[b]	0.449 ± 0.0265
	RyR3	0.307 ± 0.1018	1.847 ± 0.1042	0.307 ± 0.0854	0.973 ± 0.0405
Cardiac Muscle	RyR1a	0.483 ± 0.1895	0.422 ± 0.0203	0.472 ± 0.2141	0.444 ± 0.0222
	RyR1b	0.453 ± 0.1644	0.485 ± 0.0122	0.370 ± 0.1536	0.986 ± 0.0387
	RyR2a	2.024 ± 0.1855	1.659 ± 0.0406	2.372 ± 0.1340	1.784 ± 0.0657
	RyR2b	N/A[b]	1.932 ± 0.0576	N/A[b]	1.986 ± 0.0779
	RyR3	0.182 ± 0.0405	0.062 ± 0.0028	0.236 ± 0.0952	0.067 ± 0.0019
Brain Tissue	RyR1a	0.524 ± 0.1526	0.431 ± 0.1380	0.468 ± 0.0935	0.432 ± 0.0134
	RyR1b	0.561 ± 0.2369	0.590 ± 0.1871	0.454 ± 0.1011	0.481 ± 0.1819
	RyR2a	0.594 ± 0.1040	0.354 ± 0.0140	0.538 ± 0.0973	0.485 ± 0.0084
	RyR2b	N/A[b]	0.475 ± 0.0274	N/A[b]	0.476 ± 0.1883
	RyR3	2.124 ± 0.1540	2.412 ± 0.4493	1.999 ± 0.2063	2.181 ± 0.1320

[a]The expression levels were determined by qRT-PCR using gene-specific primers (Table 1) and are relative to the expression of the housekeeping genes, actin and elongation factor 1-alpha (ef1α). Standard error (SE) values were determined from triplicate runs of the qRT-PCR assay.
[b] The RyR2b gene was not found in the bichir genome.

Table 5: Two-tailed t-test examining the significance of co-expression differences of RyR3:RyR1a and RyR3:RyR1b between zebrafish (*D. rerio*) and bichir (*P. ornatipinnis*) (α=0.05).

		P. ornatipinnis	*D. rerio*	Z-value[a]	Confidence Interval
Actin HKG	RyR3:RyR1a ratio	0.16	0.77	-1.83286341	**(0.133, 1.037)**
	RyR3:RyR1b ratio	0.18	0.77	-1.89308697	**(0.288, 0.892)**
ef1α HKG	RyR3:RyR1a ratio	0.27	0.75	1.58875289	**(0.238, 0.792)**
	RyR3:RyR1b ratio	0.18	0.64	0.87415821	**(0.156, 0.652)**

[a] A Z value falling between −1.96 and +1.96 indicates significance at the 0.05 level.

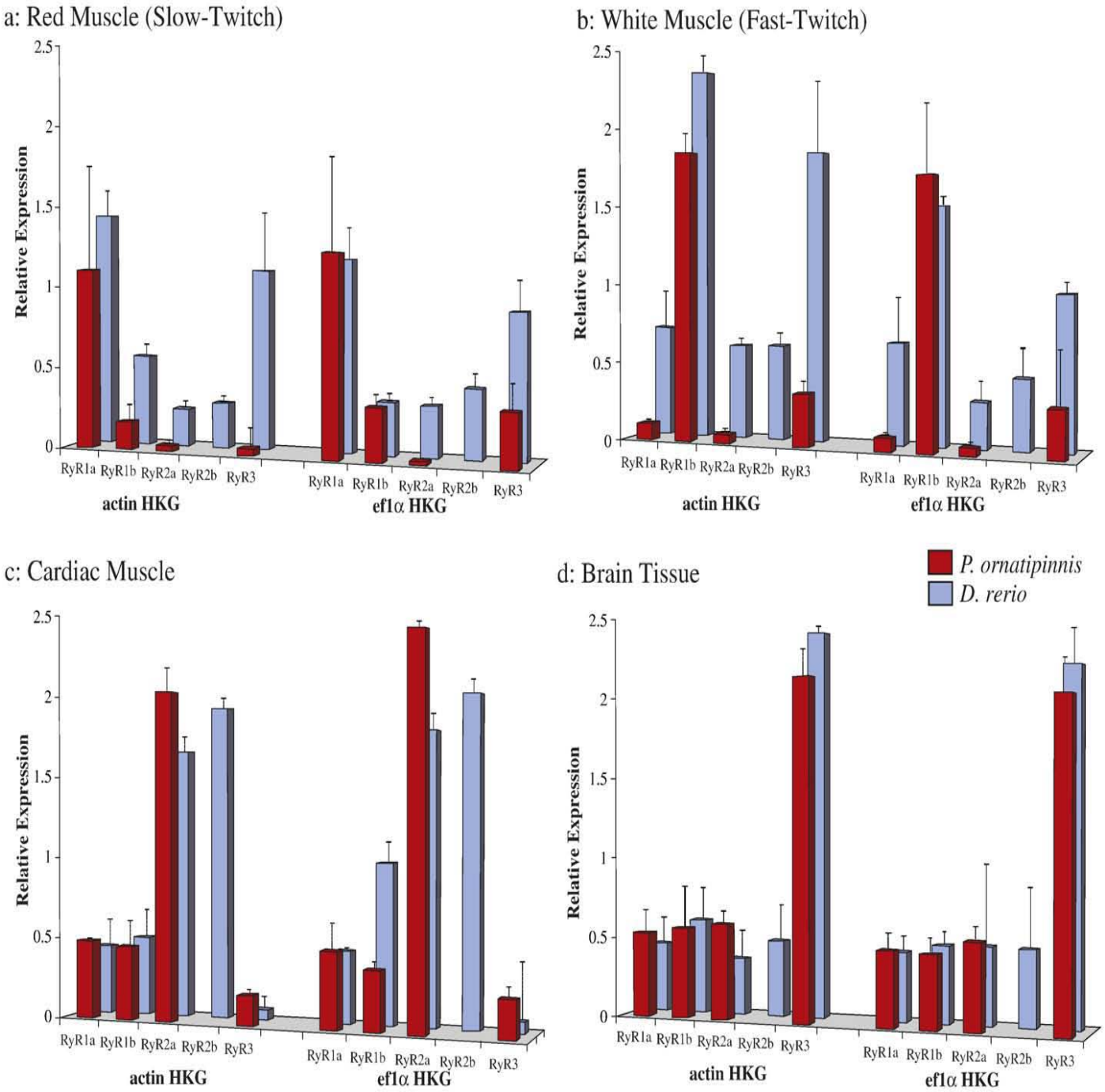

Figure 11: Relative expression levels of RyR genes in (a) red muscle (slow twitch), (b) white muscle (fast twitch), (c) cardiac and (d) brain tissue samples of bichir (*P. ornatipinnis*; red) and zebrafish (*D. rerio*, blue). The gene expression levels are quantified by qRT-PCR relative to the expression of the housekeeping genes actin (actin HKG) and elongation factor 1-alpha (ef1α). Error bars are standard error of the mean of three biological replicates for each fish species.

3.5 SUCCINATE DEHYDROGENASE STAINING

10 μm transverse sections of bichir and zebrafish were obtained utilizing a LEICA CM3050S cryostat-microtome (Figure 12a, 12c). Following staining, slides were viewed under a Nikon Stereoscopic Zoom Microscope (SMZ1500; Figure 12b, 12d). The SDH histological method darkly stained the red muscle fibers in both zebrafish and bichir. The disposition of the red muscle in the two species is different. In zebrafish, the red muscle forms a triangular wedge that does not penetrate to the center of the fish (Figure 12d) while in bichir the red muscle tissue starts as a triangular wedge and then tapers to a narrow band of tissue that extends to the center of the body (Figure 12b).

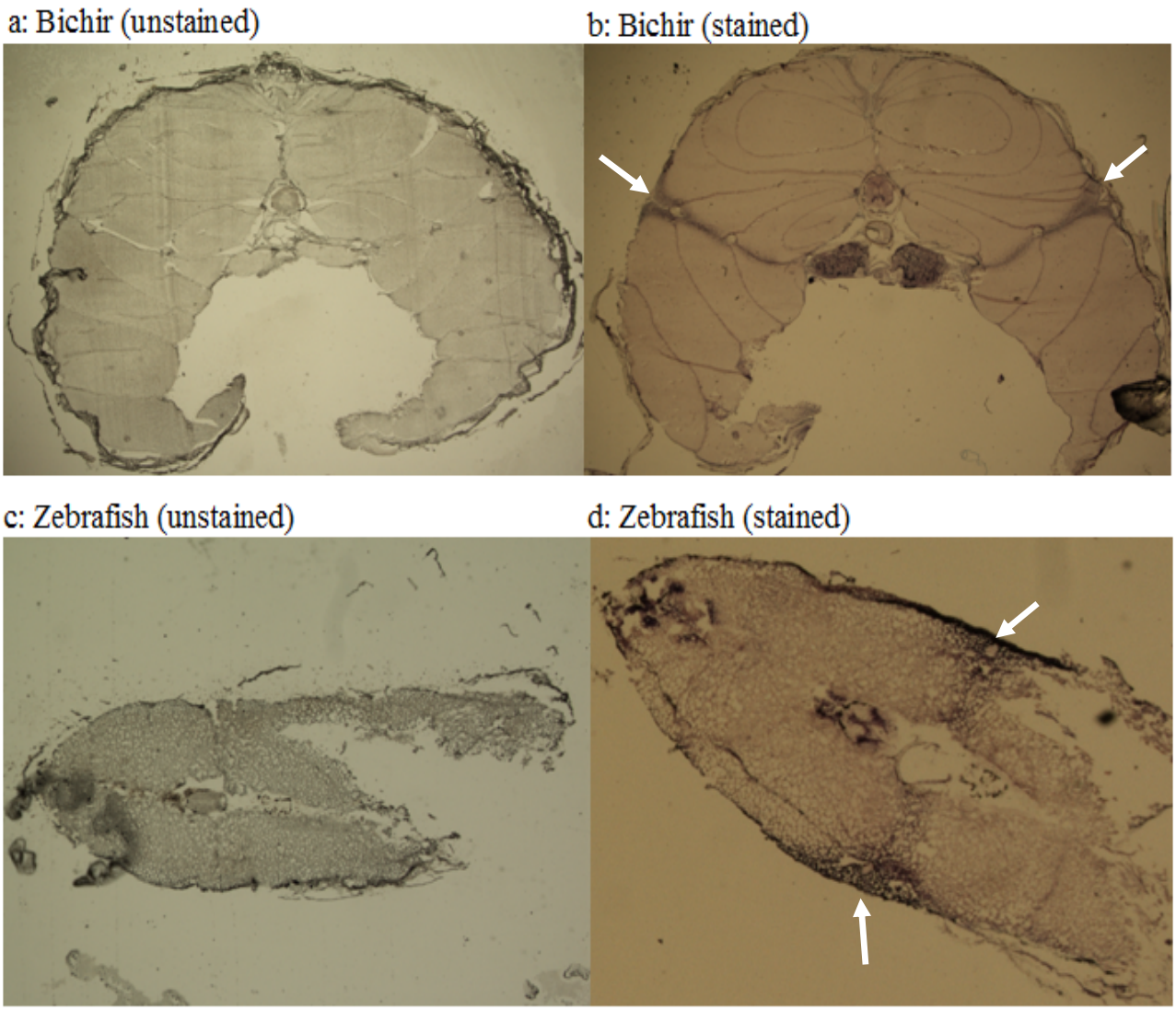

Figure 12: Cross-sections obtained from fresh embedded specimen. (a) bichir and (c) zebrafish prior to SDH staining. (b) bichir and (d) zebrafish after SDH staining. White arrows point at the red skeletal muscles in the transverse sections of bichir and zebrafish. In this staining method (SDH staining) red muscle fibers are stained dark, which determines the position, quality and quantity of red muscle fibers in bichir and zebrafish.

3.6 CRESYL VIOLET STAINING (CVS):

From SDH staining, 10 μm cross-sections of bichir and zebrafish were obtained utilizing a LEICA CM3050S cryostat-microtome (Figure 13a, 13c). Subsequent to staining, slides were viewed under a Nikon Stereoscopic Zoom Microscope (SMZ1500; Figure 13b, 13d). The cresyl violet staining provides a much greater contrast as for the disposition of different muscle fiber types in the transverse sections of bichir and zebrafish (Figure 13b and d).

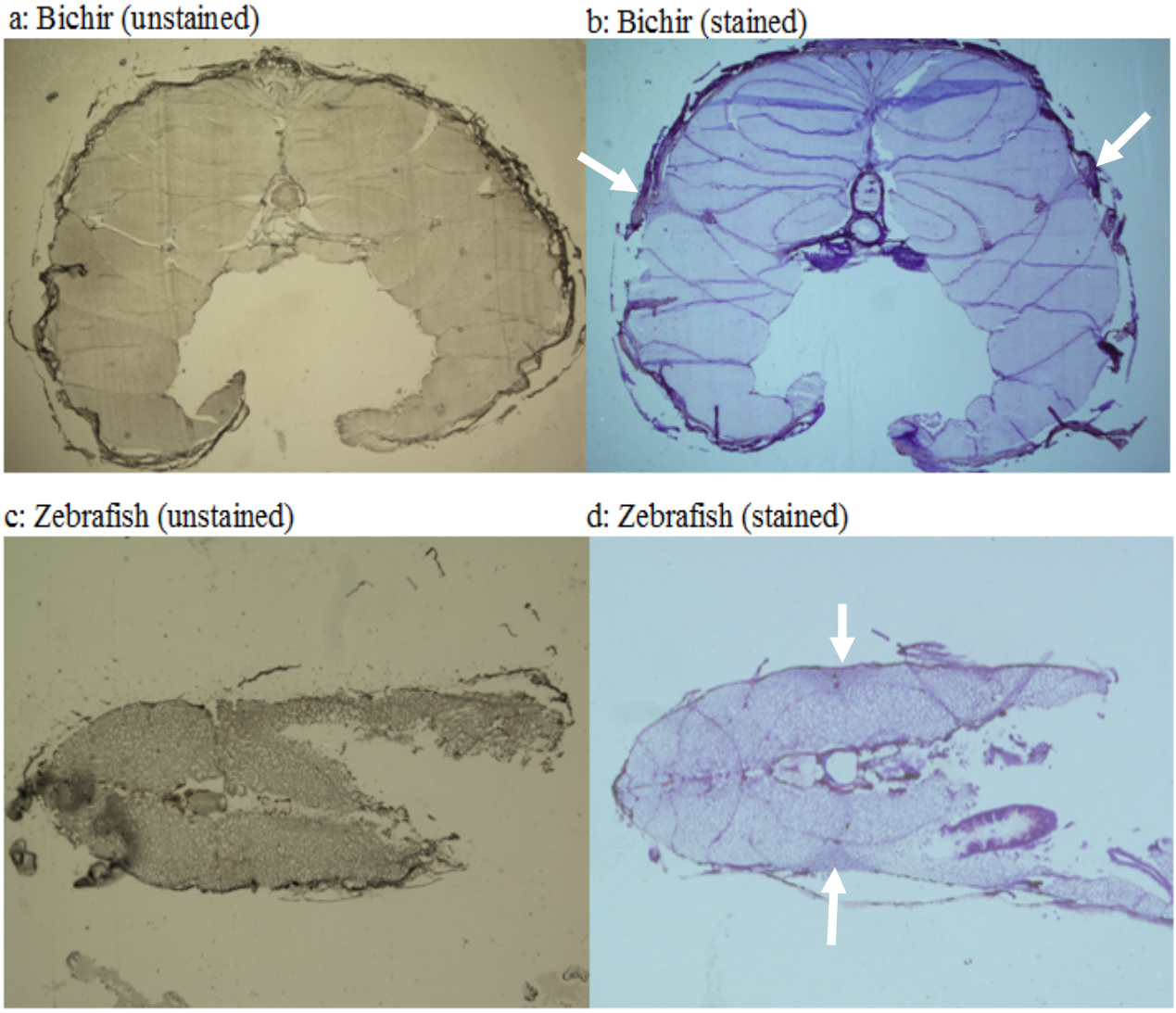

Figure 13: Cross-sections obtained from fresh embedded specimen. (a) bichir and (c) zebrafish prior to CVS staining. (b) bichir and (d) zebrafish after CVS staining. Cresyl Violet staining provides a greater contrast as for the disposition of different muscle fiber arrangement in the transverse sections of bichir and zebrafish. White arrows point at the position/location of the red skeletal muscles in bichir and zebrafish.

3.7 *IN SITU* HYBRIDIZATION (ISH):

The spatial expression levels for bichir RyR1a, RyR1b, RyR3 (Figure 14) and zebrafish RyR1a, RyR1b and RyR3 genes (Figure 15) were determined by *in situ* hybridization of ^{33}P radioactively-labelled probes to thin sections of brain, heart, and skeletal muscle of bichir. For zebrafish, the anterior half of the body including the head (brain) and thorax (heart) were embedded and sagittal sections were obtained for *in situ* hybridization. Also, transverse sections through the body were used for differentiation of spatial expression of fast and slow twitch muscle fibers. As depicted in Figure 14a and 15a RyR1a probes hybridized to the red muscle fibers of bichir and zebrafish respectively. Accordingly, RyR1b probes hybridized to the white muscle fibers of bichir and zebrafish (Figure 14b and 15b). RyR3 probes hybridized predominantly to the brain sections of both bichir and zebrafish (Figure 14i and 15i). RyR1a, RyR1b show subtle expression in cardiac muscle of bichir (Figure 14d-14f), whereas in zebrafish, in addition to RyR1a and RyR1b, RyR3 is also expressed in cardiac muscle (Figure 15d-15f). Quantitative analyses of *in situ* images were performed by utilizing ImageJ software (Figure 16), in which the mean numbers of pixels were used as a measure of signal intensity. For zebrafish the expression ratio of RyR3 to RyR1a and RyR1b is 0.84 and 0.97 for slow twitch and fast twitch muscle respectively (Table 6), while the expression ratio of RyR3 to RyR1a and RyR1b for bichir slow twitch and fast twitch muscle is 0.17 and 0.21 respectively.

In comparison, Figure 17 and 18 depict the expression pattern of *in situ* hybridization results with the histological staining (SDH and CVS) from bichir and zebrafish respectively. According to Figure 17b and 17c, bichir RyR1a probes have not

hybridized to the red muscle fibers present deep in the core of the muscle section. However, expression of RyR1a in zebrafish is consistent with the data obtained from SDH staining, regarding the disposition of red muscle fibers and location of probes hybridized to the red muscle fibers (Figure 18b and 18c). Expression of RyR1b is consistent between histological staining and *in situ* hybridization for both bichir (Figure 17e and 17f) and zebrafish (Figure 18e and 18f). Histological staining shows a distinct staining pattern in brain of bichir and zebrafish which coincides with the expression pattern of RyR3 probes to the brain sections (Figure 17g-17i and 18g-18i).

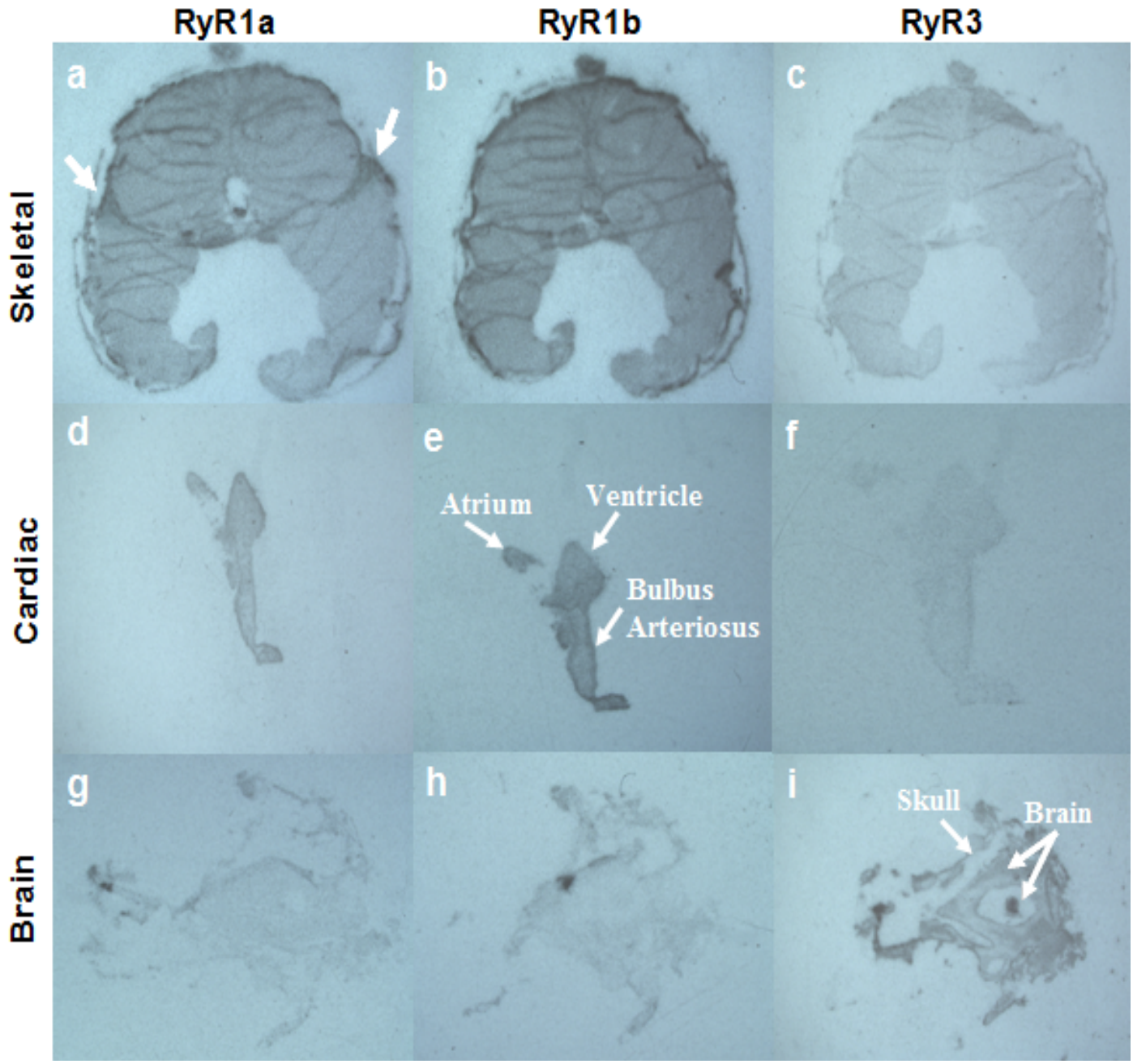

Figure 14: *In situ* hybridization of radioactively labelled probes to the transverse sections of bichir (*Polypterus ornatipinnis*). Images were taken under 300X magnification utilizing a Nikon Stereoscopic Zoom Microscope (SMZ1500). (a) White arrows point at the spatial expression of slow-twitch muscle fibers in bichir. (b) Expression of RyR1b in fast-twitch muscle fibers. (c) Lack of expression of RyR3 in bichir skeletal muscle. (d,e,f) Expression of RyR genes present in cardiac muscle fibers. (g) RyR1a and (h) RyR1b do not show any expression level in brain; however, the RyR3 gene (i) is highly expressed in the brain transverse sections of bichir.

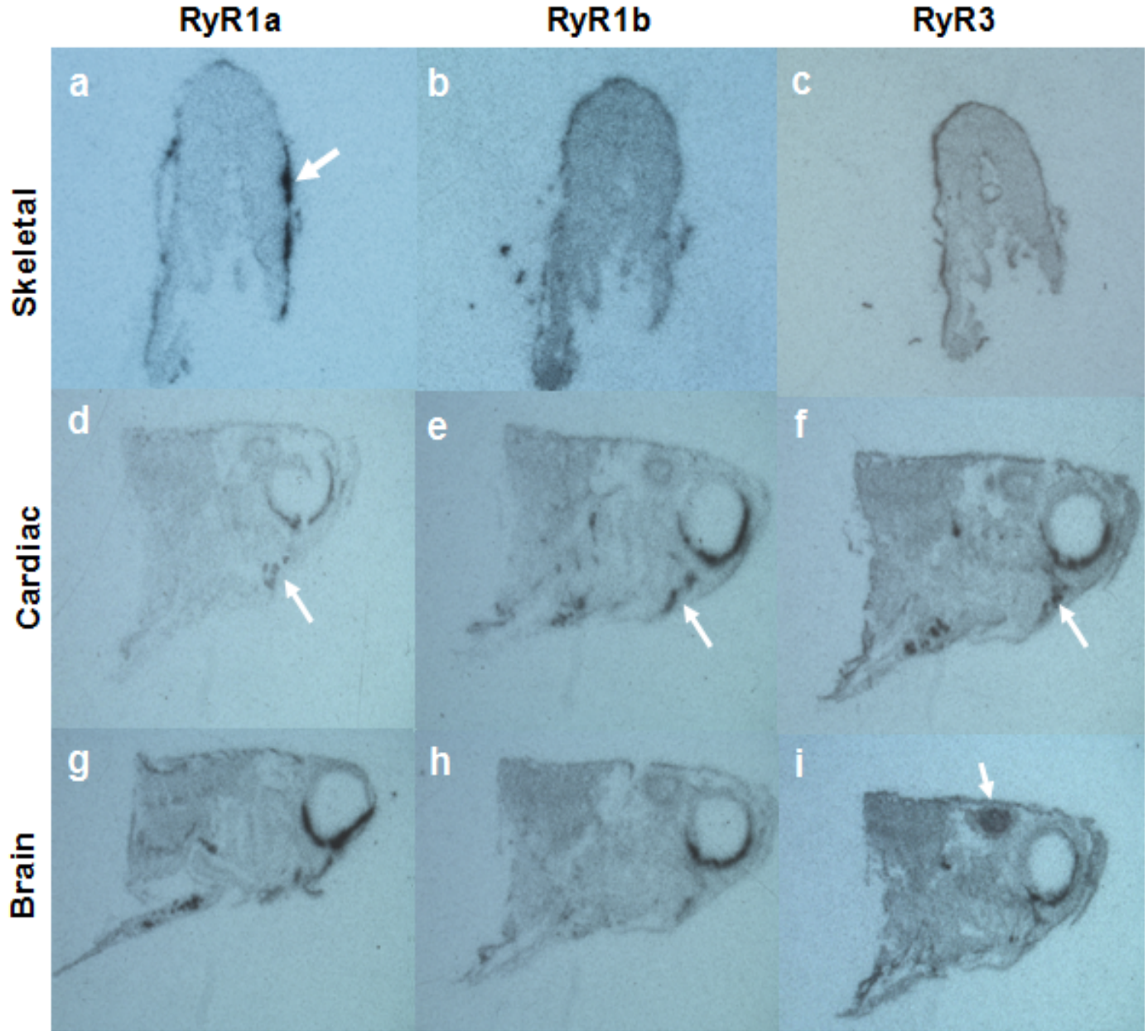

Figure 15: *In situ* hybridization of radioactively labelled probes to transverse sections of zebrafish (*Danio rerio*). Images were taken under 300X magnification utilizing a Nikon Stereoscopic Zoom Microscope (SMZ1500). (a) White arrows point at the spatial expression of slow-twitch muscle fibers in zebrafish cross section. (b) Expression of RyR1b in fast-twitch muscle fibers. (c) Presence of expression of RyR3 in zebrafish skeletal muscle confirms equal co-expression of RyR1 and RyR3 in fish skeletal muscles. (d,e,f) Expression of RyR genes present in cardiac muscle fibers. (g) RyR1a and (h) RyR1b do not show any expression level in brain; however, RyR3 gene (i) is highly expressed in the brain transverse sections of zebrafish.

Table 6: Quantification of *in situ* hybridization signal intensity in transverse sections of selected tissues of bichir (*P. ornatipinnis*) and zebrafish (*D. rerio*).

	Mean Number of Pixels ± SE	
	P. ornatipinnis	*D. rerio*
RyR1a	122.13 ± 17.71	128.65 ± 13.07
RyR1b	101.18 ± 17.28	110.04 ± 6.91
RyR3 (brain)	136.04 ± 22.11	143.14 ± 16.35
RyR3 (skeletal muscle)	21.19 ± 13.78	107.66 ± 9.05

[a]The spatial expression levels were determined by *in situ* hybridization of ^{33}P radioactively labelled oligonucleotide probes onto cross sections, through brain and skeletal muscles of fish. Mean values and standard error were calculated based on the analysis of three slides for each probe.

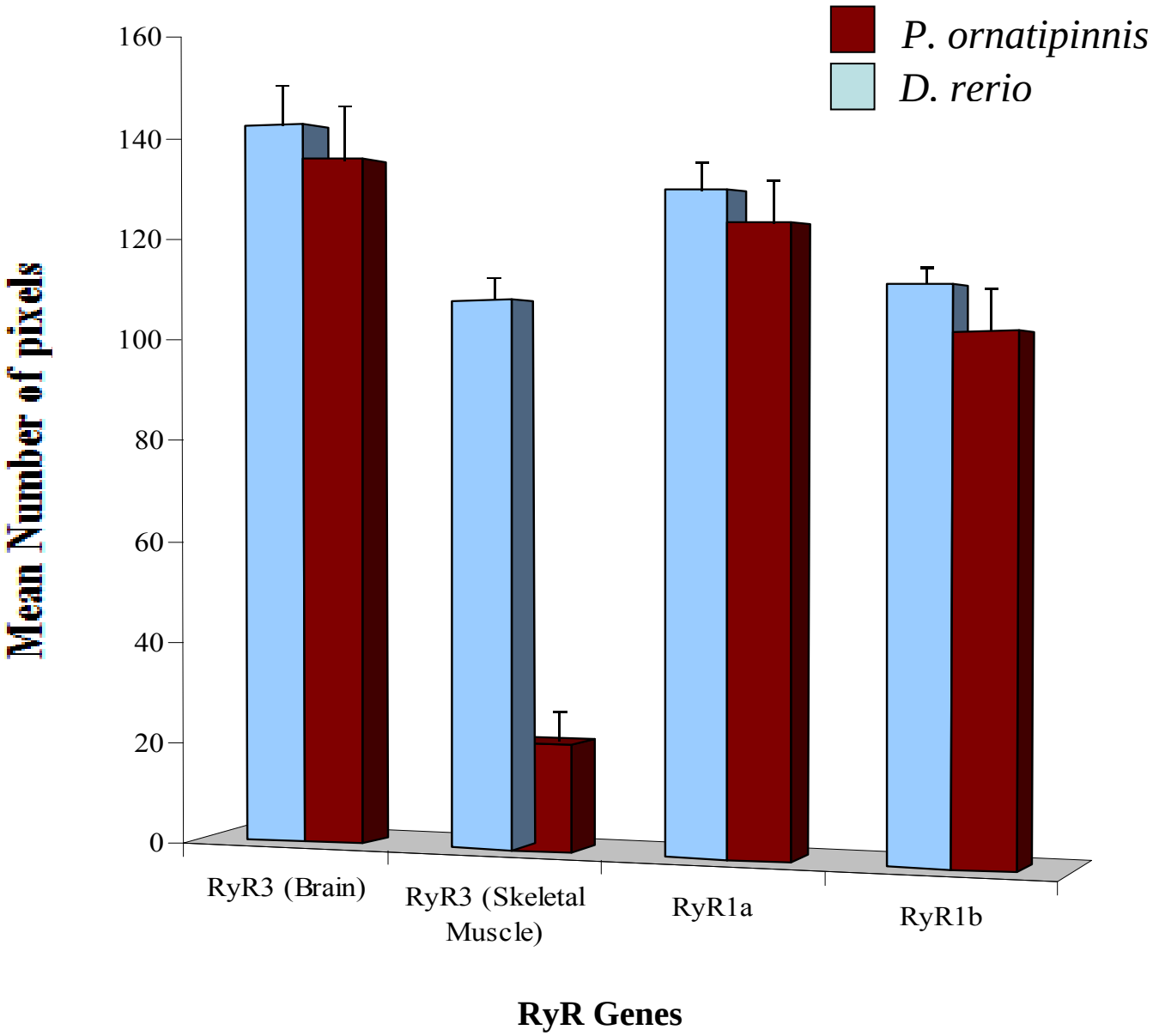

Figure 16: Quantification of *in situ* hybridization signals in bichir (*P. ornatipinnis*; red) and zebrafish (*D. rerio*; blue). The signal intensity was quantified using ImageJ software, via applying a grey scale in order to remove the background noise. Mean number of pixels was utilized as a measure to quantify the signal intensity of *in situ* hybridization. Error bars are standard error of the mean of 3 experimental replicates for each hybridized probe.

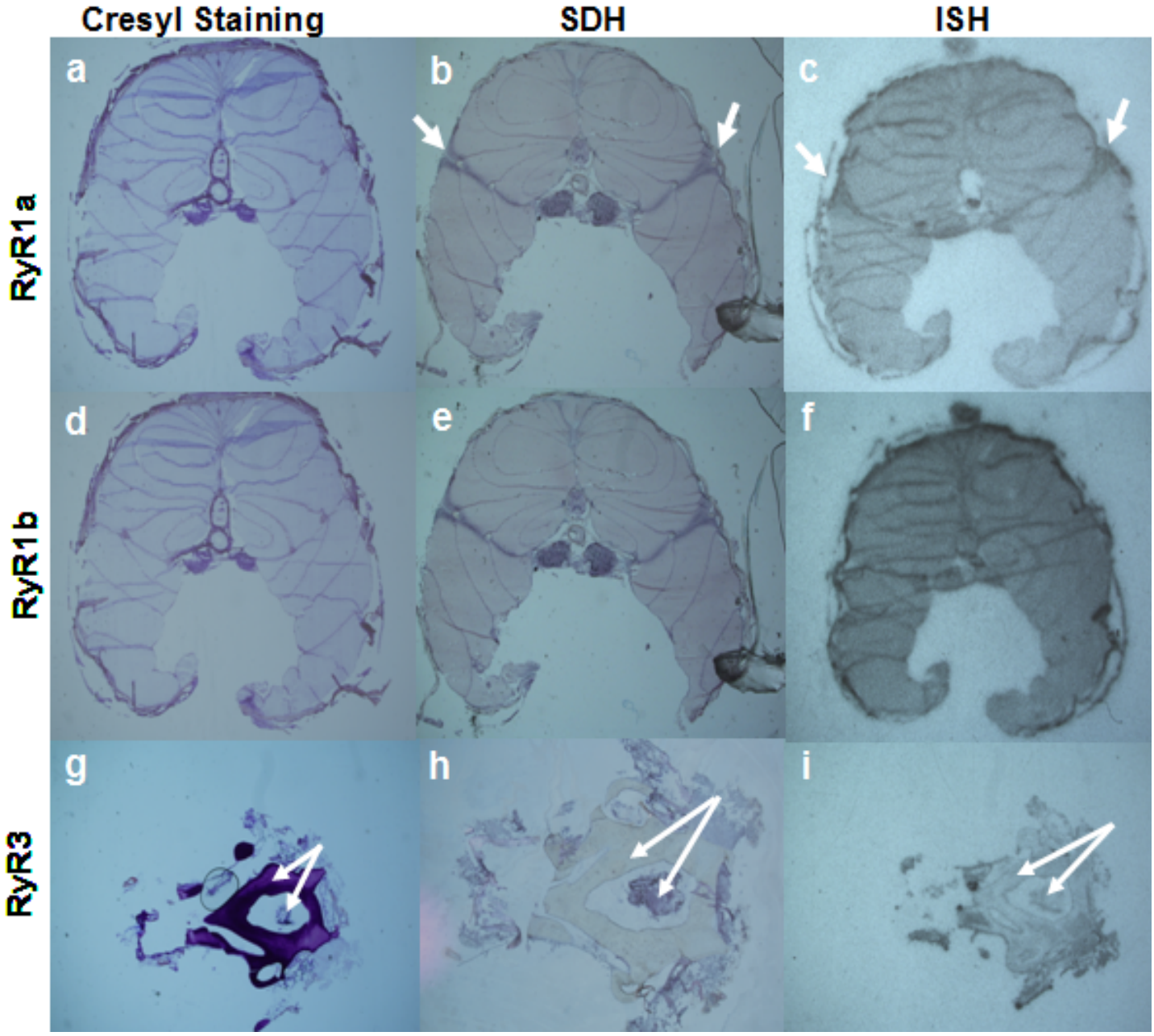

Figure 17: Comparison of bichir (*P. ornatipinnis*) *in situ* hybridization (ISH) expression pattern with the histological staining (Cresyl Violet (CVS) and Succinate Dehydrogenase (SDH) staining) performed on the transverse sections. (a,d) CVS of bichir section provided a greater contrast as per disposition of different muscle fibers. (b) SDH staining confirms presence of slow twitch (red) muscle fibers in bichir. (c)Expression pattern of RyR1a in slow twitch muscle fibers of bichir (white arrows) (e) SDH does not stain white muscle, thus is appears in a lighter shade. (f) Expression pattern of RyR1b in fast twitch muscle fibers of bichir (dark area) (g) CVS stains nissl substance present in the endoplasmic reticulum of cell bodies of neural tissue dark purple (white arrows) (h) SDH stained mitochondria present in the cell body of brain tissue (white arrows) (i) RyR3 probes have hybridized to the brain transverse section of bichir (white arrows).

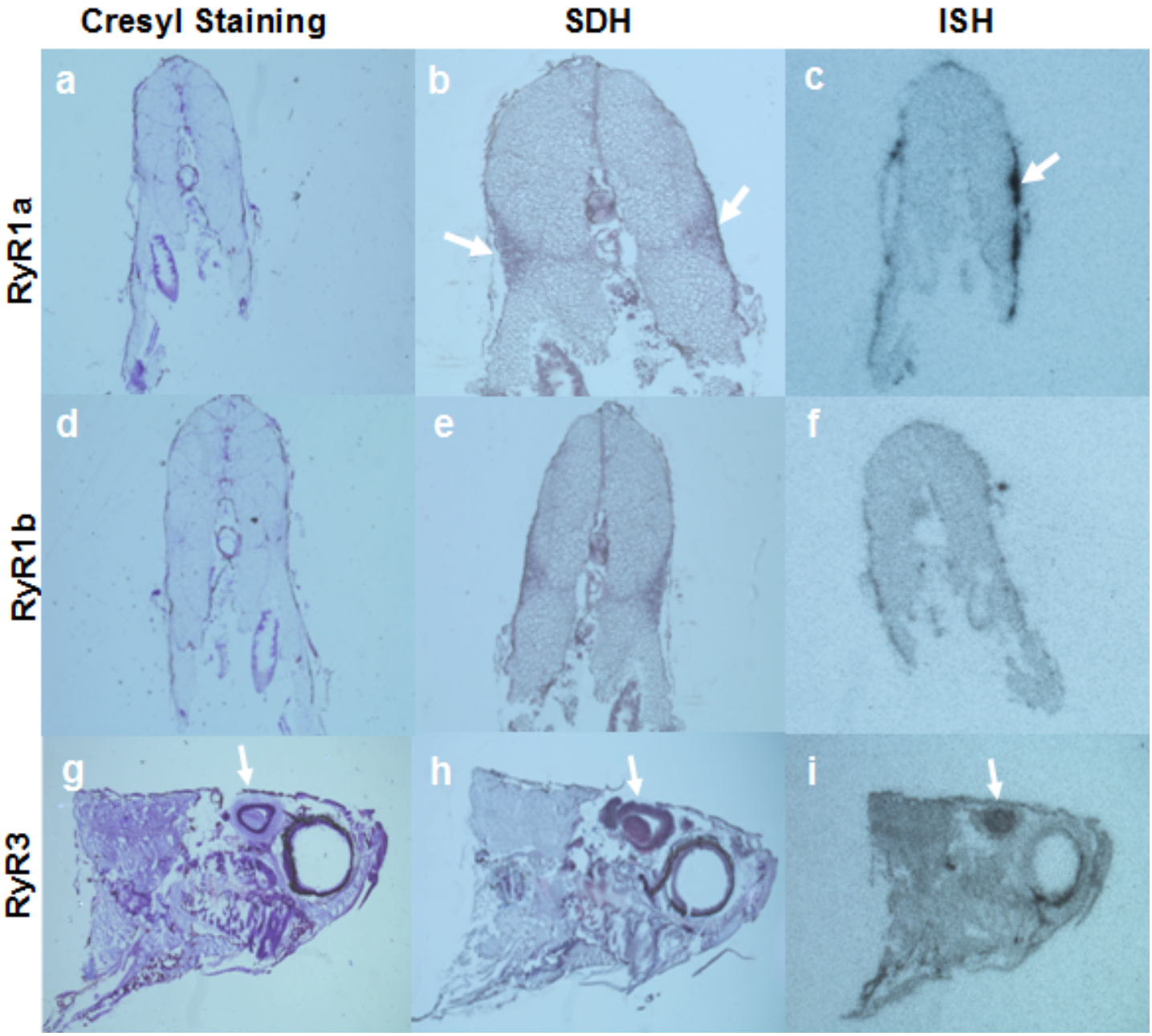

Figure 18: Comparison of zebrafish (*D. rerio*) *in situ* hybridization (ISH) expression pattern with the histological staining (Cresyl Violet (CVS) and Succinate Dehydrogenase (SDH) staining) performed on the transverse sections. (a,d) CVS of zebrafish section provided a greater contrast as per disposition of different muscle fibers. (b) SDH staining confirms presence of slow twitch (red) muscle fibers in zebrafish. (c)Expression pattern of RyR1a in slow twitch muscle fibers of zebrafish (white arrows) (e) SDH does not stain white muscle, thus is appears in a lighter shade. (f) Expression pattern of RyR1b in fast twitch muscle fibers of zebrafish (dark area) (g) CVS stains nissl substance present in the endoplasmic reticulum of cell bodies of neural tissue dark purple (white arrow) (h) SDH stained mitochondria present in the cell body of brain tissue (white arrow) (i) RyR3 probes have hybridized to the brain transverse section of bichir (white arrow).

CHAPTER 4: DISCUSSION

4.1 PHYLOGENETIC ANALYSIS OF RyR GENE FAMILY IN BICHIR

Degenerate PCR utilizes degenerate primers for DNA amplification, which provides an opportunity to amplify a pool of target sequences representing all members of a gene family in an organism. Utilizing this approach, I characterized 134 genomic clones from bichir (*P. ornatipinnis*) that share sequence identity with published RyR sequences based on BLASTx searches of GenBank databases. 134 clones were considered sufficient based on the DNA saturation studies performed on the ultracentrifugation analysis of two hundred fish genomes (Bucciarelli *et al.*, 2002) and analysis of eukaryotic genomes by density gradient centrifugation (Thiery *et al.*, 1976). DNA saturation analysis considers the size of genome of the organism, number of chromosomes as well as GC content of DNA. GC-rich genomes were of particular interest in these two studies because fish, in contrast to birds and mammals, possess DNA that is characterized by a lower heterogeneity, which implies that GC-rich sequences in fish is less GC-rich and less abundant than warm-blooded vertebrates, such as birds and mammals (Bucciarelli *et al.*, 2002; Bernardi and Bernardi, 1990b; Thiery *et al.*, 1976). In contrast, the distribution of genes is similar in all vertebrates, in that about half of the genes are located in the GC-rich sequences of the genomes, even if these sequences are less GC-rich in fishes compared to mammals and birds (Bernardi and Bernardi, 1990b). The bichir genomic clones sort into four cognate alignment groups (Appendix 2). The consensus sequences from each of the four cognate groups putatively identified the sequences as orthologs of the RyR1a, RyR1b, RyR2 and RyR3 genes based on BLASTx searches of the GenBank database (Appendix 2). The neighbour joining tree (Figure 10) identified three

monophyletic clades corresponding to the RyR1, RyR2, and RyR3 gene subfamilies. The putative orthology of the bichir sequences suggested by the BLASTx analysis is confirmed by the phylogenetic analysis as the four bichir sequences, RyR1a and RyR1b, RyR2, RyR3 are clustered within the RyR1, RyR2, and RyR3 clades respectively (Figure 10). Additionally, the bichir RyR1a and RyR1b sequences identified in the genomic survey also cluster with their zebrafish orthologs indicating that the gene duplication event of the RyR1 gene predates the divergence of the Polypteridae and Teleostei lineages. Since the bootstrap values at the node of divergence of RyR1a and RyR1b is 85%, it implies that this branch is statistically robust. Support for the orthology of the bichir RyR1a and RyR1b sequences is supported by a strong 85% bootstrap value (Fig. 10). The bichir RyR1a and RyR1b sequences cluster with their orthologs from zebrafish. The confirmation of fibre type-specific gene expression could be explained by the discrete compartmentalization of red and white muscle fibers in bichir transverse sections (Figure 12). Red muscle fibers utilize oxidative phosphorylation, which generates significantly more energy in fish skeletal muscle and is mainly used for prolonged, enhanced swimming pattern, whereas, white muscle fibers use glycolysis as the main source of energy to generate quick bursts of energy and are mainly used for quick responses to environmental stimuli. The different physiological properties of the two muscle masses could account for different selective pressure on the duplication and divergence of the RyR1a and RyR1b genes before the divergence of the Teleostei and Polypteridae lineages. The bichir RyR2 sequence is basal to the RyR2 sequences from human and mouse but is not basal to the zebrafish RyR2a and RyR2b sequences. This could be due to the relaxed selection on RyR2a and RyR2b in zebrafish, which resulted in

these genes to be more basal to other RyR2 sequences including bichir RyR2 sequence. The single bichir RyR3 gene clusters with, and is basal to, the RyR3 genes from zebrafish, human, mouse, and rabbit (Figure 10). However, as depicted in Figure 19, neighbour-joining phylogenetic analysis of full-length published RyR amino acid sequences from human, frog, mouse, and zebrafish revealed a different clustering pattern of RyR clades when compared to the neighbour-joining tree deduced from partial RyR sequences. According to Figure 19, RyR1 and RyR3 cluster together, whereas, the RyR2 clade clusters separately as a basal clade. Also, the branch length of the RyR1 clade is significantly longer than those for RyR2 and RyR3, respectively (Figure 19). This could be due to the fact that RyR1 has acquired the DICR mechanism of calcium release and has diverged functionally from RyR2 and RyR3, which utilize CICR mechanism of calcium release in the muscle and brain cells. It could also be that RyR1 is under stronger selection due to its DICR nature. Conversely, for the tree based on partial sequences (Fig. 10), RyR2 and RyR3 cluster together and RyR1 seems to have diverged separately. Also, from Figure 10, it can be deduced that even though RyR1 has acquired a different mechanism of calcium release (namely DICR) branch lengths in this clade are very short when compared to the RyR2 and RyR3 clades. Theoretically, when a gene (in this case RyR1) has diverged from the ancestral gene and has undertaken a different mode of function, a much longer branch length is expected, which would imply that those genes are more distant from other paralogous copies. The discrepancy between the tree based on full-length RyR sequences and the phylogenetic tree based on the partial RyR sequences, in which RyR2 and RyR3 cluster to the exclusion of RyR1 is likely due to the particular region selected in the partial sequence analysis. The block of sequence

amplified in bichir is from the C-terminus of RyR gene sequence, which plays a role in the TA domain which could be under a different selection pressure. Alternatively, it can be hypothesized that this short block of sequence, representing RyR multigene family in bichir, has undergone gene conversion (non-homologous recombination) which resulted in a different clustering pattern than the phylogenetic tree constructed based on the full-length amino acid sequences of published RyRs.

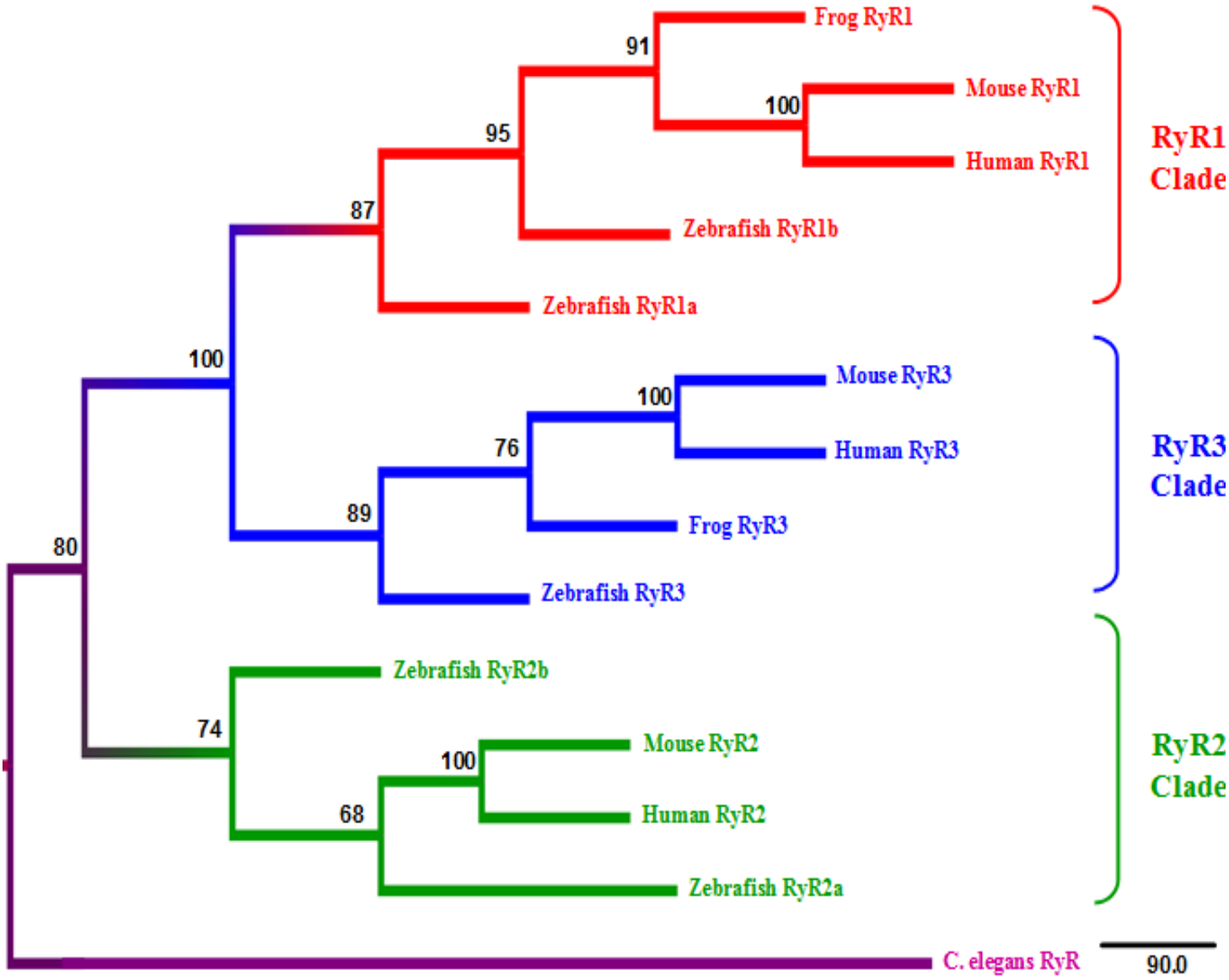

Figure 19: Bootstrapped neighbor-joining tree based on Dayhoff PAM distance matrix (Dayhoff *et al*., 1972). The multiple alignment of full-length published RyR amino acid sequence with GenBank accession numbers presented in bracket of human RyR1 (NM_001042723), human RyR2 (NP_001026), human RyR3 (NM_001036), mouse RyR1 (NM_009109), mouse RyR2 (NM_023868), mouse RyR3 (NM_177652), frog RyR1 (D21070), frog RyR3 (D21071), zebrafish RyR1a (XM_001922082), zebrafish RyR1b (NM_001102571), zebrafish RyR2a (XM_001922082), zebrafish RyR2b (XM_001921102), and zebrafish RyR3 (XM_001922078) was used to generate the phylogenetic tree. The consensus tree is based on the output of 100 bootstrap pseudoreplicates from the Neighbor program of PHYLIP (Felsenstein, 1993). The *C. elegans* RyR sequence (BAA08309) was used as a designated outgroup. Bootstrap values are given on the major nodes of the tree.

A survey of other genome databases has revealed that in addition to zebrafish, other teleost species including medaka (*Oryzia latipes*) and fugu (*Takifugu rubripes*) possess duplicate copies of the RyR2 and RyR3 genes (Franck *et al.*, in preparation). The apparent absence of RyR2 and RyR3 duplicates in the bichir genome can be explained by gene loss following the fish-specific whole-genome duplication event. The most parsimonious explanation for the paralogous RyR copies could be that the RyR1 gene duplication is the result of a local or single gene duplication event that occurred at the base of the ray-finned lineage and multiple copies of RyR2 and RyR3 are results of Fish-Specific Genome-Duplication event during the evolution of teleosts (Figure 20). Previous studies on *Hox* gene clusters in bichir indicate that the *HoxA*α and *HoxA*β duplicate clusters found in zebrafish and other derived teleosts are not present in the bichir genome, lending support for the FSGD event occurring after the divergence of the Polypteridae lineage (Chiu *et al.*, 2004).

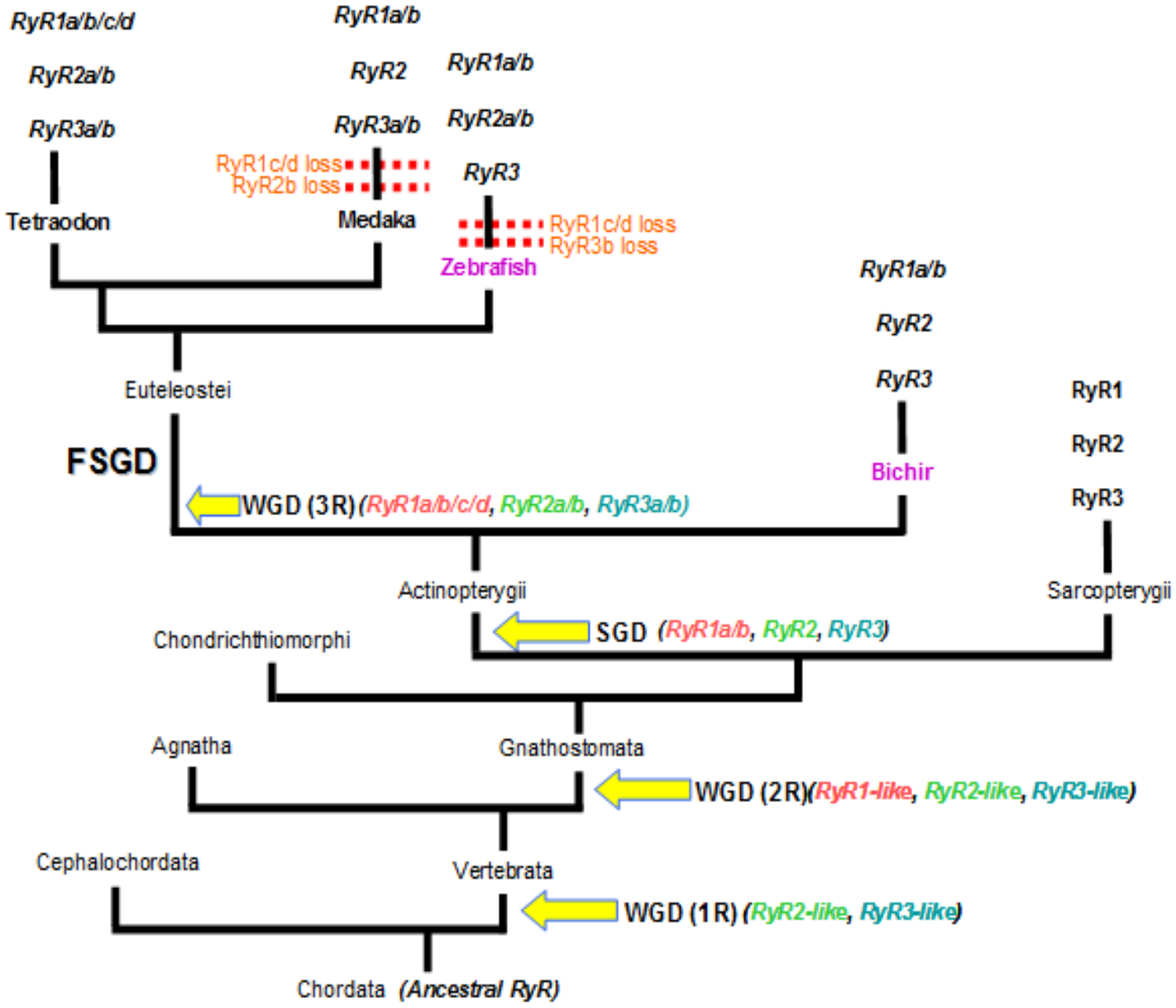

Figure 20: Proposed History of RyR Gene Duplications. The proposed molecular evolution of the RyR gene family is shown within a conventional vertebrate species tree. Based on the genomic survey of bichir, there is sufficient evidence that bichir possesses orthologs for RyR1a, RyR1b, RyR2 and RyR3 in its genome. The evolution of the fiber type-specific RyR1 genes is believed to be the result of local or single gene duplication at the base of ray-finned lineage. Multiple copies of RyR2 and RyR3 genes in the Euteleostei lineage are believed to be the result of Fish-Specific Genome-Duplication (FSGD; 3R). WGD = Whole-Genome Duplication, SGD = Single/Local Gene Duplication.

4.2 Relative Expression Levels of RyR Genes in Bichir and Zebrafish

The relative expression levels for the four bichir and five zebrafish RyR genes were measured by qRT-PCR in four tissue sources: slow twitch (red) skeletal muscle, fast twitch (white) skeletal muscle, cardiac and brain tissues. In all tissues the expression levels were assayed relative to the expression of two housekeeping genes, actin and elongation factor 1α (ef1α). Figure 11a and 11b shows the relative expression levels for the RyR1a and RyR1b paralogs in bichir and zebrafish. The expression study results indicate the tissue specific expression pattern for the RyR1 paralogs is present in the basal ray-finned bichir with marked higher expression levels for RyR1a and RyR1b in the slow twitch and fast twitch muscles respectively (Figure 11a). The expression of fiber type-specific RyR1 genes in teleost fish was first reported by Franck and colleagues (Franck *et al.*, 1998). The slow twitch RyR1 and fast twitch RyR1 specific gene transcripts are now referred to as RyR1a and RyR1b respectively since the recent publication of a full-length RyR1b fast twitch sequence from zebrafish (Hirata *et al.*, 2007). The bichir RyR2 gene and both RyR2a and RyR2b paralogs in zebrafish are expressed at the highest level in cardiac tissue with low levels for both species in slow twitch and fast twitch skeletal muscle fibres and brain tissues (Figure 11c). The zebrafish RyR2a and RyR2b paralogs are co-expressed with a ratio of 0.86 RyR2a to RyR2b. The RyR3 gene in both species is predominantly expressed in brain tissue (Figure 11d). The relative gene expression level for the RyR3 gene in the skeletal muscle tissues of bichir and zebrafish differs markedly. In bichir the RyR3 gene is expressed at low levels in both slow twitch (Figure 11a) and fast twitch (Figure 11b) skeletal muscle whereas it is up regulated in zebrafish skeletal muscle fibres. In zebrafish, the expression ratio measured

relative to the actin housekeeping gene of RyR3 to RyR1a and RyR1b is 0.77 for both slow twitch and fast twitch muscle, respectively (Table 4) while the RyR3 to RyR1a and RyR1b expression ratio for bichir slow twitch and fast twitch muscle is 0.16 and 0.18, respectively. These values are consistent with the ratios calculated relative to the ef1α housekeeping gene with a ratio of RyR3 to RyR1a and RyR1b expression of 0.75 and 0.64 in zebrafish slow twitch and fast twitch muscle and 0.27 and 0.18 for the same comparison in bichir. Previous studies of RyR expression based on immunoblot analyses describe the equal co-expression of RyR1 and RyR3 proteins in skeletal muscles of teleost fish (O'Brien *et al.*, 1993; Sutko *et al.*, 1996). Exceptions to this condition are highly specialized super high frequency muscle fibres such as extraocular eye muscle and toadfish swimbladder muscle in which RyR3 expression is not detected (O'Brien *et al.*, 1993). A Low RyR3 expression level in skeletal muscle is the normal condition in the sarcopterygian lineage (Fill *et al.*, 2002). The increased expression of RyR3 in the teleostei lineage which includes zebrafish is therefore likely due to a divergence of regulatory domains in the RyR3 gene.

4.3 HISTOLOGICAL STAINING

The dissection of the skeletal slow twitch (red muscle) and fast-twitch (white muscle) tissues for the qRT-PCR analyses relied solely on identifying the difference by colour. In order to more precisely determine the disposition of the two muscle masses in bichir and zebrafish I utilized a histological technique – Succinate Dehydrogenase Staining – that specifically differentiates slow-twitch oxidative from fast-twitch glycolytic tissues. Succinate dehydrogenase (SDH) is a bound inner mitochondrial membrane enzyme. SDH catalyses the conversion of succinate to fumarate in the citric

acid cycle (TCA cycle) accompanied by the formation of a reduced flavin moiety (Rustin *et al.*, 2002; Horák, 1983). The histochemical assay for SDH is used to distinguish between oxidative and non-oxidative muscle fibers. Sherwood and colleagues (2005) showed that fibers with a high oxidative capacity generate ATP via oxidative phosphorylation in the mitochondria. Thus, muscle cells which contain more mitochondria will have a higher oxidative capacity. It is generally accepted that muscle fiber types can be broken down into two main types. The first category is slow-twitch oxidative (Type I) muscle fibers, which utilize oxidative phosphorylation and are used during continuous, extended muscle contractions over a long period of time. Due to their slow-twitch nature, these muscle fibers can twitch for a longer period of time before fatigue is induced from continuous contraction. The second category of muscle fiber classification is fast twitch glycolytic (Type II) muscle fibers. Since fast-twitch muscles utilize anaerobic metabolism to create energy, they are much better at generating short bursts of strength than slow-twitch muscles. In mammals, fast twitch fibers can be further categorized into Type IIa (fast twitch oxidative-glycolytic; FOG) and Type IIb (fast twitch glycolytic; FG) fibers (Sherwood *et al*., 2005).

SDH staining is a convenient method to differentiate between fast and slow-twitch muscle fibers. As depicted in figure 12b and 12d, SDH staining stains slow-twitch (Type I) muscle fibers dark. Red muscle fibers are arranged quite differently in bichir when compared to zebrafish (Figure 12b and 12d). Bichir possesses a significantly lower concentration of red muscle fibers, which are positioned in a very thin sliver-like shape which expends deep into the muscle section (Figure 12b). Conversely, zebrafish possesses a higher concentration of red muscle fibers, which are more concentrated on

the peripheral side of the fish skeletal muscle in a triangular-like shape (Figure 12d). This could be explained by the fact that bichir is a nocturnal predator and feeds on smaller fishes, fresh water crustaceans, snails, and amphibians larvae (Budgett, 2001), which would require quick bursts of energy to capture its prey. Thus it is expected that bichir might possess a greater proportion of white muscle mass in its skeletal cross-sections. In contrast, zebrafish uses more time and energy to maintain a steady swimming pattern, which could be explained by the higher concentration of red muscle fibers in the cross section (Figure 12d).

4.4 *IN SITU* HYBRIDIZATION

The qRT-PCR and histological analyses indicate that bichir and zebrafish have discrete red and white muscle masses with fiber type-specific expression of the RyR1 paralogs. To accurately determine the spatial expression of the RyR genes in both species, I performed *in situ* hybridization using gene-specific oligonucleotide probes. The ^{33}P-labeled probes were hybridized directly to 10 μm thin sections of skeletal muscle and brain tissue of bichir and zebrafish. Figure 14a, 14b and 15a, 15b show the spatial expression pattern for the RyR1a and RyR1b paralogs in bichir and zebrafish. The spatial expression analyses indicate that the tissue specific expression pattern for the RyR1 paralogs is present in the basal ray-finned bichir with notably higher expression levels for RyR1a and RyR1b in the slow twitch and fast twitch muscles, respectively (Figure 14a, 14b). This expression pattern confirms the results obtained from the qRT-PCR investigation of expression analysis for the RyR multigene family in bichir and zebrafish (Figure 11a and 11b; Darbandi and Franck, 2009). The expression of muscle specific RyR1 was originally discovered by Franck and colleagues (Franck *et al.*, 1998). The slow

twitch RyR1 and fast twitch RyR1 specific gene transcripts are now referred to as RyR1a and RyR1b respectively (Hirata *et al*., 2007). The *in situ* hybridization results are consistent with the expression profile revealed by qRT-PCR. A qualitative assessment of the *in situ* hybridization results in bichir indicates that the expression of RyR3 compared to both RyR1a and RyR1b is markedly lowered in both fast twitch (white) and slow twitch (red) skeletal muscles (Figure 14c). In zebrafish, there is evidence for a significantly stronger signal for RyR3 in the skeletal muscle cross section (Figure 15c). The RyR3 gene in both species is predominantly expressed in brain tissue (Figure 14i, 15i). However, bichir shows a lower expression profile of RyR3 gene in its cardiac tissue when compared to zebrafish (Figure 14f, 15f). This evidence is further supported by the qRT-PCR analysis of relative gene expression of RyRs in both species (Figure 11c). In order to support the qualitative observations of *in situ* hybridization results, quantitative analyses of the *in situ* expression study were performed using ImageJ software. ImageJ is a public domain, Java-based image processing program developed at the National Institutes of Health (Collins, 2004). ImageJ software applies a grey scale to minimize the background noise of the image and utilizes the mean number of pixels as a measure to quantify the signal intensity. Thus, the higher mean number of pixels represents a higher signal intensity, which implies a higher expression profile. Based on the results compiled in Figure 16 and Table 5, it is apparent that the expression ratio of RyR3 to RyR1a and RyR1b is 0.17 and 0.21 in slow twitch and fast twitch skeletal muscle of bichir, respectively. Conversely, zebrafish possesses a significantly higher expression profile, in which the expression ratio of RyR3 to RyR1a and RyR1b is 0.84 and 0.97, respectively. These data confirm the fact that RyR3 gene is expressed in lower levels in bichir skeletal

muscle, which strengthens the results gathered from qRT-PCR depicted in figure 11a and 11b. Additionally, such low expression ratio in bichir compared to zebrafish, provides further evidence that bichir does not equally co-express the RyR1 and RyR3 genes in skeletal muscle. This marked difference in the expression profile for the RyR3 gene would suggest that the two component mode of E-C coupling is not essential in the skeletal muscles of primitive fish, in which activation of DICR mechanism, where RyR1 gene is the principle regulator of pattern of calcium release into the cytoplasm of muscle cells, is not paired with the CICR mechanism associated with the activity of RyR3 in skeletal muscle cells. Data gathered from qRT-PCR as well as *in situ* hybridization, also suggests that the two component mode of E-C coupling may be an important contributor to the diversification of teleost fishes by providing a greater ability to response to the environmental stimulus, which would provide a greater chance of survival for teleosts in their habitat. Quantitative analyses also validate the result obtained from qRT-PCR presented in Figure 11d, in which RyR3 is predominantly expressed in brain tissue (Table 6; Figure 16). RyR1 and RyR3 co-expression at equivalent levels may allow for flexibility or increased modulation in the control of calcium release properties in muscle cells, due to different calcium release properties of RyR1 and RyR3 as well as different regulatory potentials of these two genes (O'Brien *et al.*, 1993). Rios and Pizarro (1991) suggested that this phenomenon (RyR1-RyR3 co-expression) could be under the influence of several factors. The first and most important contributing factor is the mode of E-C coupling by each of the RyR1 and RyR3 genes. In teleost skeletal muscle, RyR1 uses DICR via mechanical association of DHPRs and RyRs in triad junctions. However, not all RyRs in triad junction are able to make direct mechanical connections (Block *et*

al., 1988). RyRs are arranged in an alternating pattern with the DHPRs so that only half of the RyRs can make direct contact (O'Brien *et al.*, 1993; O'Brien *et al.*, 1995; Rios and Pizarro, 1991). RyRs that are not directly associated with DHPRs (namely RyR3) utilize the CICR mechanism of calcium release. The presence of two RyR genes allows for greater flexibility in the calcium release response (Block *et al*., 1994). The second contributing factor is the control of calcium regulation by ligands including intracellular calcium, magnesium, adenine nucleotides, and other ligands (Tripathy *et al.*, 1995). The presence of two RyR genes (namely RyR1 and RyR3) with potentially different sensitivities to calcium and other ligands also contributes to the flexibility of the calcium release response in the skeletal muscles of teleost fish (Tripathy *et al.,* 1995; Block *et al.*, 1994). The co-expression of equivalent levels of RyR1 and RyR3 may be more suited for meeting the physiological demands of teleost muscles than one. For bichir, in which RyR3 is expressed at significantly lower levels, it can be hypothesized that bichir, similar to mammals, recruits its muscles at relatively high contraction speeds (O'Brien *et al.,* 1993; O'Brien *et al*., 1995). This may be the reason why the RyR3 gene is not co-expressed at equivalent levels with RyR1 in bichir skeletal muscles. Interestingly, results of *in situ* hybridization show a very distinct expression pattern of RyR1a, RyR1b and RyR3 genes in the eye of zebrafish, more specifically in the extraocular muscles and retina (Figure 15d – 15i). Previous studies of retinal RyR expression based on immunoblotting with specific and pan-antibodies showed that the majority of retinal RyR protein has a mobility similar to RyR3 (Shoshan-Barmatz *et al*., 2007), which could explain the unique expression pattern of RyR3 to the eye of zebrafish (Figure 15f and 15i). An investigation conducted by O'Brien and colleagues (1993) demonstrated that

extraocular eye muscles are highly specialized super high frequency muscle fibers, which possess a mixed fiber type of fast twitch and tonic (slow twitch) fiber types (O'Brien *et al.*, 1993). In addition, fast contracting extraocular muscles, which are believed to have given rise to the heater phenotype, express a single RyR1 gene similar to the one in the non-mammalian skeletal muscles (Block *et al.*, 1994). The expression of a single RyR gene in the heater and extraocular muscle is a specialized condition, presumably linked to the super fast contraction capabilities of extraocular muscle. The expression pattern for the heater and extraocular eye muscle is in sharp contrast to the slow and fast-twitch skeletal muscles of teleosts based on immunoblot analyses (Block *at al.*, 1994; O'Brien *et al.*, 1995). These facts could explain the hybridization pattern of RyR1a, RyR1b to the sagittal sections of the eye of zebrafish, since RyR1a and RyR1b share a common ancestral function. Additionally, there is sufficient evidence that RyR1a and RyR1b are expressed in low levels in cardiac tissues of bichir and zebrafish (Figure 14d, 14e and 15d, 15e), which is further supported with the results obtained from the qRT-PCR from both species (Figure 11c).

The results obtained from the histological staining and the *in situ* hybridization experiments support the presence of fiber type-specific RyR1 paralogs in basal ray-finned bichir. As depicted in Figure 17b, red muscle fibers of bichir penetrate deep into the body section but interestingly the *in situ* hybridization (Figure 17c) does not show any hybridization signal from deep portions of the skeletal muscle. This could be due to several factors. First, the lack of expression, deep into the body section of bichir could simply be due to lower red muscle fiber cell density in this area. Alternatively, it could imply that bichir possesses two different types of red muscle fibers in its muscle mass.

The *in situ* hybridization experiment indicates that the RyR1a and RyR1b genes are discretely expressed in the red and white muscle tissue respectively in bichir and zebrafish. These results along with the data obtained from the molecular evolutionary and qRT-PCR analysis of the RyR multigene family in bichir and zebrafish strengthens the hypothesis that RyR1a and RyR1b are likely the result of a single or local gene duplication of the ancestral RyR1 at the base of ray-finned lineage before the divergence of Polypteridae from the Teleostei lineage. Additionally, cresyl violet stains nissl substance – which are commonly referred to as rough endoplasmic reticulum (RER) mainly present in the cell bodies of neural tissue – dark purple (Snell, 2009). As depicted in Figure 18g cresyl violet staining produces a light and dark colouring pattern in the brain of zebrafish, which could be due to the different concentrations of cell bodies in the different parts of brain. When histological staining of zebrafish brain (Figure 18g and 18h) is compared to the *in situ* hybridization of RyR3 gene in brain (Figure 18i) it is apparent that probes have hybridized mostly to the frontal portion of the brain, which could hypothetically be designated as telencephalon, epiphysis and optic tectum based on the magnetic resonance imaging of zebrafish brain (Figure 21). This observation coincides with the SDH staining pattern (Figure 18h), which supports the qualitative observation, where the hybridization has occurred in the frontal portion of brain tissue (olfactory bulb, telencephalon and optic tectum).

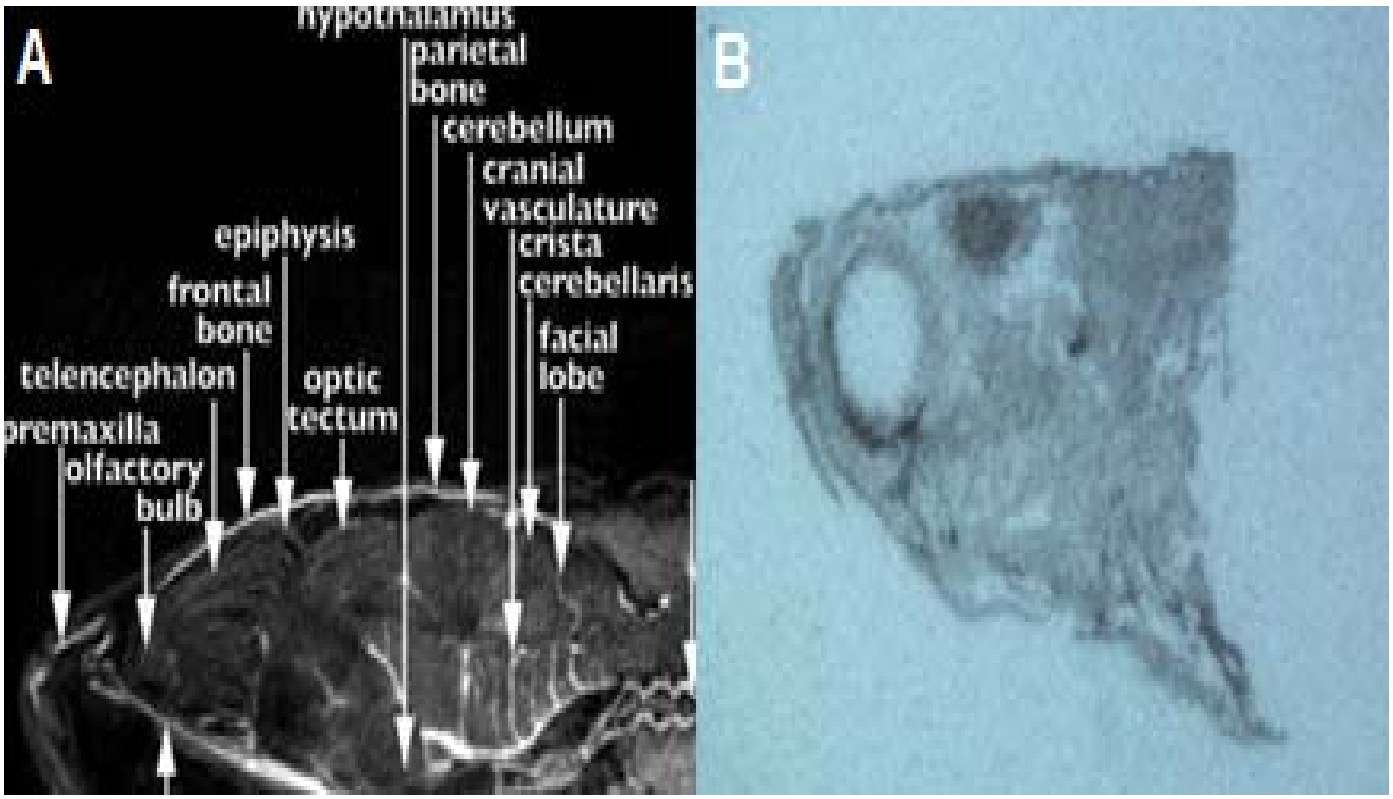

Figure 21: Magnetic Resonance Imaging (MRI) of zebrafish brain. (A) Coronal view at the midline (Adapted from Bryson-Richardson *et al*., 2007), and (B) ISH of zebrafish coronal section.

4.5 EVOLUTION OF EXCITATION-CONTRACTION COUPLING

The comparison of the expression profile of the RyR multigene family between the basal ray-finned bichir and the derived euteleost zebrafish provides important insight into the evolution of E-C coupling. The evolution of the depolarization induced calcium release (DICR) mode of calcium release is a vertebrate innovation (Inoue *et al*., 2002; Di Biase *et al*., 2005). The RyR1 channel utilizes the DICR mechanism of calcium release and is the predominant gene expressed in skeletal muscles of mammals involved in the E-C coupling. The RyR3 channel which utilizes the calcium induced calcium release (CICR) mechanism of calcium release is expressed at low levels in mammalian skeletal muscle but is co-expressed at equal levels with RyR1 in the skeletal muscle fibers of teleost fish (O'Brien *et al.,* 1993; O'Brien *et al*., 1995). The co-expression of the RyR1 and RyR3 genes in teleost fish has led to the proposal of a two component mode of E-C coupling (O'Brien *et al*., 1995). In this model, the RyR1 channels are directly opposed and mechanically gated open by the DHPR voltage sensors resulting in the release of calcium that then activates the adjacent ligand-gated RyR3 channels. This effectively results in the amplification of the original signal (Figure 22). The model is based on ultrastructural studies showing every second DHPR tetrad opposed by a RyR channel (Yin *et al*., 2008). The unopposed RyR channels are presumed to be the RyR3 channels (Di Biase *et al*., 2005). The ultrastructural arrangement of RyRs and DHPRs has not been investigated in bichir but based on the low relative expression of RyR3; it would be unlikely that the two channels are arranged in the alternating pattern found in teleost fish.

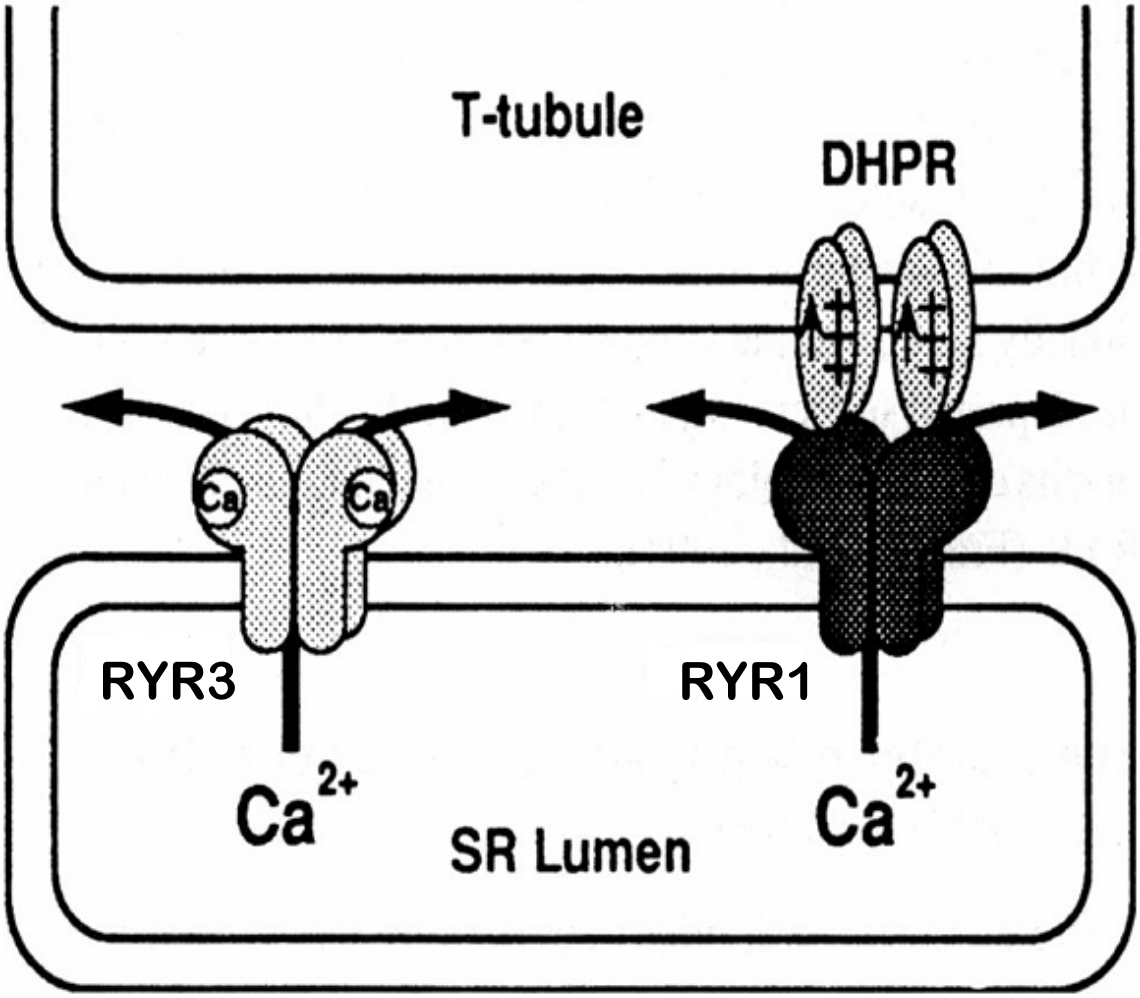

Figure 22: Schematic representation of a two component model for the calcium release process in non-mammalian vertebrate skeletal muscle. The presence of two physiologically distinct Ca^{2+} release channels in skeletal muscle of non-mammalian vertebrates suggests a model in which two different forms of E-C coupling are present. Direct, mechanically coupled channels are depicted making contact with the overlaying T-tubule DHPR, which acts as a voltage sensor. Ca^{2+} release in a depolarization-induced coupling event triggers Ca^{2+} release from the close neighbour or "slave" RYR channel. The RyR1 isoform occupies the directly coupled position, and the RyR3 isoform the Ca^{2+}-coupled position (Block *et al*., 1988). The physical dimensions of the RyR array in toadfish triad junctions are such that adjacent RyRs may actually touch one another and deliver localized Ca^{2+} currents or transmit conformational changes (Figure used with permission from O'Brien *et al*., 1995).

CHAPTER 5: CONCLUDING REMARKS

The PCR genomic survey and phylogenetic analysis indicates that bichir possess orthologs for the RyR1a, RyR1b, RyR2, and RyR3 genes. This implies that the RyR1 gene was duplicated at the base of the ray-finned fish lineage before the divergence of the Polypteridae and Teleostei lineages. Subfunctionalization of the two daughter genes, namely RyR1a and RyR1b, resulted in their discrete expression in slow twitch and fast twitch muscle fibres respectively. *In situ* hybridization and qRT-PCR gene expression analysis of the RyR multigene family in bichir and zebrafish revealed that the RyR1a and RyR1b genes of bichir and zebrafish are both expressed discretely in the slow and fast twitch skeletal muscle fibers, respectively in bichir and zebrafish. However, the comparison of expression levels for the RyR genes of bichir and zebrafish reveals that the co-expression of RyR1 and RyR3 genes is a teleost-specific condition as the RyR3 gene is expressed at lower levels in bichir. The marked difference in expression profile for the RyR3 gene would suggests that the two component mode of E-C coupling is not essential in the skeletal muscles of primitive fish. Also, equal co-expression of RyR1 and RyR3 in skeletal muscles of teleosts allows for flexibility or increased modulation in the control of calcium release in muscle cells. It is believed that flexibility or increased modulation is due to the unique calcium release properties of the RyR1 and RyR3 genes as well as the different regulatory sensitivity of RyR1 and RyR3 to the intracellular ligands. These factors may be important contributors to the diversification of teleost fishes over other evolutionary lineages. This hypothesis is further supported by the results obtained from SDH staining, in which zebrafish, representative of teleosts, possesses a higher concentration of slow twitch oxidative (red) muscle fibers than bichir. The higher volume

of red muscle fibers could contribute to the enhanced swimming ability of the Teleostei lineage, which would consequently contribute to further diversification of teleosts. Lastly, the lack of co-expression of RyR1 and RyR3 in the skeletal muscles of bichir, is similar to the mammalian groups. This might be hypothesized that bichir, similar to mammals, recruits its muscles at a higher contraction speeds and under homeostatic temperature condition at all times. This might be the reason why RyR3 expression is not up regulated in bichir skeletal muscles.

REFERENCES

Altschul, S. F., Gish, W., Miller, W., Myers, E. W., and Lipman, D.J. 1990. Basic local alignment search tool. *J Mo. Biol.* **215**: 403–410.

Amores A., Suzuki, T., Yan, Y. L., Pomeroy, J., Singer, A., Amemiya, C. and J. H. Postlethwait. 2004. Developmental roles of puffer fish hox clusters and genome evolution in ray-fin fish. *Genome Res.* **14**(1):1 – 10.

Amores, A., Force, A., Yan, Y.-L., Jolly, L., Amemiya, C. T., Fritz, A., Ho, R. K., Langeland, J., Prince, V., Wang, Y. L., et al. 1998. Zebrafish *Hox* clusters and vertebrate genome evolution. *Science.* **282**: 1711 – 1714.

Barboriak, D., Padua, A., York, G. and J. Macfall. 2005. Creation of DICOM–aware applications using ImageJ. *J Digit Imaging* **18** (2): 91–99.

Bernardi, G. and G. Bernardi. 1990b. Compositional transitions in the nuclear genomes of cold-blooded vertebrates. *J Mol Evol*. **31**: 282-293.

Bird, T. M. 2005. Extraction of RNA from cells and tissue. *Methods Mol Med*. **108**:139 – 48.

Block, B. A., Imagawa, T., Campbell, K. P., and C. Franzini-Armstrong. 1988. Structural evidence for direct interaction between the molecular components of the transverse tubule/sarcoplasmic reticulum junction in skeletal muscle. *J Cell Biol*. **107**:2587-2600.

Block, B. A., O'Brien, J. and G. Meissner. 1994. Characterization of the Sarcoplasmic Reticulum proteins in the thermogenic muscles of fish. *J Cell Biol.* **127**(5): 1275–1287.

Blomme, T., Vandepoele, K., De Bodt, S., Simillion, C., Maere, S., and Y. Van de Peer. 2006. The gain and loss of genes during 600 million years of vertebrate evolution. *Genome Biol.* **7**(5):R43.

Bryson-Richardson, R. J., Berger, S., Schilling, T. F., Hall, T. E., Cole, N. J., Gibson, A. J., Sharpe, J., and P. D. Currie. 2007. FishNet: an online database of zebrafish anatomy. *BMC Biol*. **5**(34): 1-8.

Bucciarelli, G., Bernardi, G. and G. Bernardi. 2002. An ultracentrifugation analysis of two hundred fish genomes. *Gene*. **295**: 153-162.

Budgett, J. S. 2001. In Pursuit of *Polypterus*. *American Institute of Biological Sciences.* **51**(5): 399 – 407.

Chiu, C.H., Dewar, K., Wagner, G.P., Takahashi, K., Ruddle, F., Ledje, C., Bartsch, P., Scemama, J.L., Stellwag, E., Fried, C., Prohaska, S.J., Stadler, P.F. and C. T. Amemiya. 2004. Bichir HoxA cluster sequence reveals surprising trends in ray-finned fish genomic evolution. *Genome Res*. **14**(1):11-17.

Chomczunski, P. and N. Sacchi. 1987. Single-step method of RNA isolation by acid guanidinium thiocyanate-phenol-chloroform extraction. *Anal Biochem*. **162**: 156 – 159.

Chugun, A., Taniguchi, K., Murayama, T., Uchide, T., Hara, Y., Temma, K., Ogawa, Y., and T. Akera. 2003. Subcellular distribution of ryanodine receptors in the cardiac muscle of carp (*Cyprinus carpio*). *Am J Physiol*. **285**: R601–R609.

Collins, T.J. 2007. ImageJ for microscopy. *BioTechniques* **43** (1 Suppl): 25–30.

Darbandi, S. and J. P. C. Franck. 2009. A Comparative Study of Ryanodine Receptors (RyRs) Gene Expression Levels in Basal Ray-Finned Fishes, Bichir (*Polypterus ornatipinnis*) and the Derived Euteleosts Zebrafish (*Danio rerio*). *Comparative Biochem Physiol Part B* **154:** 443 – 448.

Dayhoff, M. O., Eck, R. V., C M, P. 1972. A model of evolutionary change in proteins. *National Biomedical Research Foundation*, Washington, D.C.

Di Biase, V., and C. Franzini-Armstrong. 2005. Evolution of skeletal type E-C coupling: a novel means of controlling calcium delivery. *J Cell Biol.* **17**: 695–704.

Felsenstein, J. 1992. Estimating effective population size from samples of sequences: A bootstrap monte carlo integration method. *Genet Res* **60**(3): 209-220.

Fill, M., and J. A. Copello. 2002. Ryanodine receptor calcium release channels. *Physiol Rev.* **82**(4): 893-922.

Finn, R. N. and B. A. Kristoffersen. 2007. Vertebrate vitellogenin gene duplication in relation to the "3R hypothesis": Correlation to the pelagic egg and the oceanic radiation of teleosts. *PLoS ONE* **2**:e169.

Force, A., Lynch, M., Pickett, F.B., Amores, A., Yan, Y.-L. and Postlethwait, J. 1999. Preservation of duplicate genes by complementary, degenerative mutations. *Genetics.* **151**: 1531–1545.

Franck, J. P., Morrissette, J., Keen, J. E., Londraville, R. L., Beamsley, M. and B. A. Block. 1998. Cloning and characterization of fiber type-specific ryanodine receptor isoforms in skeletal muscles of fish. *Am J Physiol* **275**: C401-415.

Franck, J.P.C., Reimer, K.R. and K. Hill. In preparation. Molecular evolution of the RyR gene family: A phylogenetic and comparative genomic analysis.

Frank, J. 1996. Three-Dimensional Electron Microscopy of Macromolecular Assemblies. *Academic Press*, New York.

Franzini-Armstrong, C. and A. O. Jorgensen. 1994. Structure and development of E-C coupling units in skeletal muscle. *Annu Rev Physiol*. **56**: 509 – 534.

Franzini-Armstrong, C. and J. W. Kish. 1995. Alternate disposition of tetrads in peripheral couplings of skeletal muscle. *J Muscle Res Cell Motil*. **16**: 319 – 324.

Franzini-Armstrong, C. and F. Protasi. 1997. Ryanodine receptors of striated muscles: A complex channel capable of multiple interactions. *Phyiol Rev*. **77**: 699 – 729.

Franzini-Armstrong, C., Protasi, F. and V. Ramesh. 1999. Shape, size, and distribution of Ca^{2+} release units and couplons in skeletal and cardiac muscles. *Biophys J*. **77**: 1528 – 1539.

Gyorke, S., and P. Palade. 1993. Role of local Ca^{2+} domains in activation of Ca^{2+}-induced Ca^{2+} release in crayfish muscle fibers. *Am J Physiol*. **264**: C1505–C1512.

Hirata, H., Watanabe, T., Hatakeyama, J., Sprague, S.M., Saint-Amant, L., Nagashima, A., Cui, W.W., Zhou, W. and J. Y. Kuwada. 2007. Zebrafish relatively relaxed mutants have a ryanodine receptor defect, show slow swimming and provide a model of multiminicore disease. *Development* **134**: 2771–2781.

Holland, P. W. and J. Gracia-Fernandez. 1996. *Hox* genes and chordate evolution. *Dev Biol.* **173**: 382 – 395.

Horák, V. 1983. A successive histochemical staining for succinate dehydrogenasae and "reversed"-ATPase in a single section for the skeletal muscle fibre typing. *Histochemistry*. **78**: 545 – 553.

Inoue, I., Tsutsui, I. and Q. Bone. 2002. Excitation-contraction coupling in skeletal and caudal heart muscle of the hagfish *Eptatretus burgeri* Girard. *J Exp Biol* **205**: 3535 - 3541.

Inoue, I., Tsutsui, I., Bone, Q. and E. R. Brown. 1994. Evolution of skeletal muscle excitation-contraction coupling and the appearance of dihydropyridine-sensitive intramembrane charge movement. *Proc R Soc Lond B Biol Sci.* **255**: 181–187.

Ledje, C., Kim, C. B. and Francis H. Ruddle. 2002. Characterization of Hox Genes in the Bichir, *Polypterus palmas*. *Journal of experimental Zoology (Mol Dev Evol)* **294**: 107-111.

Lynch, M. and A. G. Force. 2000. The origin of interspecific genomic incompatibility via gene duplication. *The American Naturalist*. **156**(6): 590 – 605.

MacCarthy, T. and A. Bergman. 2007. The limits of subfunctionalization. *BMC Evol Biol*. **7**: 213 – 227.

McGuigan, K.., Phillips, P. C. and J.H. Postlethwait. 2004. Evolution of sarcomeric myosin heavy chain genes: Evidence from fish. *Mol Biol Evol.* **21**: 1042–1056.

Meyer, A. and Y. Van de Peer. 2005. From 2R to 3R: Evidence for fish-specific genome duplication (FSGD). *Bioessays* **27**(9): 937-945.

Morrissette, J., Xu, L., Nelson, A., Meissner, G. and B. A. Block. 2000. Characterization of RyR-slow, a ryanodine receptor specific to slow-twitch skeletal muscle. *Am J Physiol Regul Integr Comp Physiol.* **279**: R1889-1898.

Nabauer, M., Gallewaert, G., Cleemann, L. and M. Morad. 1989. Regulation of calcium release is gated by calcium current, not gating charge, in cardiac myocites. *Science*. **244**: 800–803.

Nguyen, C. 2009. Cloning and phylogenetic analysis of RyR orthologues in horn shark (*Heterodontus francisci*). *The University of Winnipeg Press.*

O'Brien, J., Meissner, G. and B. A. Block. 1993. The fastest contracting muscles of nonmammalian vertebrates express only one isoform of the ryanodine receptor. *Biophys J.* **65**: 2418–2427.

O'Brien, J., Valdivia, H. H. and B. A. Block. 1995. Physiological differences between the α and β ryanodine receptors of fish skeletal muscle. *Biophys J.* **68**: 471–482.

Prohaska, S. J. and P. F. Stadler. 2004. The duplication of the *Hox* gene cluster in teleost fishes. *Theory in Biosciences*. **123**: 89 – 110.

Radermacher, M., Rao, V., Grassucci, R., Frank, J., Timerman, A. P., Fleischer, S. and T. Wagenknecht. 1994. Cryo-electron microscopy and tree-dimensional reconstruction of the calcium release channel/ryanodine receptor from skeletal muscle. *The Journal of Cell Biology*. **127**(2): 411–423.

Page, R. D. M. 1996. TREEVIEW: An application to display phylogenetic trees on personal computers. *Comput Appl Biosci*. **12**: 357–358.

Protasi, F., Franzini-Armstrong, C. and B. Flucher. 1997. Coordinated incorporation of skeletal muscle dihydropyridine receptors and ryanodine receptors in peripheral couplings of BC3H1 cells. *J Cell Biol.* **137**: 859–870

Reimer, K. 2007. Cloning and phylogenetic analysis of RyR orthologues in primitive vertebrate species. *The University of Winnipeg Press.*

Rios, E. and G. Pizarro. 1991. Voltage sensor of excitation-contraction coupling in skeletal muscle. *Physiol Rev.* **71**: 849–908.

Rossi, D. and V. Sorrentino. 2002. Molecular genetics of ryanodine receptors Ca^{2+} release channels. *Cell Calcium*. **32**: 307–319.

Rose, T. M., Schultz, E. R., Henikoff, J. G , Pietrokovski, S., McCallum, C. M. and S. Henikoff. 1998. Consensus-degenerate hybrid oligonucleotide primers for amplification of distantly related sequences. *Nucleic Acids Res* **26**(7): 1628-1635.

Rozen, S. and H. Skaletsky. 2000. Primer3 on the WWW for general users and for biologist programmers. In: Krawetz, S., Misener, S. (Eds.), Bioinformatics Methods and Protocols: Methods in Molecular Biology. *Humana Press*, Totowa, NJ, pp. 365–386.

Rustin, P., Munnich, A. and A. Rötig. 2002. Succinate dehydrogenase and human disease: new insights into a well-known enzyme. *Euro J of Hum Genet.* **10**: 289–291.

Sharma, M. R. and T. Wagenknecht. 2004. Cryo-electron microscopy and 3D reconstruction of ryanodine receptors and their interactions with E-C coupling proteins. *Basic Appl Myol.* **14**(5): 299-306.

Sherwood, L., Klandorf, H. and P.H. Yancey. 2005. Animal Physiology: From Genes to Organisms. *Thompson Brooks/Cole*. pp. 324-430.

Snell, R. S. 2009. *Clinical Neuroanatomy* (7th ed., pp. 35-46). Philadelphia: Wolters Kluwer.

Sorrentino, V., Barone, V. and D. Rossi. 2000. Intracellular Ca^{2+} release channels in evolution. *Curr Opin Genet Dev.* **10**(6): 662-7.

Sutko, J. L. and J. A. Airey. 1996. Ryanodine receptor Ca^{2+} release channels: does diversity in form equal diversity in function? *Physiol. Rev*. **76**: 1027–1071.

Takekura, H. and C. Franzini-Armstrong. 2002. The structure of Ca^{2+} release units in arthropod body muscle indicates an indirect mechanism for excitation-contraction coupling. *Biophys. J*. **83**: 2742–2753.

Thiery, J. P., Macaya, G. and G. Bernardi. 1976. An analysis of eukaryotic genomes by density gradient centrifugation. *J Mol Biol.* **108**: 219-235.

Thompson, J. D., Gibson, T. J., Plewniak, F., Jeanmougin, F. and D. G. Higgins. 1997. The Clustalx windows interface:flexible strategies for multiple sequence alignment aided by quality analysis tools. *Nucleic Acids Res*. **25**: 4876 – 4882.

Tripathy, A., Xu, L., Mann, G. and G. Meissner. 1995. Calmodulin activation and inhibition of skeletal muscle Ca^{2+} release channels (ryanodine receptor). *Biophys J.* **69**:106 – 119.

Williams, A. J., West, D. J. and R. Sitsapesan. 2001. Light at the end of the Ca^{2+}-release channel tunnel: Structures and mechanisms involved in ion translocation in ryanodine receptor channels. *Quart Rev Biophys*. **34**: 61 – 104.

Xian-guang, H., Aldridge, R.J., Siveter, D.J., Siveter, D.J. and F. Xiang-hong. 2002. New evidence on the anatomy and phylogeny of the earliest vertebrates. *Proc Biol Sci.* **269**(1503): 1865 – 1869.

Yin, C.-C., D'Cruz, L.G. and F. A. Lai. 2008. Ryanodine receptor arrays: Not just a pretty pattern? *Trends Cell Biol.* **18**: 149–156.

Zhao, M., Li, P., Li, X., Zhang, L., Winkfein, R. J. and S. R. W. Chen. 1999. Molecular identification of the ryanodine receptor pore-forming segment. *J Biol Chem.* **274**: 25971 – 25974.

APPENDICES

APPENDIX 1: pGEM® - T Easy Vector Map

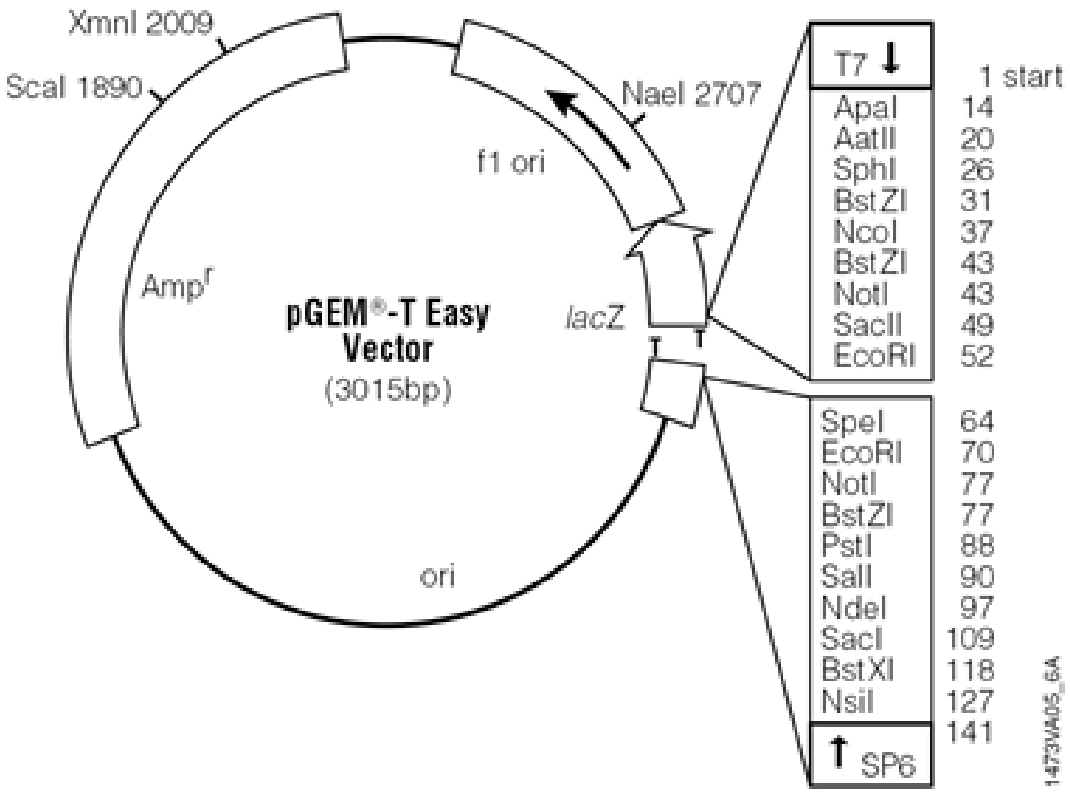

pGEM®-T Easy Vector

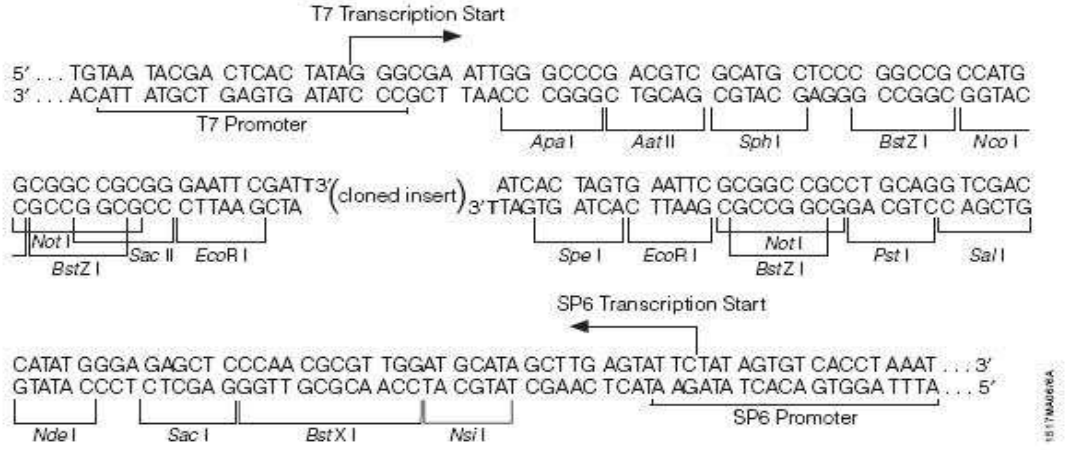

APPENDIX 2: Nucleotide alignment of RyR sequences amplified via genomic survey of bichir using degenerate PCR. Alignment shows that bichir sequences grouped into four separate cognates of RyR1a (red), RyR1b (yellow), RyR2 (blue), and RyR3 (green).

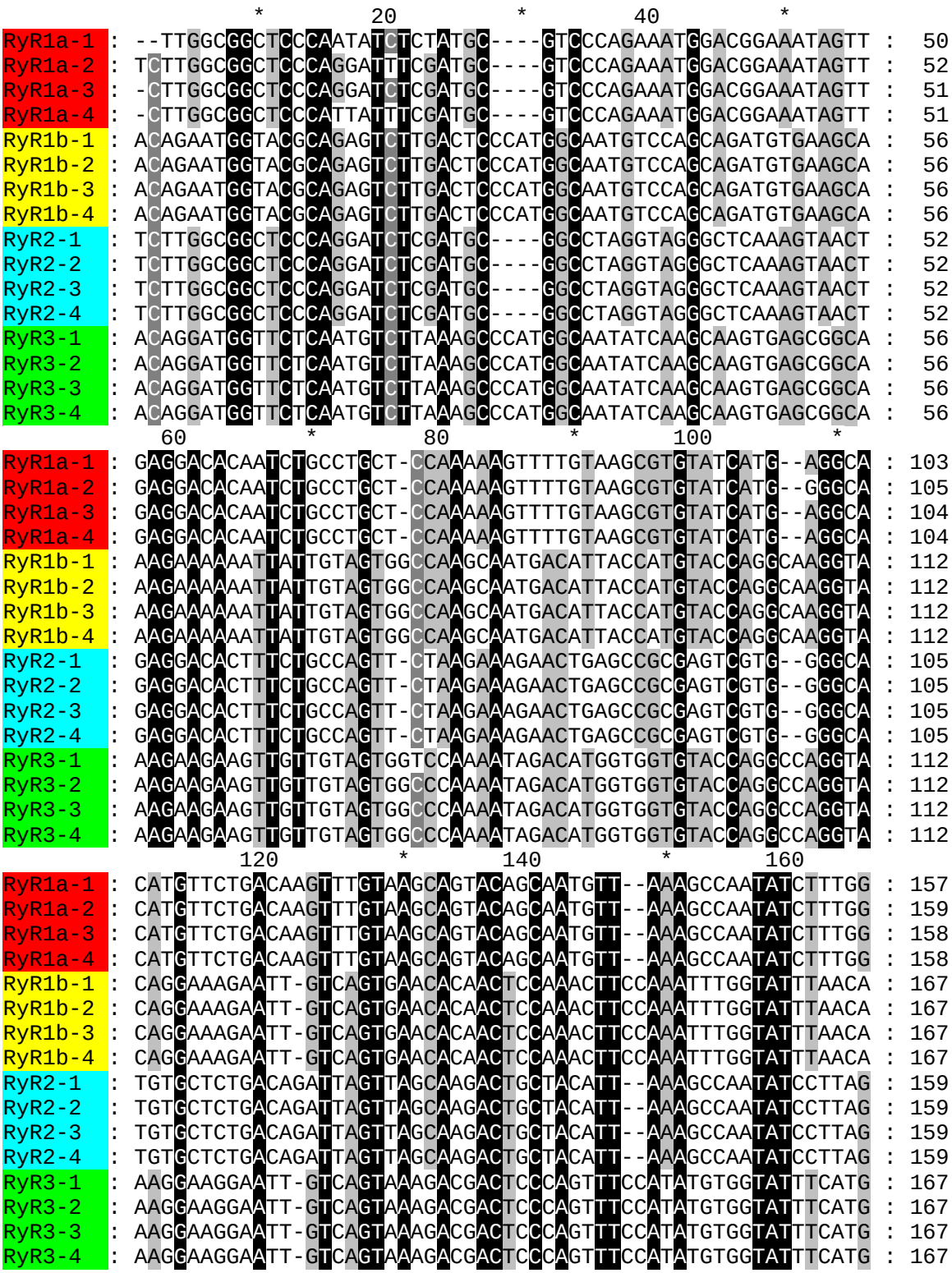

```
          *       180         *       200         *       220
RyR1a-1 : CTGGCTCTTGAAATCGATTAGCAAACTCCTCATAATTGATCATTTCATTCTCATCT : 213
RyR1a-2 : CTGGCTCTTGAAATCGACTAGCAAACTCCTCATAATTGATCATTTCATTCTCATCT : 215
RyR1a-3 : CTGGCTCTTGAAATCGATTAGCAAACTCCTCATAATTGATCATTTCATTCTCATCT : 214
RyR1a-4 : CTGGCTCTTGAAATCGATTAGCAAACTCCTCATAATTGATCATTTCATTCTCATCT : 214
RyR1b-1 : TCTACTGAAGTAATCCAAGTGAATA-TGGAACTGTCTGGCTCAGGCTTCTTCTCAT : 222
RyR1b-2 : TCTACTGAAGTAATCCAAGTGAATA-TGGAACTGTCTGGCTCAGGCTTCTTCTCAT : 222
RyR1b-3 : TCTACTGAAGTAATCCAAGTGAATA-TGGAACTGTCTGGCTCAGGCTTCTTCTCAT : 222
RyR1b-4 : TCTACTGAAGTAATCCAAGTGAATA-TGGAACTGTCTGGCTCAGGCTTCTTCTCAT : 222
RyR2-1  : CAGGCTCATGGAAACGATCTACAAACTCTTTATAGCTAAACATGTCATTCTCATCA : 215
RyR2-2  : CAGGCTCATGGAAACGATCTACAAACTCTTTATAGCTAAACATGTCATTCTCATCA : 215
RyR2-3  : CAGGCTCATGGAAACGATCTACAAACTCTTTATAGCTAAACATGTCATTCTCATCA : 215
RyR2-4  : CAGGCTCATGGAAACGATCTACAAACTCTTTATAGCTAAACATGTCATTCTCATCA : 215
RyR3-1  : TCAATAGAGCTCAACCATGACACCAGTGTGGCTTCTTTGG--GGGCAGTCTCTTCT : 221
RyR3-2  : TCAATAGAGCTCAACCATGACACCAGTGTGGCTTCTTTGG--GGGCAGTCTCTTCT : 221
RyR3-3  : TCAATAGAGCTCAACCATGACACCAGTGTGGCTTCTTTGG--GGGCAGTCTCTTCT : 221
RyR3-4  : TCAATAGAGCTCAACCATGACACCAGTGTGGCTTCTTTGG--GGGCAGTCTCTTCT : 221

            *       240         *       260         *       280
RyR1a-1 : GCTTCTGAGCAGGATAGTAGAAACTGGATCTCACTGGGAGAGTATTGCTTCTGACT : 269
RyR1a-2 : GCTTCTGAGCAGGATAGTAGAAACTGGATCTCACTGGGAGAGTATTGCTTCTGACT : 271
RyR1a-3 : GCTTCTGAGCAGGATAGTAGAAACTGGATCTCACTGGGAGAGTATTGCTTCTGACT : 270
RyR1a-4 : GCTTCTGAGCAGGATAGTAGAAACTGGATCTCACTGGGAGAGTATTGCTTCTGACT : 270
RyR1b-1 : GTTGGGCACTGATATCCAAAGATGCCAAGCCCATCCCCAGAA----GCTCAGCAAT : 274
RyR1b-2 : GTTGGGCACTGATATCCAAAGATGCCAAGTCCATCCCCAGAA----GCTCAGCAAT : 274
RyR1b-3 : GTTGGGCACTGATATCCAAAGATGCCAAGTCCATCCCCAGAA----GCTCAGCAAT : 274
RyR1b-4 : GTTGGGCACTGATATCCAAAGATGCCAAGTCCATCCCCAGAA----GCTCAGCAAT : 274
RyR2-1  : GCCTCTGCACATGATAACAAGAATTCAATTTCTGATTGAGTGTACTGCTTTTGGCT : 271
RyR2-2  : GCCTCTGCACATGATAACAAGAATTCAATTTCTGATTGAGTGTACTGCTTTTGGCT : 271
RyR2-3  : GCCTCTGCACATGATAACAAGAATTCAATTTCTGATTGAGTGTACTGCTTTTGGCT : 271
RyR2-4  : GCCTCTGCACATGATAACAAGAATTCAATTTCTGATTGAGTGTACTGCTTTTGGCT : 271
RyR3-1  : GTTGGGT--TGAAGTCCAGAGCACTTTTGTCCAAACCCAAGA----GTTCAGCAAT : 271
RyR3-2  : GTTGGGT--TGAAGTCCAGAGCACTTTTGTCCAAACCCAAGA----GTTCAGCAAT : 271
RyR3-3  : GTTGGGT--TGAAGTCCAGAGCACTTTTGTCCAAACCCAAGA----GTTCAGCAAT : 271
RyR3-4  : GTTGGGT--TGAAGTCCAGAGCACTTTTGTCCAAACCCAAGA----GTTCAGCAAT : 271

                *       300         *       320         *
RyR1a-1 : ATCCATGGCTTTCTGGAAGTCTTTTTTAGAGATAAGTCCTCGAGGATCTGTCACAT : 325
RyR1a-2 : ATCCATGGCTTTCTGGAAGTCTTTTTTAGAGATAAGTCCTCGAGGATCTGTCACAT : 327
RyR1a-3 : ATCCATGGCTTTCTGGAAGTCTTTTTTAGAGATAAGTCCTCGAGGATCTGTCACAT : 326
RyR1a-4 : ATCCATGGCTTTCTGGAAGTCTTTTTTAGAGATAAGTCCTCGAGGATCTGTCACAT : 326
RyR1b-1 : CCGCTCTCGTCCATAGATATCACCATACTTGTCCAGGACCTTCCGTTTGACAAATT : 330
RyR1b-2 : CCGCTCTCGTCCATAGATATCACCATACTTGTCCAGGACCTTCCGTTTGACAAATT : 330
RyR1b-3 : CCGCTCTCGTCCATAGATATCACCATACTTGTCCAGGACCTTCCGTTTGACAAATT : 330
RyR1b-4 : CCGCTCTCGTCCATAGATATCACCATACTTGTCCAGGACCTTCCGTTTGACAAATT : 330
RyR2-1  : TTCCATAGCTTTCTGAAACTCTTTCTTGGAGATGACTCCCTTTCCATCAGGATCAT : 327
RyR2-2  : TTCCATAGCTTTCTGAAACTCTTTCTTGGAGATGACTCCCTTTCCATCAGGATCAT : 327
RyR2-3  : TTCCATAGCTTTCTGAAACTCTTTCTTGGAGATGACTCCCTTTCCATCAGGATCAT : 327
RyR2-4  : TTCCATAGCTTTCTGAAACTCTTTCTTGGAGATGACTCCCTTTCCATCAGGATCAT : 327
RyR3-1  : TCTCTCAGCTCCATAGAGATCCCCATATTTGTTAATGACCTTACGTTTCACAAACT : 327
RyR3-2  : TCTCTCAGCTCCATAGAGATCCCCATATTTGTTAATGACCTTACGTTTCACAAACT : 327
RyR3-3  : TCTCTCAGCTCCATAGAGATCCCCATATTTGTTAATGACCTTACGTTTCACAAACT : 327
RyR3-4  : TCTCTCAGCTCCATAGAGATCCCCATATTTGTTAATGACCTTACGTTTCACAAACT : 327
```

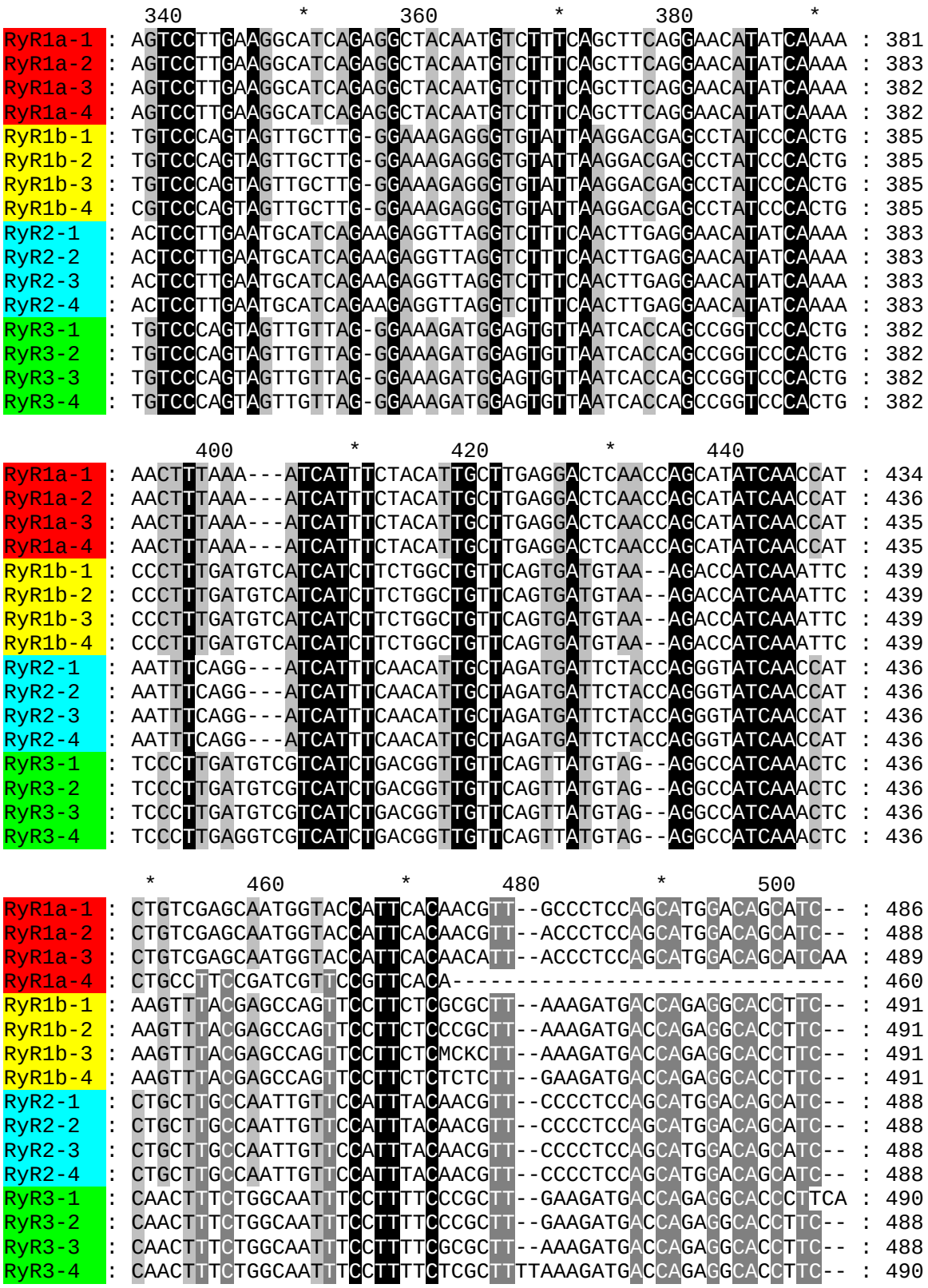
340 * 360 * 380 *
RyR1a-1 : AGTCCTTGAAGGCATCAGAGGCTACAATGTCTTTCAGCTTCAGGAACATATCAAAA : 381
RyR1a-2 : AGTCCTTGAAGGCATCAGAGGCTACAATGTCTTTCAGCTTCAGGAACATATCAAAA : 383
RyR1a-3 : AGTCCTTGAAGGCATCAGAGGCTACAATGTCTTTCAGCTTCAGGAACATATCAAAA : 382
RyR1a-4 : AGTCCTTGAAGGCATCAGAGGCTACAATGTCTTTCAGCTTCAGGAACATATCAAAA : 382
RyR1b-1 : TGTCCCAGTAGTTGCTTG-GGAAAGAGGGTGTATTAAGGACGAGCCTATCCCACTG : 385
RyR1b-2 : TGTCCCAGTAGTTGCTTG-GGAAAGAGGGTGTATTAAGGACGAGCCTATCCCACTG : 385
RyR1b-3 : TGTCCCAGTAGTTGCTTG-GGAAAGAGGGTGTATTAAGGACGAGCCTATCCCACTG : 385
RyR1b-4 : CGTCCCAGTAGTTGCTTG-GGAAAGAGGGTGTATTAAGGACGAGCCTATCCCACTG : 385
RyR2-1 : ACTCCTTGAATGCATCAGAAGAGGTTAGGTCTTTCAACTTGAGGAACATATCAAAA : 383
RyR2-2 : ACTCCTTGAATGCATCAGAAGAGGTTAGGTCTTTCAACTTGAGGAACATATCAAAA : 383
RyR2-3 : ACTCCTTGAATGCATCAGAAGAGGTTAGGTCTTTCAACTTGAGGAACATATCAAAA : 383
RyR2-4 : ACTCCTTGAATGCATCAGAAGAGGTTAGGTCTTTCAACTTGAGGAACATATCAAAA : 383
RyR3-1 : TGTCCCAGTAGTTGTTAG-GGAAAGATGGAGTGTTAATCACCAGCCGGTCCCACTG : 382
RyR3-2 : TGTCCCAGTAGTTGTTAG-GGAAAGATGGAGTGTTAATCACCAGCCGGTCCCACTG : 382
RyR3-3 : TGTCCCAGTAGTTGTTAG-GGAAAGATGGAGTGTTAATCACCAGCCGGTCCCACTG : 382
RyR3-4 : TGTCCCAGTAGTTGTTAG-GGAAAGATGGAGTGTTAATCACCAGCCGGTCCCACTG : 382
400 * 420 * 440
RyR1a-1 : AACTTTAAA---ATCATTTCTACATTGCTTGAGGACTCAACCAGCATATCAACCAT : 434
RyR1a-2 : AACTTTAAA---ATCATTTCTACATTGCTTGAGGACTCAACCAGCATATCAACCAT : 436
RyR1a-3 : AACTTTAAA---ATCATTTCTACATTGCTTGAGGACTCAACCAGCATATCAACCAT : 435
RyR1a-4 : AACTTTAAA---ATCATTTCTACATTGCTTGAGGACTCAACCAGCATATCAACCAT : 435
RyR1b-1 : CCCTTTGATGTCATCATCTTCTGGCTGTTCAGTGATGTAA--AGACCATCAAATTC : 439
RyR1b-2 : CCCTTTGATGTCATCATCTTCTGGCTGTTCAGTGATGTAA--AGACCATCAAATTC : 439
RyR1b-3 : CCCTTTGATGTCATCATCTTCTGGCTGTTCAGTGATGTAA--AGACCATCAAATTC : 439
RyR1b-4 : CCCTTTGATGTCATCATCTTCTGGCTGTTCAGTGATGTAA--AGACCATCAAATTC : 439
RyR2-1 : AATTTCAGG---ATCATTTCAACATTGCTAGATGATTCTACCAGGGTATCAACCAT : 436
RyR2-2 : AATTTCAGG---ATCATTTCAACATTGCTAGATGATTCTACCAGGGTATCAACCAT : 436
RyR2-3 : AATTTCAGG---ATCATTTCAACATTGCTAGATGATTCTACCAGGGTATCAACCAT : 436
RyR2-4 : AATTTCAGG---ATCATTTCAACATTGCTAGATGATTCTACCAGGGTATCAACCAT : 436
RyR3-1 : TCCCTTGATGTCGTCATCTGACGGTTGTTCAGTTATGTAG--AGGCCATCAAACTC : 436
RyR3-2 : TCCCTTGATGTCGTCATCTGACGGTTGTTCAGTTATGTAG--AGGCCATCAAACTC : 436
RyR3-3 : TCCCTTGATGTCGTCATCTGACGGTTGTTCAGTTATGTAG--AGGCCATCAAACTC : 436
RyR3-4 : TCCCTTGAGGTCGTCATCTGACGGTTGTTCAGTTATGTAG--AGGCCATCAAACTC : 436
* 460 * 480 * 500
RyR1a-1 : CTGTCGAGCAATGGTACCATTCACAACGTT--GCCCTCCAGCATGGACAGCATC-- : 486
RyR1a-2 : CTGTCGAGCAATGGTACCATTCACAACGTT--ACCCTCCAGCATGGACAGCATC-- : 488
RyR1a-3 : CTGTCGAGCAATGGTACCATTCACAACATT--ACCCTCCAGCATGGACAGCATCAA : 489
RyR1a-4 : CTGCCTTCCGATCGTTCCGTTCACA---------- : 460
RyR1b-1 : AAGTTTACGAGCCAGTTCCTTCTCGCGCTT--AAAGATGACCAGAGGCACCTTC-- : 491
RyR1b-2 : AAGTTTACGAGCCAGTTCCTTCTCCCGCTT--AAAGATGACCAGAGGCACCTTC-- : 491
RyR1b-3 : AAGTTTACGAGCCAGTTCCTTCTCMCKCTT--AAAGATGACCAGAGGCACCTTC-- : 491
RyR1b-4 : AAGTTTACGAGCCAGTTCCTTCTCTCTCTT--GAAGATGACCAGAGGCACCTTC-- : 491
RyR2-1 : CTGCTTGCCAATTGTTCCATTTACAACGTT--CCCCTCCAGCATGGACAGCATC-- : 488
RyR2-2 : CTGCTTGCCAATTGTTCCATTTACAACGTT--CCCCTCCAGCATGGACAGCATC-- : 488
RyR2-3 : CTGCTTGCCAATTGTTCCATTTACAACGTT--CCCCTCCAGCATGGACAGCATC-- : 488
RyR2-4 : CTGCTTGCCAATTGTTCCATTTACAACGTT--CCCCTCCAGCATGGACAGCATC-- : 488
RyR3-1 : CAACTTTCTGGCAATTTCCTTTTCCCGCTT--GAAGATGACCAGAGGCACCCTTCA : 490
RyR3-2 : CAACTTTCTGGCAATTTCCTTTTCCCGCTT--GAAGATGACCAGAGGCACCTTC-- : 488
RyR3-3 : CAACTTTCTGGCAATTTCCTTTTCGCGCTT--AAAGATGACCAGAGGCACCTTC-- : 488
RyR3-4 : CAACTTTCTGGCAATTTCCTTTTCTCGCTTTTAAAGATGACCAGAGGCACCTTC-- : 490

APPENDIX 3: Nucleotide alignment of RyR sequences amplified via genomic survey of zebrafish using degenerate PCR. After plasmids were sequenced, zebrafish RyR gene specific primers were designed and used to amplify the target for qRT-PCR. Subsequent to amplification, PCR products were directly sequenced.

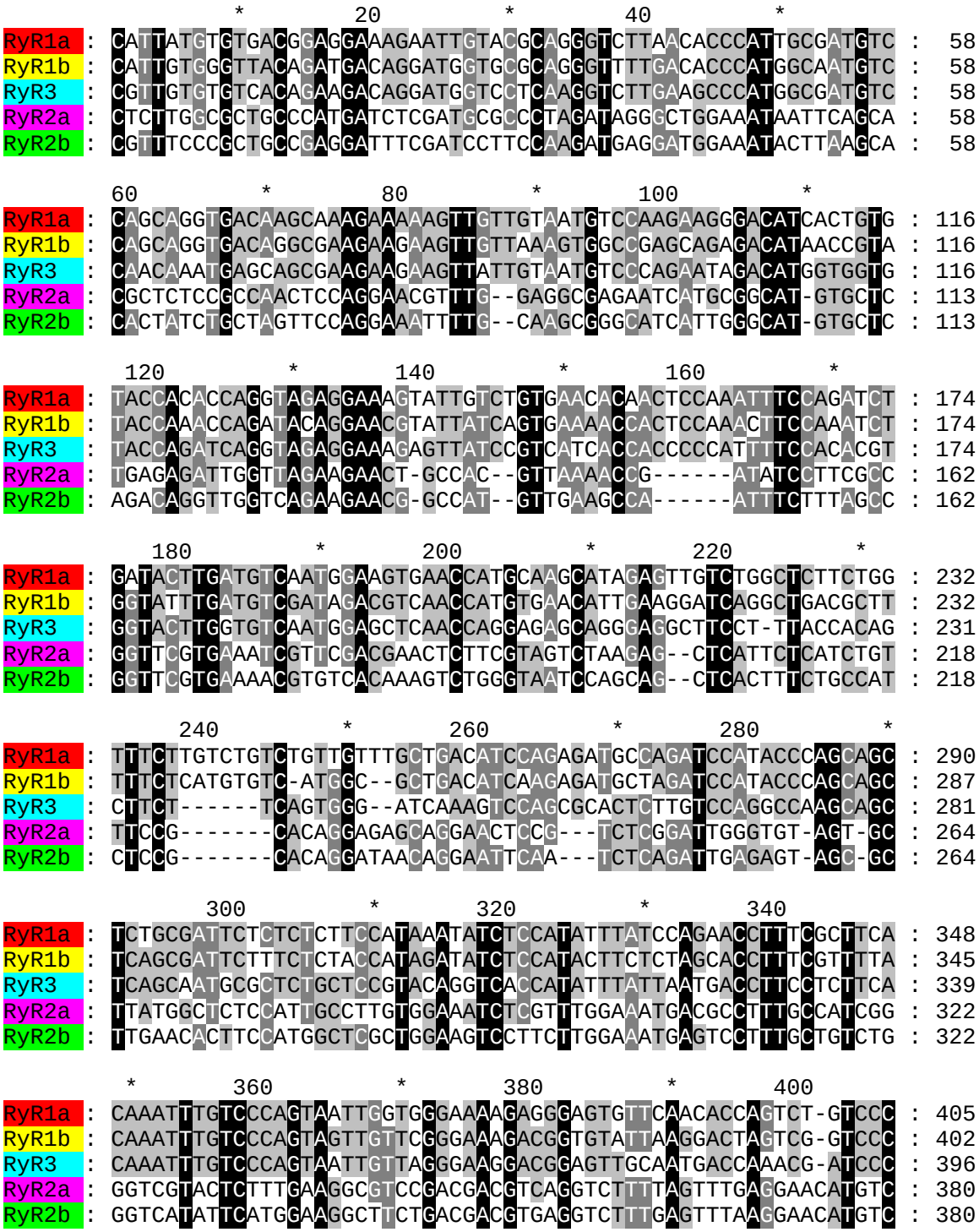

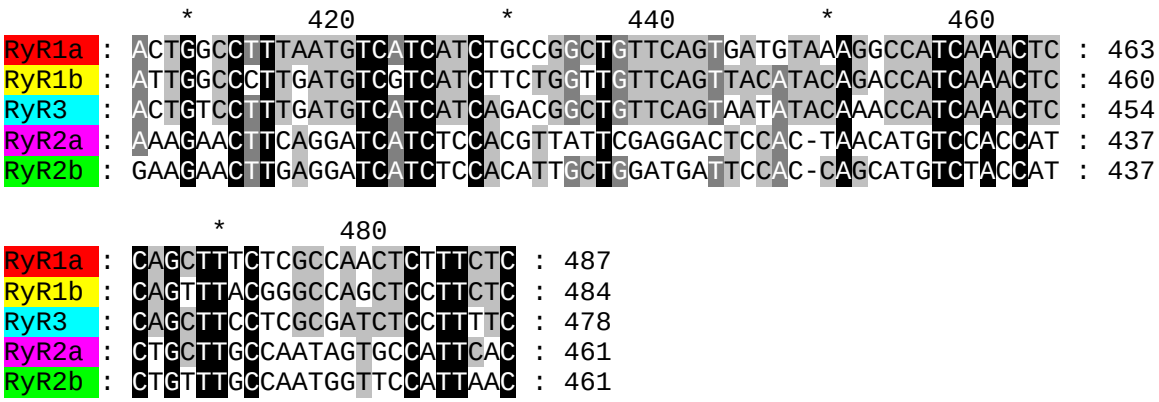
* 420 * 440 * 460
RyR1a : ACTGGCCTTTAATGTCATCATCTGCCGGCTGTTCAGTGATGTAAAGGCCATCAAACTC : 463
RyR1b : ATTGGCCCTTGATGTCGTCATCTTCTGGTTGTTCAGTTACATACAGACCATCAAACTC : 460
RyR3 : ACTGTCCTTTGATGTCATCATCAGACGGCTGTTCAGTAATATACAAACCATCAAACTC : 454
RyR2a : AAAGAACTTCAGGATCATCTCCACGTTATTCGAGGACTCCAC-TAACATGTCCACCAT : 437
RyR2b : GAAGAACTTGAGGATCATCTCCACATTGCTGGATGATTCCAC-CAGCATGTCTACCAT : 437
* 480
RyR1a : CAGCTTTCTCGCCAACTCTTTCTC : 487
RyR1b : CAGTTTACGGGCCAGCTCCTTCTC : 484
RyR3 : CAGCTTCCTCGCGATCTCCTTTTC : 478
RyR2a : CTGCTTGCCAATAGTGCCATTCAC : 461
RyR2b : CTGTTTGCCAATGGTTCCATTAAC : 461

APPENDIX 4: Nucleotide alignment of bichir (Bi) and zebrafish (ZF) actin gene amplified from genomic DNA and used as one of the housekeeping genes during qRT-PCR. Blue colouring represents the binding site of bichir actin HKG qRT-PCR primers, and red colouring is the annealing site of actin HKG primers in zebrafish.

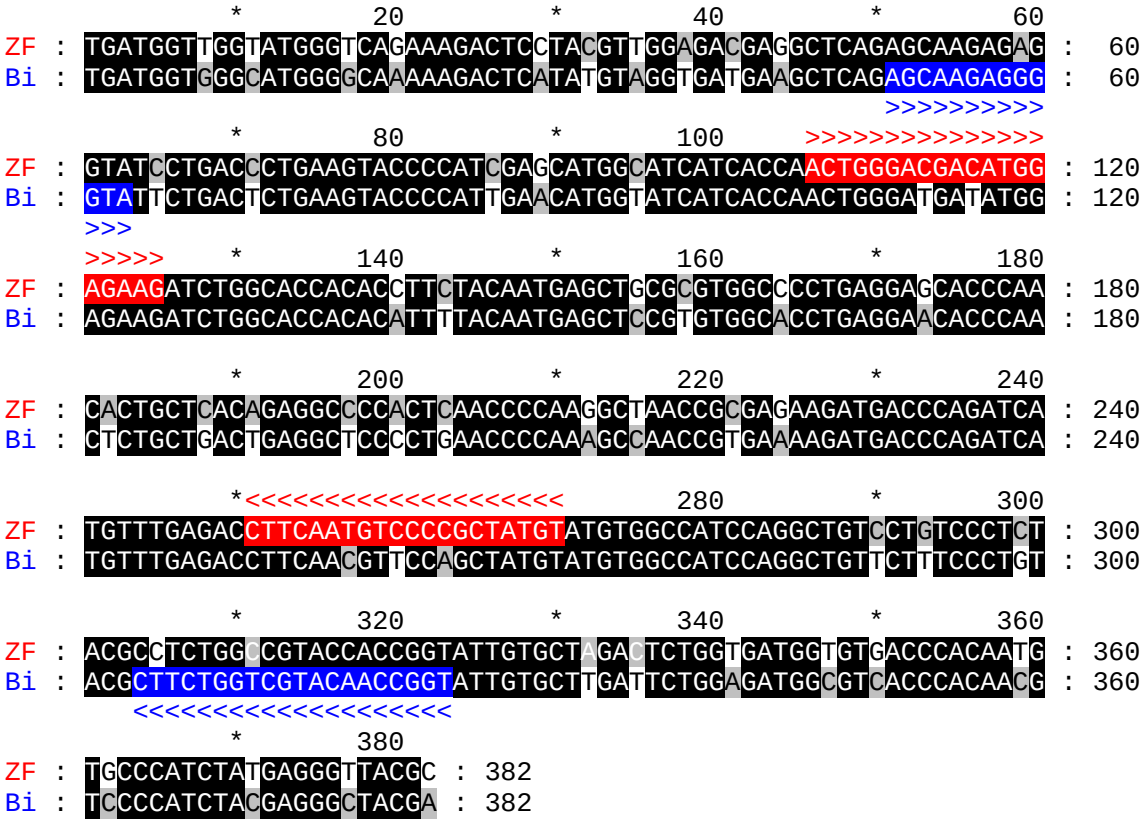

APPENDIX 5: Nucleotide alignment of bichir (Bi) and zebrafish (ZF) ef1α gene amplified from genomic DNA and used as one of the housekeeping genes during qRT-PCR. Blue colouring represents the binding site of bichir actin HKG qRT-PCR primers, and red colouring is the annealing site of actin HKG primers in zebrafish.

```
                *         20         *         40         *         60
ZF : TAGCCGTCCCACCGACAAGCCCCTCCGTCTGCCACTTCAGGATGTGTACAAAATTGGAGG : 60
Bi : CACCCGGCCCACTGACAAGCCTCTTCGGCTGCCTCTCCAAGATGTGTATAAGATTGGAGG : 60

                *         80         *        100         *        120
ZF : TATTGGAACTGTACCTGTGGGTCGTGTGGAGACTGGTGTCCTCAAGCCTGGTATGGTTGT : 120
Bi : TATAGGAACAGTTCCAGTGGGCAGGGTTGAGACTGGAGTTCTGCGGCCAGGAATGGTGGT : 120
                                                    >>>>>>>>>
                *         140        *        160        >>>>>>>>>>>>>>>
ZF : GACCTTCGCCCCTGCCAATGTAACCACTGAGGTCAAGTCTGTTGAGATGCACCACGAGTC : 180
Bi : GACCTTTGCTCCTGTCAATATAACCACAGAGGTGAAATCAGTTGAAATGCATCATGAGGC : 180
     >>>>>>>>>>>
     >>>>>     *         200        *        220         *        240
ZF : TCTGACTGAGGCCACTCCTGGTGACAACGTTGGCTTCAACGTTAAGAACGTGTCTGTCAA : 240
Bi : TTTGAGTGAAGCCCTGCCTGGTGATAACGTAGGCTTTAATGTCAAGAACGTTTCAGTCAA : 240

                *         260        *        280         *        300
ZF : GGACATCCGTCGTGGTAATGTGGCTGGAGACAGCAAGAACGACCCACCCATGGAGGCTGC : 300
Bi : GGATATCCGCCGAGGAAATGTGTGTGGAGACAGCAAGAATGATCCCCCCAGGAGGCGGC : 300

        <<<<<<<<<<<<<<<<<<<<         *        340         *        360
ZF : CAACTTCAACGCTCAGGTCATCATCCTGAACCACCCTGGTCAGATCTCTCAGGGTTACGC : 360
Bi : TCAGTTTGTTGCTCAGGTGATCATCTTGAACCATCCTGGACAGATCAGCGCTGGCTACTC : 360
                                 <<<<<<<<<<<<<<<<<<<<
                *         380        *        400         *        420
ZF : CCCAGTGCTGGATTGCCACACTGCTCACATCGCCTGCAAGTTTGCTGAGCTCAAGGAGAA : 420
Bi : GCCTGTGATTGACTGTCACACGGCTCACATTGCCTGCAAGTTTGCTGAGCTAAAAGAGAA : 420

                *         440        *        460         *        480
ZF : GATCGACCGTCGTTCTGGCAAGAAGCTTGAAGACAACCCCAAGGCTCTCAAATCCGGAGA : 480
Bi : GATTGACAGACGTTCTGGCAAAAAACTTGAAGACAACCCTAAATCTTTAAAGTCTGGTGA : 480

                *         500        *        520         *        540
ZF : TGCCGCCATTGTTGAGATGGTCCCTGGCAAGCCCATGTGTGTGGAGAGCTTCTCTACCTA : 540
Bi : TGCAGCCATTGTGGATATGGTGCCTGGTAAACCCATGTGTGTAGAGAGCTTCTCACAGTA : 540

                *         560        *        580         *        600
ZF : CCCTCCTCTTGGTCGCTTTGCTGTGCGTGACATGAGGCAGACCGTTGCTGTCGGCGTCAT : 600
Bi : CCCACCATTGGGGCGCTTTGCCGTGAGAGACATGCGACAGACAGTGGCAGTTGGGGTAAT : 600

                *         620        *        640         *        660
ZF : CAAGAGCGTTGAGAAGAAAATCGGTGGTGCTGGCAAGGTCACAAAGTCTGCACAGAAGGC : 660
Bi : CAAAAATGTGGAGAAGAAAGCCGCAGGAGCGGGCAAAGTCACCAAGTCCGCCCAGAAGGC : 660


ZF : T : 661
Bi : A : 661
```

APPENDIX 6: Composition of Media and Reagents

SALINE SOLUTION

0.85 g Sodium Chloride in 100 ml of distilled water.

PHOSPHATE BUFFER, pH=7.4

19.5 mL of Sodium phosphate, monobasic (0.69 g/50 mL distilled water)
80.8 mL of sodium phosphate, dibasic (1.41 g/ 100mL distilled water)
Store at 4℃.

NITRO BLUE TETRAZOLIUM (NBT) SOLUTION

100 mg NBT in 50 mL distilled water.